

**REGULATION OF INTRACELLULAR pH IN CULTURED FOETAL RAT
HIPPOCAMPAL PYRAMIDAL NEURONES**

by

KEITH ALLEN BAXTER

B.Sc. (Chemistry), The University of British Columbia, 1991

A THESIS SUBMITTED IN PARTIAL FULFILLMENT OF
THE REQUIREMENTS FOR THE DEGREE OF

MASTER OF SCIENCE

in

THE FACULTY OF GRADUATE STUDIES

(Department of Anatomy)

We accept this thesis as conforming to the required standard

THE UNIVERSITY OF BRITISH COLUMBIA

February, 1995

© Keith Allen Baxter, 1995

In presenting this thesis in partial fulfilment of the requirements for an advanced degree at the University of British Columbia, I agree that the Library shall make it freely available for reference and study. I further agree that permission for extensive copying of this thesis for scholarly purposes may be granted by the head of my department or by his or her representatives. It is understood that copying or publication of this thesis for financial gain shall not be allowed without my written permission.

Department of Anatomy

The University of British Columbia
Vancouver, Canada

Date Feb. 21, 1995

ABSTRACT

The mechanisms regulating intracellular pH (pH_i) were investigated in cultured foetal rat hippocampal pyramidal neurones loaded with the pH-sensitive fluorescent indicator 2',7'-bis(carboxyethyl)-5(or 6)-carboxyfluorescein. At room temperature ($\sim 20^\circ\text{C}$), steady-state pH_i was 6.85 in the nominal absence of external HCO_3^- , and increased to 7.15 in the presence of HCO_3^- . In HCO_3^- -free medium at 37°C , steady-state pH_i rested at the substantially higher level of 7.23, whereas in HCO_3^- -containing solutions at 37°C , pH_i was reduced to 7.13. Regardless of temperature and in the absence of HCO_3^- , the removal of extracellular Na^+ caused an immediate and sustained intracellular acidification, suggesting the dominance of a Na^+ -dependent mechanism(s) maintaining steady-state pH_i . In $\text{HCO}_3^-/\text{CO}_2$ -buffered medium at room temperature, a moderate intracellular acidification was observed during the application of the anion exchanger inhibitor 4,4'-diisothiocyanatostilbene-2,2'-disulphonic acid (DIDS) or after the removal of HCO_3^- , indicating the contribution of $\text{HCO}_3^-/\text{Cl}^-$ exchange to the maintenance of baseline pH_i . Moreover, this anion exchanger could participate in pH_i regulation even in the absence of extracellular Na^+ . At 37°C , however, DIDS did not alter steady-state pH_i in the presence of HCO_3^- . Though extremely sensitive to the removal of extracellular Na^+ at both temperatures, neither steady-state pH_i nor the rate of pH_i restoration from an imposed acid load were influenced by the application of ethylisopropylamiloride, a potent inhibitor of Na^+/H^+ exchange. Following an NH_4^+ -induced intracellular acidification, the rate of pH_i recovery to baseline levels was faster at 37°C than at room temperature. Furthermore, in contrast to experiments performed at room temperature, the addition of HCO_3^- to the perfusate did not increase the rate of pH_i recovery at 37°C . The results of this study suggest that at 37°C , the dominant regulator of pH_i in hippocampal neurones is a Na^+ -dependent, HCO_3^- -independent acid extrusion mechanism (probably an amiloride insensitive variant of the Na^+/H^+ exchanger). At

room temperature, this Na^+ -dependent acid extrusion mechanism remains active, but the regulation of pH_i appears to be supplemented by the activity of a Na^+ -independent $\text{HCO}_3^-/\text{Cl}^-$ exchanger.

TABLE OF CONTENTS

	Page
Abstract	ii
Table of Contents	iv
List of Tables	vi
List of Figures	vii
Acknowledgments	x
 INTRODUCTION	 1
Physiology, pathophysiology, and pH_i	3
pH_i and cell excitability	6
pH_i and ionic conductances	9
pH_i and Ca^{2+}	12
Distribution of protons across the limiting membrane	14
Regulation of pH_i	15
Intracellular buffering	19
Overview	21
 MATERIALS AND METHODS	
Cell preparation	22
Loading the neurones with BCECF	23
Experimental setup	24
Solutions	25
Calculation of pH_i	28
Analysis of data	32
 RESULTS	
Steady-state pH_i regulation	
Regulation of pH_i at room temperature	42
Regulation of pH_i at 37°C	43
Na^+ -dependent or -independent anion exchange	46
Modulation of pH_i by shifts in pH_o and the application of weak acids and bases	46
pH_i recovery from an imposed acid load	86
Recovery from an acid load at room temperature	88
Recovery from an acid load at 37°C	89

	Page
DISCUSSION	122
Regulation of pH_i at 37°C	122
Regulation of pH_i at room temperature	130
Comparison of pH_i regulation at 37°C and room temperature	133
Modulation of pH_i by pH_o	137
Conclusions	140
REFERENCES	144

LIST OF TABLES

	Page
Table 1 Composition of HEPES-buffered experimental solutions	34
Table 2 Composition of $\text{HCO}_3^-/\text{CO}_2$ -buffered experimental solutions at room temperature	35
Table 3 Composition of $\text{HCO}_3^-/\text{CO}_2$ -buffered experimental solutions at 37°C	36
Table 4 Composition of $\text{HCO}_3^-/\text{CO}_2$ -buffered experimental solutions at varying pHs at 37°C	37
Table 5 Steady-state pH_i in HCO_3^- -free and HCO_3^- -containing media at room temperature and at 37°C , and the change in pH_i caused by the exposure to the experimental solutions indicated	49
Table 6 pH_i recoveries from an NH_4^+ -induced intracellular acidification	95

LIST OF FIGURES

		Page
Figure 1	Relationship between the concentration of HCO_3^- and the resulting solution pH when equilibrated with 5% CO_2 in balance air at 37°C	39
Figure 2	Sample calibration plot for BCECF	41
Figure 3	Distribution of steady-state pH_i	51
Figure 4	Effect of 0 $[\text{Cl}^-]_o$ on steady-state pH_i in the presence of HCO_3^- at room temperature	53
Figure 5	Effect of DIDS on steady-state pH_i in the presence of HCO_3^- at room temperature	55
Figure 6	Steady-state pH_i in the presence and absence of $\text{HCO}_3^-/\text{CO}_2$ at room temperature	57
Figure 7	Effect of 0 $[\text{Na}^+]_o$ on steady-state pH_i in the absence of HCO_3^- at 37°C	59
Figure 8	Effect of 0 $[\text{Cl}^-]_o$ on steady-state pH_i in the absence of HCO_3^- at 37°C	61
Figure 9	Effect of EIPA on steady-state pH_i in the absence of HCO_3^- at 37°C ...	63
Figure 10	Combined effect of 0 $[\text{Na}^+]_o$ and EIPA on steady-state pH_i in the absence of HCO_3^- at 37°C	65
Figure 11	Effect of MGCMA and HOE 694 on steady-state pH_i in the absence of HCO_3^- at 37°C	67
Figure 12	Effect of 0 $[\text{Na}^+]_o$ on steady-state pH_i in the presence of HCO_3^- at 37°C	69
Figure 13	Effect of EIPA on steady-state pH_i in the presence of HCO_3^- at 37°C ...	71
Figure 14	Effect of 0 $[\text{Cl}^-]_o$, and the combined effect of 0 $[\text{Cl}^-]_o$ plus DIDS on steady-state pH_i in the presence of HCO_3^- at 37°C	73
Figure 15	Effect of DIDS on steady-state pH_i in the presence of HCO_3^- at 37°C ...	75
Figure 16	Steady-state pH_i in the presence and absence of $\text{HCO}_3^-/\text{CO}_2$ at 37°C ...	77

	Page
Figure 17 Effect of $\text{HCO}_3^-/\text{CO}_2$ on steady-state pH_i during 0 $[\text{Na}^+]_o$ perfusion at room temperature	79
Figure 18 Effect of 0 $[\text{Cl}^-]_o$ during 0 $[\text{Na}^+]_o$ perfusion on steady-state pH_i in the presence of HCO_3^- at 37°C	81
Figure 19 Effect of changes in pH_o on steady-state pH_i in the presence of HCO_3^- at 37°C	83
Figure 20 Effect of propionate and TMA on steady-state pH_i in the presence of HCO_3^- at room temperature	85
Figure 21 Sample acid load with NH_4Cl	94
Figure 22 Initial rate of acid load recovery as a function of pH_i , preload pH_i , minimum pH_i , and net pH_i decrease	97
Figure 23 pH_i recovery from an acid load in the absence and presence of HCO_3^- at room temperature	99
Figure 24 Effect of DIDS on pH_i recovery from an acid load in the presence of HCO_3^- at room temperature	101
Figure 25 Effect of 0 $[\text{Cl}^-]_o$ on pH_i recovery from an acid load in the presence of HCO_3^- at room temperature	103
Figure 26 pH_i recovery from an acid load in the absence and presence of HCO_3^- at 37°C	105
Figure 27 Effect of 0 $[\text{Na}^+]_o$ on pH_i recovery from an acid load in the absence of HCO_3^- at 37°C	107
Figure 28 Effect of EIPA on pH_i recovery from an acid load in the absence of HCO_3^- at 37°C	109
Figure 29 Effect of DIDS on pH_i recovery from an acid load in the absence of HCO_3^- at 37°C	111
Figure 30 Effect of 0 $[\text{Na}^+]_o$ on pH_i recovery from an acid load in the presence of HCO_3^- at 37°C	113

	Page
Figure 31 Effect of EIPA on pH_i recovery from an acid load in the presence of HCO_3^- at 37°C	115
Figure 32 Effect of 0 $[\text{Cl}^-]_o$ on pH_i recovery from an acid load in the presence of HCO_3^- at 37°C	117
Figure 33 Effect of DIDS on pH_i recovery from an acid load in the presence of HCO_3^- at 37°C	119
Figure 34 Effect of DIDS on pH_i recovery from an enhanced acid load in the presence of HCO_3^- at 37°C	121
Figure 35 Diagrammatic representation of pH_i recovery from an acid load in the presence and absence of HCO_3^- , at room temperature and at 37°C	139
Figure 36 Schematic presentation of pH_i regulating mechanisms in cultured foetal hippocampal pyramidal neurones at 37°C and room temperature	143

ACKNOWLEDGMENTS

There are many to which I would like to extend my sincerest appreciation and gratitude. Firstly, I am indebted to Dr. John Church for his enduring guidance, encouragement, and insight. John, you have been instrumental in my growth as a scientist and as an individual.

For their consideration and time, I thank the other members of my supervisory committee, Drs. Ken Baimbridge and Vladimir Palatý. I would especially like to extend my deepest gratitude to Dr. Palatý for sharing his breadth of knowledge, even beyond the scope of science. Furthermore, I humbly acknowledge Monika Grunert and Garth Smith for their technical expertise and experimental assistance.

To the Faculty, Graduate Students, and Staff in the Department of Anatomy, I thank you for creating an atmosphere that has fostered a relentless pursuit of knowledge. I will look fondly upon friendships and memories of my time here. I would particularly like to express my heartfelt appreciation to my esteemed friend and colleague, Sean Virani, for his persistent yet genuine ability to keep me on an even keel.

Foremost, a debt of gratitude is owed to my family for their continued support and inspiration. Mum and Dad, I am especially grateful to you both for your patience and unconditional love.

Financial support was provided by an operating grant to Dr. John Church from the Medical Research Council of Canada.

INTRODUCTION

pH fluctuations in the brain have been shown to accompany many physiological and pathophysiological events (reviewed by Chesler, 1990; Chesler and Kaila, 1992). For example, a transient extracellular alkalization has been demonstrated to follow electrical stimulation of the CA1 region of the rat hippocampus (Voipio and Kaila, 1993). Jarolimek *et al* (1989) have noted a similar, albeit enhanced, extracellular pH (pH_o) shift induced by the application of neurotransmitters to the CA3 region of guinea pig hippocampal slices. Following electrical stimulation of presynaptic pathways in the rat hippocampus, a long-lasting extracellular alkaline shift has also been observed to accompany excitatory synaptic transmission (Krishtal *et al*, 1987; Gottfried and Chesler, 1994). In addition to the pH_o shifts associated with normal neuronal activity, tissue pH changes are also associated with various pathologies (reviewed by Siesjö, 1985). For instance, complete brain ischemia has been shown to result in the accumulation of extracellular protons (Harris *et al*, 1987), caused primarily by the production of lactic acid due to the anaerobic consumption of glycogen and glucose stores (Siesjö *et al*, 1990). Furthermore, extracellular acidosis has been recorded in the rat parietal cortex during spreading depression (Mutch and Hansen, 1984), whereas biphasic changes in the acid-base balance of the interstitial fluid have been shown to occur during seizure activity in the rat hippocampus (Somjen, 1984; Jarolimek *et al*, 1989).

Not only has it become increasingly apparent that many normal and abnormal events relating to neuronal activity will cause alterations in the tissue pH but, in turn, tissue pH may alter or modulate many of these physiological or pathological occurrences. The clinic implications of changes in tissue pH were described as early as the 1930's. Lennox *et al* (1936) remarked that voluntary hyperpnea, an action in which one blows off CO_2 , can cause seizure-like brain patterns in epilepsy-prone patients. Conversely, the inhalation of elevated CO_2 concentrations has been described as a means of attenuating

seizure activity (Lennox *et al*, 1936). Recent evidence points towards pH changes as the cause for these CO₂-induced alterations in seizure activity. Aram and Lodge (1987) and Velišek *et al* (1994) have demonstrated that the lowering of pH_o, by either direct titration with HCl or increasing the partial pressure of CO₂ (PCO₂), will suppress the induction of seizure activity in the rat cortex and hippocampus. Fornai *et al* (1994) observed that acidic conditions, produced by the application of lactate, exert a similar anti-epileptiform action on rat cortical neurones. In contrast, alkalosis induces epileptiform activity (Aram and Lodge, 1987; Church and McLennan, 1989; Jarolimek *et al*, 1989). The induction of mild brain acidosis, produced by hypercarbic ventilation, has also been shown to serve a neuroprotective role during focal ischemia (Simon *et al*, 1993), possibly via inhibition of the rise in intracellular Ca²⁺ that normally characterizes the onset of ischemia (Ebine *et al*, 1994, Kristián *et al*, 1994). In addition, hypoxia-induced spreading depression in hippocampal slices can be prevented by exposure to acidic artificial cerebrospinal fluid, whereas an alkaline pH_o will predispose neurones to spreading depression after oxygen deprivation (Tombaugh, 1994). Whilst mild extracellular acidity exerts a protective effect during neural pathologies (Kaku *et al*, 1993), excessive acidosis (pH_o < 5.3) has been correlated with the death of brain tissue following complete ischemia (Kraig *et al*, 1987). Similarly, Nedergaard *et al* (1991) have shown that the prolonged exposure of neurones and glia to lactic acid or HCl (pH_o < 6.8) produced toxic effects leading to cell death.

The susceptibility of these pathologies to changes in tissue pH is reflected in pH-induced alterations in many normal physiological events. For instance, a fall in the interstitial pH, caused either by elevated H⁺ or CO₂ concentrations, has been shown to have a depressant effect on neuronal excitability in the hippocampal formation (Somjen *et al*, 1987; Balestrino and Somjen, 1988; Church and McLennan, 1989). Similarly, Taira *et al* (1993) have shown that synaptic transmission is sensitive to changes in pH_o, whereby an increase or decrease in pH_o will reduce or potentiate excitatory transmission,

respectively. The effect of tissue pH on the excitable properties of cells may in fact reflect the pH-induced modulation of various ionic conductances, such as Ca^{2+} , through voltage- and ligand-gated ion channels (Ou-Yang *et al*, 1994).

Regardless of the mechanisms involved, it is clear that many physiological and pathological events are modulated by fluctuations in the external pH. In most vertebrate studies, however, the influence of changes in intracellular pH (pH_i) on neuronal excitability, injury, or mortality has not been thoroughly investigated. This is surprising since recent evidence indicates that changes in pH_i will accompany changes in pH_o (Preissler and Williams, 1981; Aicken, 1984; Tolkovsky and Richards, 1987; Chesler, 1990; Ou-yang *et al*, 1993; Katsura *et al*, 1994; Sun and Vaughan-Jones, 1994). Furthermore, Katsura *et al* (1994) concluded that the regulation of pH_i is dependent on pH_o in neurones and glia. The fact that changes in pH_o may have a significant impact on pH_i implies a possible role for pH_i in some of the aforementioned events modulated by changes in tissue pH. Indeed, as explained below, there appears to be an interdependence between pH_i and many physiological and pathological occurrences, which, though examined in invertebrate neuronal and vertebrate non-neuronal preparations, has not been extensively studied in mammalian central neurones.

Physiology, pathophysiology, and pH_i :

Many normal and abnormal cell functions can modulate, or are modulated by, the intracellular acid-base balance. For instance, pH_i changes affect many aspects of muscle dynamics. An intracellular alkalosis in cardiac Purkinje fibres produces an increase in the muscle twitch tension, whereas an intracellular acidosis is associated with a fall of muscle force generation (Vaughan-Jones *et al*, 1987; Bountra *et al*, 1988). Kaila and Voipio (1990) have reported that the resting tension in crayfish muscle fibres is increased by an reduction of pH_i , and decreased by an elevation of pH_i . Changes in pH_i also affect vascular tone. Raising pH_i increases the tension of rat vascular smooth muscle fibres in a

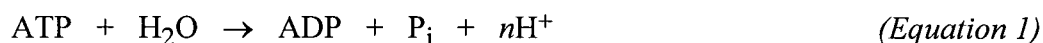
fashion that is independent of pH_o (Austin and Wray, 1993). Studies on the rat portal vein reveal similar results, and may provide a possible explanation for the observed decrease in contractile activity during pathological situations such as hypoxia (Taggart *et al*, 1994).

Cellular enzymatic activity and metabolism is also closely tied to intracellular acidity (Busa, 1986). Cells exposed to perturbations in pH_i may experience shifts in the normal operation of intracellular enzymes whose activity kinetics are pH dependent (Busa, 1986). Active sites on enzymes may contain ionizable groups which are involved in the binding of substrates and cofactors (Roos and Boron, 1981). Fluctuations in intracellular proton levels will affect the ionization of these groups, thus influencing enzyme conformational states and the ability to form enzyme-substrate complexes (Roos and Boron, 1981). The arrangement of cytoskeletal proteins can also be modulated by the internal pH. The polymerization of tubulin, for example, increases as pH_i rises (Busa, 1986). Furthermore, the bundling and cross-linking of microfilaments is sensitive to intracellular acid shifts. In *Dictyostelium* amoebae, an intracellular acidification inhibits the arrangement of microfilaments, as opposed to an alkalization which promotes filamentous organization (Busa, 1986). pH_i -dependent variations in the synthesis of these cytoskeletal components may in fact be a consequence of pH_i -dependent fluctuations in the activities of enzymes associated with these elements.

pH_i has also been shown to play a modulatory role in cellular proliferation and development. Hesketh *et al* (1985), for example, have identified pH_i perturbations in mouse thymocytes and Swiss 3T3 fibroblasts stimulated by the application of mitogens, demonstrating a possible relationship between pH_i and the regulation of cell division. It has also been observed that a pH_i increase accompanies fertilization of frog, axolotl, and sea urchin ova (reviewed by Roos and Boron, 1981). Fertilization-induced pH_i rises have been attributed to the activation of a Na^+/H^+ exchanger, which acts to extrude intracellular protons (Roos and Boron, 1981). Such changes in pH_i may in turn modulate

the cascade of biosynthetic pathways involved in early embryonic development including metabolism, stimulus-response coupling, DNA replication, and mitosis (Busa and Nuccitelli, 1984).

In addition to the previously mentioned association of pH_o with neural pathologies, it also appears that pH_i may play an important role in events such as brain ischemia and seizures (Siesjö, 1985). During cerebral ischemia, there is a marked decline in pH_i , which is predominantly caused by the production of lactic acid during anaerobic glycolysis (Siesjö, 1985). As cerebral energy states deteriorate during an hypoxic insult, ATP hydrolysis also contributes to the ischemic-induced intracellular acidification, which proceeds according to the following reaction:



where n has been approximated at 0.7 (Wilkie, 1979). The overall reduction of pH_i during ischemia may then act to protect the cell from excessive damage. Indeed, intracellular acid shifts are believed to reduce membrane excitability and inhibit cellular metabolism during ischemia (Tombaugh and Sapolsky, 1993). Nevertheless, although a neuroprotective function is associated with mild acidosis, excessive accumulations of intracellular equivalents have been shown to induce both neuronal and glial death in cells cultured from rat forebrains (Nedergaard *et al*, 1991). Glutamate neurotoxicity may also, at least in part, involve the detrimental effects of abnormally high intracellular proton concentrations induced by glutamate receptor activation (Hartley and Dubinsky, 1993). In addition, a mild intracellular acidosis has been observed to accompany neuronal epileptiform activity (Siesjö *et al*, 1985). This acidification is thought to occur as a result of increased intracellular lactic acid production, whose effects are delayed or relieved by Na^+/H^+ exchange (Siesjö *et al*, 1985). Fluctuations in pH_i have also been noted to proceed many of these pathological occurrences. For example, Mabe *et al* (1983) have demonstrated that pH_i rises to alkaline levels in rat cortical neurones immediately following ischemic insult. The reason for this post-ischemic alkalosis remains unclear,

but may be a result of the degradation of accumulated intracellular lactic acid, or the resumed production of ATP (Mabe *et al*, 1983).

pH_i and cell excitability:

Electrical activity, including the depolarization of cell membranes, can produce intracellular pH shifts in neurones (Chesler, 1990). Meech and Thomas (1987) have reported that a Ca²⁺-sensitive reduction in pH_i follows the depolarization of molluscan nerve cells. It has also been shown that the application of a depolarizing agent (i.e. high extracellular K⁺) onto cultured bovine chromaffin cells produces an intracellular acidification that can be reduced by lowering extracellular Ca²⁺ levels (Rosario *et al*, 1991). Moreover, trains of action potentials evoked in molluscan nerve cell bodies have been demonstrated to cause a decrease in pH_i (Ahmed and Connor, 1980), and the degree of intracellular acidification appears to depend on the frequency of the action potentials (Bountra *et al*, 1988). Activity-dependent changes in pH_i, in addition to reflecting changes in intracellular Ca²⁺ (see below), may also be caused by the release of acidic metabolic products (Siesjö, 1985) or the entry of acid equivalents through membrane potential sensitive transport mechanisms (Fitz *et al*, 1992). Interestingly, *in vivo* stimulation of cortical astrocytes produces an cytoplasmic alkalinization (Chesler and Kraig, 1987). This observation suggests that the intra-neuronal acidification caused by electrical stimulation may occur as a result of proton transfer between neurones and their supporting structures.

It has recently become apparent that the application of neuromodulators and neurotransmitters, including hormones and excitatory amino acids, can alter pH_i (reviewed by Chesler, 1990). Barber *et al* (1989), for instance, have shown that pH_i in cultured canine enteric endocrine cells can be altered by the application of epinephrine and somatostatin in a manner independent of their established effects on cAMP production. Epinephrine, acting on the β₂-adrenergic receptor, activates a Na⁺/H⁺

exchanger which leads to an intracellular alkalinization, whereas somatostatin inhibits this exchanger producing a cytosolic acidification (Barber *et al*, 1989). The activation of other cell surface receptors has also been shown to modify Na^+/H^+ exchange independent of the concomitant changes in cAMP. Stimulation of prostaglandin E1 and parathyroid hormone receptors on a variety of non-neuronal preparations results in a pH_i rise by enhancing Na^+/H^+ exchange (Ganz *et al*, 1990). In contrast, the activation of D_2 -dopaminergic receptors act to reduce pH_i via an inhibition of this exchanger (Ganz *et al*, 1990). Though all of the above neuromodulators or neurotransmitters alter pH_i in a manner independent of any associated fluctuations in intracellular cyclic nucleotide levels, Conner and Hockberger (1984) have shown that the injection of cyclic AMP or cyclic GMP into gastropod neurones will also induce cytoplasmic pH changes. Two other cell surface receptors that, when activated, alkalinize the interior of NG108-15 cells by accelerating Na^+/H^+ exchange are muscarinic cholinergic and δ -opiate receptors (Isom *et al*, 1987). Moreover, Ludt *et al* (1991) have indicated that protein kinase C, which is linked to muscarinic receptor activation, is involved in pH_i modulation of primate renal cells through the regulation of a $\text{HCO}_3^-/\text{Cl}^-$ exchanger.

Other hormones and growth factors have been shown to produce fluctuations in pH_i . Arginine vasopressin (AVP) raises steady-state pH_i in renal mesangial cells in the absence of extracellular HCO_3^- , whereas AVP reduces pH_i in the presence of extracellular HCO_3^- (Ganz *et al*, 1989). Ganz *et al* (1989) speculated that AVP stimulates both Na^+ - and HCO_3^- -dependent exchangers, which, depending on the composition of the interstitial fluid, will act to increase or decrease pH_i . Indeed, the exposure of rat mesangial cells to AVP, epidermal growth factor, or serotonin has recently been shown to cause increases in the activities of various acid extrusion mechanisms, including the Na^+/H^+ , Na^+ -independent $\text{HCO}_3^-/\text{Cl}^-$, and Na^+ -dependent $\text{HCO}_3^-/\text{Cl}^-$ exchangers (Ganz and Boron, 1994). The application of a combination of mitogens (platelet-derived growth factor, vasopressin, and insulin) has been reported to

cause an increase in pH_i by stimulating the Na^+/H^+ exchanger present on mouse 3T3 cells (Schuldiner and Rozengurt, 1982). Other mitogenic activators, such as epidermal growth factor and serum growth factor, have been demonstrated to alter Na^+/H^+ exchange in human diploid fibroblasts (Moolenaar *et al*, 1982). The tumour promoter, okadaic acid, which inhibits protein phosphatase activity, is also believed to stimulate fibroblast Na^+/H^+ exchange which leads to an intracellular alkalinization (Sardet *et al*, 1991). Interestingly, studies on mouse thymocytes and Swiss 3T3 fibroblasts have indicated that intracellular Ca^{2+} ($[\text{Ca}^{2+}]_i$) may serve as an intermediate to growth factor-induced changes in pH_i (Hesketh *et al*, 1985).

Extracellular changes in pH have been shown to modulate ionic conductances through channels activated by excitatory amino acids. Traynelis and Cull-Candy (1991), for example, have reported that conductances through *N*-methyl-D-aspartate (NMDA), α -amino-3-hydroxy-5-methyl-4-isoxazole propionate (AMPA), and kainate receptor channels can be inhibited by accumulations of extracellular protons. Furthermore, the blockade of the NMDA receptor by interstitial protons occurs well within the physiological pH range (Vyklícký *et al*, 1990; Giffard *et al*, 1990; Tang *et al*, 1990; Gottfried and Chesler, 1994). The application of excitatory amino acids has more recently been linked to alterations in pH_i . NMDA, quisqualate, and kainate have been shown to produce concentration-dependent intracellular acidifications in frog motoneurons (Endres *et al*, 1986). Irwin *et al* (1994) have proposed that an influx of Ca^{2+} may be required for the internal acidosis of foetal rat hippocampal neurones induced by the activation of NMDA receptors. Moreover, increasing pH_o does not significantly alter the degree of intracellular acidification caused by NMDA, suggesting that the agonist-induced fall in pH_i is not a consequence of transmembrane proton fluxes (Irwin *et al*, 1994). It appears that the activation of metabotropic receptors may also contribute to the intracellular acidosis resulting from the application of glutamate possibly by modulating the activity of a $\text{Na}^+/\text{HCO}_3^-$ cotransporter (Amos and Richards, 1994).

Neuronal excitability associated with L-glutamate receptor activation is therefore dependent not only on the pH of the extracellular environment but also on the pH of the intracellular milieu because changes in pH_i are known to modulate a wide variety of ionic conductances (see below).

The mechanism by which γ -aminobutyric acid (GABA) alters pH_i is unique among neurotransmitters. Examined on crayfish skeletal muscle, GABA induces an intracellular acidification by activating a HCO_3^- conductance (Kaila and Voipio, 1987). The application of GABA, according to Kaila *et al* (1990), leads to an influx of CO_2 , which is hydrated into carbonic acid through a catalyzed reaction involving carbonic anhydrase. The dissociation of carbonic acid into bicarbonate liberates intracellular protons, and in concert with an increase in membrane permeability to HCO_3^- , a decline in pH_i is produced (Kaila *et al*, 1990). Further investigation of GABA-induced changes in pH_i using crayfish stretch-receptor neurones produced findings supporting the notion that the intracellular acidification is mediated by a net efflux of HCO_3^- through GABA-gated channels (Voipio *et al*, 1991). Therefore, the reduction of pH_i produced by GABA is unlike the actions of other hormones and transmitters in that it directly involves the movement of acid equivalents across the plasma membrane.

pH_i and ionic conductances:

The evidence outlined above demonstrates that neuronal activity is associated with changes in pH_i . In turn, it is known that pH_i is able to influence cell excitability by modulating a wide variety of ionic conductances (reviewed by Moody, 1984). Injecting low pH solutions into isolated ventricular myocytes shortens the duration and amplitude of evoked action potentials, whereas the intracellular application of high pH solutions has the opposite effect (Kurachi, 1982). The specific currents underlying pH_i -induced changes in cell excitability have been examined. For example, voltage gated K^+ conductances in human lymphocytes are enhanced by an elevation in pH_i (Deutsch and

Lee, 1989). Conversely, an intracellular acidification has been associated with a blockade of inward rectifying K^+ currents in starfish oocytes (Moody and Hagiwara, 1982). In crayfish slow muscle fibres, low pH_i mediates the amplification of inward Ca^{2+} conductances, which is believed to occur as a result of proton-induced inhibition of the overlapping outward K^+ currents (Moody, 1980). The delayed rectifier K^+ conductance can also be modified by an accumulation of intracellular protons in squid axons (Wanke *et al*, 1979). Furthermore, an intracellular acidification inhibits conductances through Ca^{2+} -activated K^+ channels in pancreatic B-cells (Cook *et al*, 1984) which Laurido *et al* (1991), in studying rat skeletal muscle, attributed to a proton-induced weakening of Ca^{2+} binding to conformational sites on the channel. Kume *et al* (1989) report that a fall in pH_i can also reduce the likelihood of finding Ca^{2+} -activated K^+ channels in an open state. Indeed, suppression of Ca^{2+} -activated K^+ conductances by intracellular acidosis have been observed in type I cells of the rat carotid body (Peers and Green, 1991), as well as CA1 pyramidal neurones of the rat hippocampus (Church, 1992).

In addition to K^+ currents, other ionic conductances can be modulated by fluctuations in pH_i . Na^+ -dependent Ca^{2+} influx was first shown to be inhibited by a fall in pH_i in squid axons (Baker and Honerjäger, 1978). Umbach (1982) later observed decreases in Ca^{2+} channel permeability in *Paramecium* caused by an intracellular acidification; conversely, an intracellular alkalization increased Ca^{2+} conductances. High voltage activated (HVA) Ca^{2+} currents appear to be particularly sensitive to pH_i shifts (Kaibara and Kameyama, 1988). Takahashi *et al* (1993) have demonstrated that an intracellular acidification will suppress while an intracellular alkalization will enhance HVA Ca^{2+} conductances in catfish retinal cells. Prod'homme *et al* (1987) have reported that the conduction kinetics of HVA Ca^{2+} channels are influenced by protons directly occupying a channel regulatory site. Inhibition of HVA Ca^{2+} currents has also been associated with the activation of glutamate receptors (Zeilhofer *et al*, 1993; Dixon *et al*, 1993). Zeilhofer *et al* (1993) attributed this inhibition to glutamate receptor-mediated

Ca^{2+} influx and subsequent Ca^{2+} -dependent inactivation of Ca^{2+} channels, whereas Dixon *et al* (1993) suggested that a glutamate-induced Ca^{2+} -dependent change in pH_i is responsible for the modulation of HVA Ca^{2+} currents.

Variations in voltage-dependent Na^+ conductances caused by changes in pH_i have been studied in frog skeletal muscle (Nonner *et al*, 1980; Wanke *et al*, 1980) and squid giant axons (Carbone *et al*, 1981). Interestingly, results regarding the influence of pH_i on Na^+ currents have been quite variable. In squid axons, low pH_i depresses Na^+ conductances through the enhanced inactivation of Na^+ channels, whereas high pH_i reduces this inactivation, thereby increasing Na^+ conductances (Carbone *et al*, 1981). Opposite results were achieved in studies of frog muscle: lowering pH_i nearly eliminates channel inactivation, thus enhancing Na^+ channel conductances (Nonner *et al*, 1980; Wanke *et al*, 1980). An analysis of conductance kinetics reveals the possibility that two (membrane potential sensitive) proton binding affinities exist for the Na^+ channel (one with a pK_a of 4.6, and the other with a pK_a of 5.6), which may explain the observed differences in Na^+ conductance sensitivities to pH_i (Wanke *et al*, 1980). Furthermore, in contrast to most other ionic currents, the inhibition of Na^+ conductances by pH_i is voltage dependent (Moody, 1984). Ionic currents associated with $\text{Na}^+/\text{Ca}^{2+}$ exchange are also susceptible to changes in the cytoplasmic pH (Doering and Lederer, 1993). Measured in guinea-pig heart cells, an intracellular acidification suppresses the activity of the $\text{Na}^+/\text{Ca}^{2+}$ exchanger, whereas an intracellular alkalinization has the opposite effect (Doering and Lederer, 1993). Moreover, the recovery of $[\text{Ca}^{2+}]_i$ in hippocampal neurones after stimulus-evoked Ca^{2+} entry, which may require $\text{Na}^+/\text{Ca}^{2+}$ exchange, is retarded by an intracellular acidification (Koch and Barish, 1994).

The modulation of Cl^- conductances by pH has not been extensively documented. Barnes and Bui (1991) have noted that the sensitivity of Ca^{2+} -activated Cl^- currents in amphibian cone photoreceptors to alterations in pH_o is possibly a consequence of pH-induced shift in Ca^{2+} channel gating. Changes in pH_i , on the other hand, have been

observed to significantly affect basolateral Cl^- conductances in colonic epithelial cells (Chang *et al*, 1991). These results, along with the others outlined above, indicate a common link between cell excitability and pH_i in many preparations. Not only is the intracellular proton environment shifted by the electrical behavior of the cell, but pH_i has the ability to modulate many ionic conductances that underlie basic membrane excitability.

Finally, gap junctional conductances are also susceptible to changes in pH_i (Spray and Bennett, 1985). In fact, it is suggested that intracellular protons may modulate these conductances more effectively than other intracellular ions, including Ca^{2+} (Spray *et al*, 1982; Moody, 1984). A decrease in Lucifer yellow dye-coupling in guinea pig hippocampal slices has been associated with a fall in pH_i (MacVicar and Jahnsen, 1985). Conversely, Church and Baimbridge (1991) have shown that there is an increased incidence of dye-coupling caused by the exposure of rat hippocampal pyramidal neurones to high pH extracellular medium, presumably related to the fact that raising pH_o will result in an increase in pH_i (see Discussion). pH_i transients in amphibian embryos have been similarly correlated with coupling changes in a manner that is independent of the extracellular proton milieu (Spray and Bennett, 1985; Busa, 1986).

pH_i and Ca^{2+} :

A complex interdependence appears to exist between pH_i and intracellular free Ca^{2+} . For example, pH_i can be modulated by fluctuations in the intracellular concentration of Ca^{2+} (Ahmed and Connor, 1980). Observed in snail neurones, the intracellular injection of Ca^{2+} causes an immediate fall in pH_i that is proportional to the amount of Ca^{2+} injected (Meech and Thomas, 1977). Busa and Nuccitelli (1984) have postulated that Ca^{2+} -dependent alterations in pH_i may involve the exchange of Ca^{2+} for protons by various intracellular organelles, such as the mitochondria or smooth endoplasmic reticulum. Furthermore, slow Ca^{2+} iontophoresis has been observed to

produce a decrease in pH_i without affecting the membrane potential, which avoids possible secondary effects on pH_i caused by changes in ion distribution across the membrane (Meech and Thomas, 1977). The exposure of avian neural crest cells to Ca^{2+} -free media induces a cytoplasmic acidification, which is believed to occur as a result of the subsequent fall in $[\text{Ca}^{2+}]_i$ (Dickens *et al*, 1990). Sánchez-Armass *et al* (1994) have recently reported that a rise in $[\text{Ca}^{2+}]_i$ can increase the efflux of intracellular protons via the stimulation of Na^+/H^+ exchange (see below). This conclusion is supported by data showing that the application of Ca^{2+} ionophores on rat brain synaptosomes induces Na^+ -dependent increases in pH_i (Sánchez-Armass *et al*, 1994).

pH_i has in turn been shown to modulate intracellular free Ca^{2+} (Dickens *et al*, 1990; Martínez-Zaguilán *et al*, 1991). The exposure of barnacle muscle cells to CO_2 leads to an increase in $[\text{Ca}^{2+}]_i$, which Lea and Ashley (1978) attribute to a CO_2 -induced reduction in pH_i . An elevation in cytosolic protons is thought to displace Ca^{2+} from intracellular organelles and other Ca^{2+} -binding proteins present in the sarcoplasm (Lea and Ashley, 1978). Siskind *et al* (1989) also credit the low pH_i -induced rise in internal Ca^{2+} in vascular smooth muscle to the release of Ca^{2+} from intracellular sources. Interestingly, pH_i has also been shown to modulate the intracellular levels of other divalent cations. In cultured chicken heart cells, for example, changes in cytosolic Mg^{2+} have been inversely correlated with induced shifts in pH_i (Freudenrich *et al*, 1992).

In studying the relationship between pH_i and internal free Ca^{2+} using fluorescent indicators in a variety of cell types, Ganz *et al* (1990) raised three possibilities for pH_i -dependent changes in $[\text{Ca}^{2+}]_i$. In agreement with previously mentioned theories, a pH_i shift may alter Ca^{2+} fluxes across various intracellular membranes. However, Ganz *et al* (1990) caution that artifacts may be responsible for perceived changes in cytosolic Ca^{2+} levels because perturbations in pH_i may alter: 1) the association of Ca^{2+} with its fluorescent indicator, and 2) the interaction of the Ca^{2+} indicator with internal membranes. Under both of these conditions, an apparent change in $[\text{Ca}^{2+}]_i$ would be

recorded, when, in fact, none actually occurred. Therefore, it is necessary to take these factors into account when evaluating the significance of cytosolic Ca^{2+} changes caused by altering pH_i .

Distribution of protons across the limiting membrane:

Measurements of pH_i in a variety of cell types have determined that protons are not passively distributed across the plasma membrane (reviewed by Roos and Boron, 1981). This was, in fact, first observed in muscle by Fenn and Cobb in the mid-1930's. With an extracellular pH of 7.0, Fenn and Cobb (1934) measured pH_i to be 7.0, which is much higher than the predicted value of 5.62 based on a Donnan equilibrium with K^+ . The Donnan rule states that, at equilibrium, the ratios of all diffusable ion concentrations on either side of a permeable membrane will be equal. With a high K^+ concentration inside cells in comparison to the outside, one would expect, based on this law of membrane equilibria, that proton concentrations would be higher on the outside in comparison to the inside. If this rule held true, then pH_i would rest at 5.6 if pH_o was near neutrality. Further calculations on frog muscle by Fenn and Maurer (1935) yielded a value of 6.9 for pH_i while pH_o rested at 7.34, but even this difference was not large enough to be explained simply by equilibrium across the membrane. This observation was concurred with by Hill (1955) who, in studies on frog muscle, concluded that "...the Donnan equilibrium does not control, and does not greatly influence, the distribution of hydrogen ions across the fibre membrane."

Chesler (1990) outlines, from a membrane potential perspective, the unlikelihood of having a passive H^+ distribution across the plasma membrane. If protons passively moved across the membrane, then the distribution of intracellular and extracellular protons would be governed by the resting membrane potential (E_m) as represented by the Nernst equation:

$$E_m = E_{H^+} = \frac{RT}{F} \ln \frac{[H^+]_o}{[H^+]_i} \quad (\text{Equation 2})$$

where E_{H^+} is the equilibrium potential for H^+ , F is Faraday's constant, R is the ideal gas constant, and T is the temperature. Given approximate values of 7.4 for pH_o and 7.0 for pH_i (see Chesler, 1990, for a summary of resting pH_i levels in a variety of cells), the above equation yields an equilibrium potential for the H^+ ion (E_{H^+}) of -23.6 mV at 25°C. Due to the difference between E_{H^+} and E_m , which normally rests between -50 and -60 mV in excitable cells, an inward proton gradient is established. This, and the fact that some cellular metabolic processes produce acid equivalents (e.g. glucose \rightarrow 2 lactate $^-$ + 2 H^+), forces cells to continually extrude acid in order to maintain pH_i near neutrality (Thomas, 1984). Whether a conclusion is based on calculations of the Donnan equilibrium function or the Nernst equation, it is clear that protons are not passively distributed across the limiting membrane. The regulation of pH_i by acid extrusion and/or acid buffering is therefore a common property of most cell types.

Regulation of pH_i :

As an electrochemical gradient favours the influx of protons from the interstitial space into the cytoplasm, cells must continually extrude acid equivalents in order to maintain a constant resting pH_i . These extrusion mechanisms also participate in the restoration of pH_i back to normal physiological levels after cells have been burdened with an induced acid load. Accordingly, in addition to monitoring steady-state conditions, many studies on pH_i regulation have investigated acid extrusion mechanisms through the analysis of pH_i recovery from an imposed acidification.

The idea of trans-membrane fluxes of H^+ or HCO_3^- was initially suggested by Messeter and Siesjö (1971) in their study of rat brain tissue. These authors noted that the extrusion of acid equivalents is at least partially responsible for the recovery from a CO_2 -

induced intracellular acidification. Intracellular proton loading was also used by Roos (1975) in studying pH_i regulation in rat diaphragm muscle. Roos reasoned that intracellular buffering (discussed below) does not sufficiently explain why pH_i is only moderately affected by considerable intracellular proton loads. Proton extrusion must therefore play a substantial role in maintaining a constant intracellular acid-base balance (Roos, 1975). Recovery from an intracellular acidification, induced by the addition and subsequent removal of extracellular NH_4Cl , has produced additional evidence supporting the presence of acid extruding mechanisms on various invertebrate neurones, including the squid giant axon (Boron and DeWeer, 1976).

The study of intracellular proton extrusion has concentrated on the identification of transporting mechanisms that exchange intracellular or extracellular ions for proton equivalents. Murer *et al* (1976) first identified a Na^+/H^+ antiport system present on the membranes of rat intestinal and renal cells which was thought to be involved in acid extrusion. This group observed that the antiporter operates in a non-electrogenic fashion to exchange intracellular H^+ ions for extracellular Na^+ ions (Murer *et al*, 1976). Furthermore, Johnson *et al* (1976) found that the activity of Na^+/H^+ exchange is susceptible to inhibition by the diuretic drug amiloride (1-(3,5-diamino-6-chloropyrazinoyl)guanidine). The ability of this drug to block Na^+/H^+ exchange on other cell types, such as renal or intestinal epithelial cells, has been extensively documented (e.g. Sardet *et al*, 1989; Tse *et al*, 1993; Mrkic *et al*, 1993; Rowe *et al*, 1994).

A second acid transporter has been described which involves the inward flux of HCO_3^- in exchange for an intracellular anion (Thomas, 1976a). Thomas speculated that Cl^- was in fact the anion in question, a possibility that was confirmed by Russell and Boron (1976) in their investigation of squid axons. Both groups demonstrated that this anion exchanger, which operates in a Na^+ -independent fashion, could be blocked by stilbene derivatives such as SITS (4-acetamido-4'-isothiocyanatostilbene-2,2'-disulphonic acid) and DIDS (4,4'-diisothiocyanatostilbene-2,2'-disulphonic acid). The $\text{HCO}_3^-/\text{Cl}^-$

exchanger acts to reduce intracellular proton accumulations by presenting the cytosol with HCO_3^- , which enters the cell in exchange for Cl^- . HCO_3^- ions sequester protons to form H_2CO_3 which then, utilizing the enzyme carbonic anhydrase, dissociates into CO_2 and H_2O . Both CO_2 and H_2O freely diffuse out of the cell, and then combine to regenerate extracellular HCO_3^- levels. The net result of this mechanism is the reduction of intracellular H^+ ion concentrations via the influx of HCO_3^- and subsequent efflux of Cl^- , CO_2 and H_2O .

In their examination of mouse soleus muscle fibres, Aicken and Thomas (1977) revealed the possible presence of multiple pH_i regulating systems in a single cell type. These authors concluded that both Na^+/H^+ exchange, which is primarily driven by the transmembrane Na^+ gradient, and $\text{HCO}_3^-/\text{Cl}^-$ exchange independently maintain constant resting levels of pH_i (Aicken and Thomas, 1977). As demonstrated by Thomas (1977) on snail neurones, these two mechanisms may also operate in conjunction with one another. This particular regulating system, classified as Na^+ -dependent $\text{HCO}_3^-/\text{Cl}^-$ exchange, relies on the availability of extracellular Na^+ as a requisite for the counter-transport of HCO_3^- and Cl^- . Similar to the Na^+ -independent subtype, the Na^+ -dependent $\text{HCO}_3^-/\text{Cl}^-$ exchanger is susceptible to inhibition with SITS or DIDS (Thomas, 1977). Thus, by the early 1980's, three separate electroneutral mechanisms were targeted as significant regulators of pH_i : Na^+/H^+ exchange, Na^+ -independent $\text{HCO}_3^-/\text{Cl}^-$ exchange, and Na^+ -dependent $\text{HCO}_3^-/\text{Cl}^-$ exchange (Thomas, 1984). All of these transporters have been shown, for example, to be active to varying extents in freshly isolated rat glomerular mesangial cells (Boyarski *et al*, 1990a and b). Moreover, the activities of these exchangers can be modulated by the application of various neurotransmitters and hormones, or fluctuations in the concentration of intracellular ions such as Ca^{2+} (see above).

Other proton extruding mechanisms present on some cell membranes include a $\text{Na}^+/\text{HCO}_3^-$ transporter and a proton pump. Boron and Boulepaep (1983) identified an

electrogenic $\text{Na}^+/\text{HCO}_3^-$ co-transporter on the basolateral membranes of salamander renal proximal tubules. This mechanism, which is sensitive to stilbene derivatives, inwardly directs extracellular Na^+ , HCO_3^- , and a net negative charge across the plasma membrane (Boron and Boulepaep, 1983). A nonelectrogenic H^+ pump, involved in gastric acid secretion, was first described by Sachs *et al* (1976), stemming from studies on the hog stomach. In response to a variety of secretagogues, extracellular K^+ is exchanged for intracellular H^+ with the consumption of ATP (Sachs, 1987). Also known as the H^+,K^+ -ATPase, this proton pump is exclusively found on gastric parietal cells whose principal function is the acidification of the stomach milieu (Boron, 1989).

Though studied extensively in invertebrates, pH_i regulating mechanisms in vertebrate neurones have not been thoroughly investigated, primarily because their relatively small size hampers the utilization of pH-sensitive microelectrodes (Chesler, 1990). With the advent of fluorescent pH dyes, studies on mammalian central neurones have recently emerged. Various fluorescein derivatives, whose spectra shift according to the surrounding proton environment, are now employed as indicators of pH in biological systems (reviewed by Tsien, 1989). The most popular probe of pH_i in vertebrate neurones is 2',7'-bis(carboxyethyl)-5(or 6)-carboxyfluorescein (BCECF) because of its high sensitivity to small changes in pH_i , ease of intracellular entrapment, and physiologically relevant pK_a (~6.98) (Rink *et al*, 1982). Utilizing BCECF in cultured rat sympathetic neurones, Tolkovsky and Richards (1987) reported that the main regulator of pH_i is a Na^+/H^+ exchanger that is sensitive to inhibition by amiloride. Though the exchange of HCO_3^- for Cl^- does not appear to be active in these cells, the authors provide evidence for the presence of some other HCO_3^- -dependent intracellular acid regulator, perhaps HCO_3^- sensitive Na^+/H^+ exchange, which may play a minor role in pH_i regulation. Nachshen and Drapeau (1988) and Sánchez-Armass *et al* (1994) have also shown that the Na^+/H^+ antiporter is the primary pH_i regulator in rat brain synaptosomes. Gaillard and DuPont (1990) have demonstrated that cultured cerebellar Purkinje cells

utilize Na^+/H^+ exchange and $\text{HCO}_3^-/\text{Cl}^-$ exchange to control intracellular acid-base levels. This combination of acid transporters has also been implicated in the maintenance of pH_i in cultured rat cortical neurones (Ou-yang *et al*, 1993). Raley-Susman *et al* (1991) have observed that pH_i in cultured foetal rat hippocampal neurones is maintained by an amiloride insensitive Na^+/H^+ antiporter, with a minor contribution from a Na^+ - and HCO_3^- -dependent acid extrusion mechanism. Schwiening and Boron (1994) have also demonstrated that regulation of pH_i in freshly isolated neurones from the adult rat hippocampus is possibly governed by an amiloride insensitive Na^+/H^+ exchanger, in addition to a DIDS sensitive Na^+ -dependent $\text{HCO}_3^-/\text{Cl}^-$ exchanger. The insensitivity of the Na^+/H^+ exchanger present on hippocampal neurones to amiloride supports emerging evidence regarding the structural diversity of the cation counter-transporter (reviewed by Clark and Limbird, 1991). Four isoforms of the Na^+/H^+ exchanger have so far been cloned, each representing unique molecular compositions, localizations in the body, and sensitivities to amiloride and its analogues (see Discussion). Though results are still quite sparse, it is becoming increasingly evident that the regulation of neuronal pH_i in the mammalian central nervous system is maintained by various combinations of acid extruding exchangers.

Intracellular buffering:

Any chemical system that contains a well proportioned mixture of acids and bases acts to buffer any displacement of pH. By this notion, the intracellular milieu, which is rich in many proton acceptors and donators, is able to resist changes in its pH due to the buffering capacity of its constituents. In discussing pH_i , it is therefore necessary to include an examination of the cytosol's ability to buffer proton fluxes, both in terms of steady-state pH_i regulation and recovery from acid or alkali transients.

Cells are internally buffered by the acid-base pairs formed from bicarbonate, proteins, phosphates, and dipeptides (Burton, 1978). Together, these species sequester or release protons to minimize pH_i shifts according to the equation:

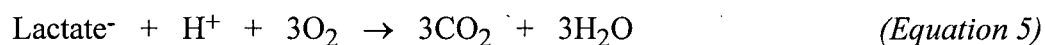


where M is a weak base having a valence of n , and MH is its conjugate acid having a valence of $n+1$ (Roos and Boron, 1981). This type of buffering, which utilizes a balanced distribution of intracellular weak acids and bases, is known as physiochemical buffering (Boron, 1989).

Another manner by which changes in pH_i are minimized is via biochemical reactions. Such reactions may act to consume or liberate H^+ ions in response to intracellular acid-base shifts. Acid production, for example, that occurs in response to alkaline loads may involve the conversion of intracellular carbohydrates into lactic acid according to:



(Siesjö, 1985). Conversely, in response to acid loads, the concentrations of lactate, pyruvate, or citrate may decrease (Siesjö and Messeter, 1971). Acid consumption, in the case of lactic acid, would proceed as:



(Siesjö, 1985). The consumption of protons by intracellular acids and their subsequent oxidation produces freely diffusable CO_2 (and H_2O), which can readily leave the cell to reduce the effects of acid loading.

A final form of intracellular buffering is the movement of acid-base equivalents between the cytoplasm and the interior of various cytosolic organelles (Roos and Boron, 1981). Known as organellar buffering, it is thought that many intracellular inclusions, such as endosomes and lysosomes, are able to transport protons across their membranes, possibly in an electrogenic fashion (Boron, 1989). This transporter has been identified as a H^+ pump, driven by the hydrolysis of ATP (Boron, 1989). The inner mitochondrial

membrane is also believed to be an active site of proton exchange (Roos and Boron, 1981). Responding to intracellular acidifications, for instance, such buffering would act to transport H^+ ions into acidic vesicles or limit H^+ flux out of alkaline organelles.

It should be emphasized that buffering, whether physiochemical, biochemical, or organellar, does not eliminate pH_i shifts, but instead acts to minimize them. Buffering offers only a short term and partial solution to acid-loading, but when combined with acid extrusion, cells are better able to maintain constant pH_i levels.

Overview:

Tissue pH in the central nervous system can modulate, or be modulated by, many physiological and pathological processes. It is becoming increasingly apparent that many of these processes may have specific effects on pH_i . Changes in pH_o and the application of neurotransmitters or neuromodulators can influence pH_i . In turn, fluctuations in pH_i can regulate ionic conductances in excitable cells, alter cellular metabolism, and modulate seizure activity and neurodegenerative processes. pH_i is, in all cell types so far studied, actively regulated. These regulating mechanisms have been extensively investigated in invertebrate neuronal and vertebrate non-neuronal preparations. As studies on mammalian central neurones are limited, this thesis will examine the regulation of pH_i in pyramidal neurones cultured from embryonic rat hippocampi, a region known to be particularly sensitive to epileptiform activity and ischemic conditions. A ratiometric technique, utilizing the pH sensitive fluorophore BCECF, was employed to determine pH_i regulating mechanisms operating while at rest and during the recovery from an induced acidification.

MATERIALS AND METHODS

Cell preparation:

Neuronal cell cultures were prepared according to Banker and Cowen (1977) with some minor modifications. Hippocampal sections were obtained from 18 day embryonic-age Wistar rat fetuses, and stored in a Ca^{2+} and Mg^{2+} -free balanced salt solution (CMF-BSS). The CMF-BSS contained 10% Hank's balance salt solution, 55.5 mM glucose, 10.05 mM 4-(2-hydroxyethyl)-1-piperazineethanesulfonic acid (HEPES), 4.95 mM HEPES Na^+ -salt, and 2 mM NaHCO_3 . The hippocampi were subsequently transferred into 6 mL of an enzymatic solution containing aliquots of trypsin and DNase dissolved in CMF-BSS, for 20 minutes at 37°C. The enzyme-based dissociation was followed by a trituration procedure in which tissue was suspended in a test tube containing DNase, CMF-BSS, and 10% foetal bovine serum (FBS), and was mechanically siphoned 20 times through fire polished pasteur pipettes of decreasing tip diameter. The triturated mixture was then diluted with an additional 1 mL of 10% FBS, and cold centrifuged at 150 g for 4 to 5 minutes. The supernatant was removed and the resulting cell pellet was re-suspended in 6 mL of Dulbecco's Modified Eagle's Medium (D-MEM) containing 10% FBS (D-MEM/FBS). All D-MEM solutions were buffered by 22 mM NaHCO_3 , 10 mM HEPES, and 5% CO_2 in air.

A 50 μL sample of the cell suspension was removed from the D-MEM suspension and mixed into 410 μL CMF-BSS and 40 μL trypan blue. The living pyramidal cells were then counted on a hemocytometer (Neubauer) chamber. In order to compute the percent dilution to be applied to the total cell suspension, this sampling count was multiplied by a factor of 0.01. This dilution constant accounted for the number of chambers on the hemocytometer, the size of the coverslips, and the final density (10^5 cells/cm²) at which the coverslips were to be plated. The cell-containing medium was subsequently diluted with D-MEM/FBS by the factor determined in the sample count

calculation. Coverslips, previously coated with poly-D-lysine and laminin for cell adhesion and growth, were then plated with 0.2 mL of the diluted culture medium. After 1 hour, the coverslips were transferred face down into 6-well culture plates containing 2 mL of D-MEM/FBS in each well, and stored in a 5% CO₂ in air environment at 35°C. The cells were cultured in a face-down position due to the high rate of mortality associated with face-up growth (see Brewer and Cotman, 1989). After 3 to 4 hours of incubation, half of the culture medium was replaced by 1 mL of serum-free D-MEM containing 5 mg/L transferrin, 6.2 µg/L progesterone, 8.8 mg/L putrescine, 5.19 µg/L selenium, and 5 mg/L insulin. This D-MEM/FBS replacement procedure was repeated seven days after the initial culture date. The presence of non-neuronal cells was checked following 2 to 3 days of storage, and the cultures were treated with 5-fluorodeoxyuridine to arrest glial multiplication. Experiments were performed at both room temperature and 37°C using 6 to 14 day old cultures.

Loading the neurones with BCECF:

BCECF acetoxymethyl ester (BCECF-AM), the cell-permeant form of the fluorescent hydrogen ion indicator BCECF (Rink *et al*, 1982), was obtained from Molecular Probes Inc. (Eugene, Oregon). The fluorescent probe was prepared in advance as a 1.0 mM stock in anhydrous DMSO, separated into 60 µL aliquots, and stored at -60°C. Loading medium, made up on the day of the experiment, contained the same elements as *solution 1* (Table 1) with the isoosmotic addition of 3.0 mM NaHCO₃ in place of NaCl. 5 µL of the 1.0 mM BCECF-AM stock was thawed and diluted to 2 µM in 2.5 mL of the loading medium contained in a single well of a 6-well tissue culture plate. An 18 mm coverslip, plated with the hippocampal neurones, was placed face-up in the dye-containing medium for 30 minutes at room temperature. The coverslip was then mounted in a temperature-controlled perfusion chamber so as to form the base of the chamber. The neurones were perfused at a rate of 2.4 mL/minute for 15 minutes with the

initial experimental buffer at the appropriate temperature prior to the start of an experiment. The polyethylene perfusion line was contained within an aluminum block that was heated when necessary to raise the perfusate temperature to 37°C. During perfusion with $\text{HCO}_3^-/\text{CO}_2$ -buffered solutions, the atmosphere in the recording chamber consisted of 5% CO_2 in balance air.

Experimental setup:

pH values were measured utilizing the dual-excitation fluorescence ratio method, employing an Attofluor Digital Fluorescence System (Atto Instruments Inc.) operating in conjunction with a Zeiss Axiovert 10 microscope (Carl Zeiss Canada Ltd.). BCECF was used as a dual-excitation indicator, with the ratio of the emitted fluorescence intensities from excitations at 488 nm and 460 nm providing the pH determination. Exciting the dye at 488 nm, the emitted fluorescence, measured at 510 nm, was pH sensitive. The dye was subsequently excited at 460 nm, a wavelength in close proximity to the indicator's isoexcitation point, and thus at this wavelength the emitted fluorescence was nearly completely insensitive to pH. The ratiometric method has been shown to substantially reduce signal errors caused by variations in optical path length, dye concentration, dye leakage, and photobleaching (Bright *et al*, 1989). The limits and potential artifacts of fluorescence ratio imaging microscopy have been discussed by Bright *et al* (1987) and Silver *et al* (1992).

The source of the excitation photons was a 100 W mercury arc burner whose light path was interrupted by a computer actuated high speed shutter. The shutter served to restrict the illumination of the BCECF to periods of data acquisition (usually once every 10 to 60 seconds) in order to minimize any photo-induced damage to the dye or cells. Such degradation was also reduced by placing variable neutral density filters in the light path. 488 and 460 nm short band-pass filters were mounted on a computer-controlled filter changer which, during excitation, sequentially interrupted the light path. The

excitation radiation was reflected by a long band-pass dichroic mirror (FT-495) and was focused through a x40 Neofluar objective (numerical aperture 0.75) onto the cells in the recording chamber. The emitted fluorescent light passed back through the dichroic beam splitter before being filtered by a 510 nm long-pass filter, the wavelength at which the emission was monitored.

Fluorescence emissions were measured by an intensified charge-coupled device camera mounted onto the microscope. The camera gain was set by maximizing the image intensity while minimizing the possibility of camera saturation, and was held constant throughout an experiment. Images were digitized to 8 bit resolution with a 512×480 pixel frame size. During acquisition, a single image was captured for each of the two excitation wavelengths. A video terminal sequentially displayed each pseudocoloured image, which were used not only to visually monitor the progress of the study, but to also select areas for analysis. These selected regions of interest (ROI's), 10 pixels by 10 pixels in size, were set at the start of the experiment over multiple (maximum 99) neuronal somata having an approximate pyramidal shape: one defined long process, and two or more shorter processes. To aid in the rough focusing of the neurones and the selection of the ROI's, the cell population was visualized under phase illumination using a 12 V, 100 W halogen lamp. Throughout the course of an experiment, the computer calculated and graphically displayed the emission intensities for both excitation wavelengths, and the ratio of the emitted fluorescence for all, or a chosen single, region(s) of interest. In all cases, the recorded values reflected the mean emitted intensity within each ROI, computed in real time.

Solutions:

The solutions utilized during the course of these experiments are listed in Tables 1 to 4. A Corning 240 pH meter, calibrated daily, was employed to measure all pHs. Those solutions lacking bicarbonate (Table 1) were buffered by 10 mM HEPES and then

titrated to the appropriate pH with 10 M NaOH, except when noted. The Na⁺-free saline (*solution 2*) was prepared by equimolar substitution of all Na⁺ salts found in the standard medium (*solution 1*) with *N*-methyl-D-glucamine (NMDG⁺), which then required the use of 10 M HCl to lower the pH to the 7.4 range. Cl⁻ was removed through the use of sodium, potassium, and hemi-calcium gluconate in place of NaCl, KCl, and CaCl₂, respectively (*solution 3*). The addition NH₄Cl (*solution 4*) to the HEPES buffered saline was achieved through equimolar replacement of NaCl. Calibration solutions were prepared using the ionophore nigericin, a cation-hydrogen exchanger that is highly selective for K⁺ (Chaillet and Boron, 1985). Nigericin was prepared as a 10 mM stock solution in ethanol, divided into 100 μ L volumes, and then stored at -60°C. When needed, a 10 mM aliquot was diluted to 10 μ M in a solution containing a concentration of K⁺ near intracellular levels (*solution 5*). Nigericin-containing solutions were titrated to appropriate pHs with 10 M KOH, with the exception of the pH 5.5 solution employed during full calibrations (see below) that required 1 M HCl.

Regardless of the temperature at which a given experiment was being performed, all HEPES buffered media were prepared at room temperature (18°C to 22°C). In order to account for the pH fluctuation associated with raising the solution temperature, the pH at room temperature (pH_{RT}) was adjusted to reflect the ensuing temperature-induced pH change, such that at 37°C the desired pH would be reached (pH₃₇). The different pHs for HCO₃⁻/CO₂-free, HEPES-buffered solutions at room temperature and 37°C were related by the equation:

$$\text{pH}_{37} = 0.18 + 0.96 \times \text{pH}_{\text{RT}} \quad (\text{Equation 6})$$

This equation was determined during preliminary experiments (n=8) in which the pHs of HEPES buffered solutions, prepared at 22°C, were compared to the resulting pH when heated to 37°C.

The composition of solutions buffered by a combination of HCO₃⁻ and CO₂ at room temperature are summarized in Table 2. All HCO₃⁻-containing solutions, at room

temperature and 37°C, were equilibrated with 5% CO₂ in balance air. For experiments at room temperature, the standard HCO₃⁻/CO₂-buffered medium contained 26.0 mM NaHCO₃ (*solution 6*), resulting in a pH of 7.32 ± 0.01 (mean \pm standard error of the mean, n=19). The preparation of Na⁺-free saline was accomplished by replacing NaCl and NaHCO₃ with choline chloride and choline bicarbonate, respectively (*solution 7*). Solutions lacking Cl⁻ were produced by substituting gluconate in place of Cl⁻ (*solution 8*). Propionate (*solution 9*), trimethylamine (*solution 10*) and NH₄Cl (*solution 11*) were added by equimolar substitution of NaCl; when equilibrated with 5% CO₂, these mixtures resulted in pHs of 7.30 (n=1), 7.31 (n=1), and 7.32 (n=2), respectively.

At 37°C, the concentration of bicarbonate in the standard medium was reduced to 20.0 mM (*solution 12*, Table 3), yielding a pH of 7.36 ± 0.01 (mean \pm S.E.M., n=19). Na⁺-free (*solution 13*; pH₀ 7.38 ± 0.01 , n=4), Cl⁻-free (*solution 14*; pH₀ 7.38 ± 0.01 , n=7), and NH₄Cl-containing (*solution 16*; pH₀ 7.35 ± 0.01 , n=7) solutions were prepared in an similar fashion to their room temperature counterparts. A mixture lacking both Na⁺ and Cl⁻ was formed using free choline base, choline bicarbonate, free gluconic acid, potassium and hemi-calcium gluconate, and normal concentrations of MgSO₄ and D-glucose (*solution 15*; pH₀ 7.38, n=1).

In order to vary the pH of a solution buffered by HCO₃⁻/CO₂, it was necessary to adjust the concentration of NaHCO₃ via isoosmotic substitution with NaCl (Table 4). Preliminary experiments established that, at 37°C, the solution pH was related to its bicarbonate concentration (in mM) by the equation:

$$\text{pH} = 6.03 + 1.03 \times \log[\text{HCO}_3^-] \quad (\text{Equation 7})$$

This formula was derived from a series of pH versus concentration of HCO₃⁻ data points that are shown in Figure 1, and was employed to create *solutions 17, 18, 20, 21, and 22* (Table 4). The NH₄Cl-containing solution at pH 6.8 was isoosmotically balanced by substitution of NaCl with 20 mM NH₄Cl (*solution 19*). The pHs of all solutions were re-measured at the appropriate temperature following each experiment.

Ethylisopropylamiloride (EIPA) was prepared as a 50 mM stock solution in dimethylsulphoxide (DMSO) prior to a 1 in 1000 dilution in the perfusion solution. 4,4'-diisothiocyanatostilbene-2,2'-disulphonic acid (DIDS) was dissolved in DMSO at a concentration of 100 mM, and used at a final concentration of 200 μ M. All stock solutions were prepared on the day of the experiment, and the final concentration of DMSO in the perfusion solution never exceeded 0.5%. Control experiments demonstrated that, at this concentration, DMSO had no effect on pH_i (data not shown). Compounds were purchased from Sigma Chemical Company (St. Louis, Missouri), with the exception of 3-methylsulfonyl-4-piperidinobenzoyl guanidine hydrochloride (HOE 694), and 5-(*N*-methyl-*N*-guanidinocarbonylmethyl) amiloride (MGCMA). HOE 694 was obtained from Hoechst A.G. (Frankfurt, Germany), while MGCMA was a generous gift from Dr. V. Palatý (Department of Anatomy, University of British Columbia); both chemicals were prepared as 100 mM stock solutions in DMSO, and utilized at a final concentration of 100 μ M.

Calculation of pH_i :

Experimental results were stored in computer-generated data files containing pixel intensities for each region of interest. During acquisition periods the following information was stored: the intensity of the fluorescent signal after excitation at 488 nm, the 460 nm-induced fluorescent signal, and a ratio (I_{488}/I_{460}) of the fluorescence intensities. Utilizing a stand-alone DOS based graphing program (ATTOGRAF, Atto Instruments Inc, version 5.41), regions of interest corresponding to neurones that remained viable throughout an experiment were selected for analysis. Viability was judged by the capacity of the neurones to retain the fluorescent indicator (as judged by raw intensity values) throughout the entire course of the experiment (see Schwiening and Boron, 1992; Schwiening and Boron, 1994).

The determination of pH_i was initiated by the subtraction of background fluorescence intensities from the raw intensity values in each selected ROI. Background levels were determined by measuring the fluorescence signal in a region devoid of cellular processes at each excitation wavelength. Transformation of the background-corrected ratios into pH_i values utilized conversion equations derived from *in situ* calibration experiments (Figure 2). In such experiments, the neurones were exposed to variety of HEPES-buffered solutions at room temperature having differing pHs (Figure 2A). All calibration solutions contained 10 μM of the ionophore nigericin, which was added to a solution containing high concentrations of K^+ (solution 5, Table 1). Each solution was titrated to a different pH in the 5.5 to 8.5 range using 10 M KOH or 1 M HCl. Nigericin is a charged electron carrier that acts to balance pH_i and pH_o if the intracellular and extracellular K^+ activities are equal (Chaillet and Boron, 1985). Thus, in the presence of high extracellular K^+ concentrations, pH_i was controlled merely by the pH of the superfusing medium.

The resulting intensity ratios produced by exposing the neurones to various pH solutions containing 10 μM nigericin were used to construct a calibration curve. Following subtraction of background fluorescence values from the 488 and 460 nm-induced fluorescence signals, the ratios (I_{488}/I_{460}) were normalized such that the ensuing curve passed through unity at pH 7.0 (Figure 2B.). A full calibration experiment resulted in the determination of parameters fitting a standard curve which could then be used to transform other normalized ratios into pH_i values. The derivation of the equation fitting this standard curve stems from the Henderson-Hasselbalch expression for the dissociation of a weak acid:

$$\text{pH} = \text{pK}_a + \log \frac{[\text{A}^-]}{[\text{HA}]} \quad (\text{Equation 8})$$

where $[A^-]$ is the concentration of the ionized form of the acid, $[HA]$ is the neutral form of the acid, and K_a is the acid dissociation constant. Taking into consideration the total acid concentration, denoted by $[Total]$, as equaling the sum of the ionized $[A^-]$ and non-ionized $[HA]$ forms of the acid, the above equation becomes:

$$pH = pK + \log \frac{[A^-]}{[Total] - [A^-]} \quad (\text{Equation 9})$$

For BCECF, the concentration of the ionized form is proportional to the ratio ("R") of the fluorescence intensities at 488 nm and 460 nm. Thus the total acid concentration is proportional to the maximal obtainable ratio ("b"). Substituting these variables into Equation 9 yields:

$$pH = pK_a + \log \frac{R}{b - R}, \quad \text{or} \quad R = b \cdot \frac{10^{(pH - pK_a)}}{1 + 10^{(pH - pK_a)}} \quad (\text{Equation 10})$$

If R is constrained to pass through unity at pH 7.0, then the value of R at pH 7.0 must be subtracted from the Equation 10, followed by the addition of 1. This normalized R term, now denoted R_n , can be expressed as:

$$R_n = b \cdot \frac{10^{(pH - pK_a)}}{1 + 10^{(pH - pK_a)}} - b \cdot \frac{10^{(7 - pK_a)}}{1 + 10^{(7 - pK_a)}} + 1 \quad (\text{Equation 11})$$

The fitted values for b and pK_a varied with the setup of the microscope. For this reason, any changes to the experimental equipment (for example, the replacement of the mercury arc burner) was accompanied by the execution of a full calibration experiment, and revised calibration parameters were determined. Equation 11 was simplified by determining the theoretical maximum and minimum obtainable values for the normalized ratio. These values, symbolized by $R_{n(\max)}$ and $R_{n(\min)}$, can be represented as:

$$R_{n(\max)} = 1 + b - b \cdot \frac{10^{(7 - pK_a)}}{1 + 10^{(7 - pK_a)}} \quad (\text{Equation 12})$$

and

$$R_{n(\min)} = 1 - b \cdot \frac{10^{(7-pK_a)}}{1 + 10^{(7-pK_a)}} \quad (\text{Equation 13})$$

Using the determined values for b and pK_a , the maximum and minimum normalized ratios were calculated.

In order to create an equation which converts normalized ratios into pH values, it is necessary to express the regression equation as a function of pH. Manipulation of Equation 11 yields:

$$10^{(pH-pK_a)} = \frac{R_n - \left[1 - b \cdot \frac{10^{(7-pK_a)}}{1 + 10^{(7-pK_a)}} \right]}{\left[1 + b - b \cdot \frac{10^{(7-pK_a)}}{1 + 10^{(7-pK_a)}} \right] - R_n} \quad (\text{Equation 14})$$

Substituting $R_{n(\max)}$ and $R_{n(\min)}$ into Equation 14 gives rise to:

$$10^{(pH-pK_a)} = (R_n - R_{n(\min)}) / (R_{n(\max)} - R_n) \quad (\text{Equation 15})$$

Isolating the pH term utilizing a logarithmic manipulation produces the following equation:

$$pH = \log[(R_n - R_{n(\min)}) / (R_{n(\max)} - R_n)] + pK_a \quad (\text{Equation 16})$$

Equation 16 was then utilized in the conversion of all normalized ratios into pH values, using the predetermined parameters for $R_{n(\min)}$, $R_{n(\max)}$, and pK_a . These factors were calculated for each full calibration experiment. For the seven full calibration experiments utilized in analyzing all experiments, the mean values of pK_a , $R_{n(\min)}$, and $R_{n(\max)}$ were 6.98 ± 0.02 , 0.49 ± 0.02 , and 1.49 ± 0.02 , respectively. Furthermore, the values of these calculated parameters did not appear to be dependent on changes in the experimental temperature, which typically varied between 20°C and 30°C. For example, in a calibration performed at 30°C, the determined pK_a value was 6.98, whereas in a separate study at 21°C, pK_a was found to be 6.97.

Most experiments were concluded by exposing the neurones to a single pH 7.0 nigericin-containing solution (see Figures 4, 7, and 12). The resulting (background-corrected) ratio at pH_i 7.0 was used as the normalization factor for that particular

experiment. As outlined by Boyarski *et al* (1988), the advantage of this normalization step is that it provides a one-point calibration for each cell population studied. After dividing all experimentally-derived (background-corrected) intensity ratios by the determined normalization value, each R_n was converted to pH_i utilizing Equation 16 and the appropriate fitted calibration parameters.

Analysis of data:

Each experiment typically required the analysis of 10 or more regions of interest, and thus it became necessary to automate the conversion of I_{488}/I_{460} into pH_i employing either a DOS-based transformation program (courtesy of Dr. K. Abdel-Hamid, Department of Physiology, University of British Columbia) or personally designed Visual Basic macros running in Microsoft Excel 5.0. Absolute pH_i levels are reported for neurones under steady-state conditions in the presence and absence of HCO_3^- , at both room temperature and 37°C. At steady-state, any perturbations in pH_i were measured relative to the resting pH_i before the change.

In experiments designed to analyze the restoration of pH_i back to steady-state levels after an imposed acid load, the recovery portion of the experiment was fitted to a single exponential function having a format:

$$pH_i = a + b(1 - 10^{(-ct)}) \quad (\text{Equation 17})$$

where a , b , and c are the exponential parameters. The differentiated form of Equation 17 represents the change in pH_i as a function of time, and was used to analyze the recovery rate (dpH_i/dt) at any point during the restoration to steady-state pH_i levels:

$$\frac{dpH_i}{dt} = -bc10^{(-ct)} \quad (\text{Equation 18})$$

Recovery rates were determined immediately after the peak acidification, and at 50% and 80% recovery relative to the steady-state pH_i before the induced acid load.

Statistical comparisons were carried out using Student's t test with a 95% confidence limit. If a preconceived directionality existed in making a comparison, a one-tailed test was used, otherwise the two-tailed version was utilized. In all cases, unpaired t values were calculated, with supplemental paired data added when appropriate. Any indicated errors are expressed as the standard error of the mean (S.E.M.), with the accompanying n value referring to the number of cell populations (i.e. number of coverslips) analyzed.

Periodically, variations in the emission intensities arose which were caused by brief fluctuations in the incident radiation (see Boyarski *et al*, 1988a). In order to smooth the resulting graphical representation of the pH_i versus time record, a moving average (period = 3) was applied to all plots (Boyarski *et al*, 1988a).

Table 1: Composition of HEPES-buffered experimental solutions
(all concentrations in mM):

	Solution				
	1 Standard	2 Na ⁺ free	3 Cl ⁻ free	4 NH ₄ Cl	5 High K ⁺
NaCl	136.5	-	-	116.5	-
KCl	3.0	3.0	-	3.0	-
CaCl ₂	2.0	2.0	-	2.0	2.0
NaH ₂ PO ₄	1.5	-	1.5	1.5	1.5
MgSO ₄	1.5	1.5	1.5	1.5	1.5
Na Glu	-	-	136.5	-	10.0
K Glu	-	-	3.0	-	130.5
½Ca Glu	-	-	4.0	-	-
D-glucose	10.0	10.0	10.0	10.0	10.0
NMDG ⁺	-	136.5	-	-	-
NH ₄ Cl	-	-	-	20.0	-
HEPES	10.0	10.0	10.0	10.0	10.0
Titrated	10 M	10 M	10 M	10 M	10 M
with:	NaOH	HCl	NaOH	NaOH	KOH

Abbreviations: Na Glu, sodium gluconate; K Glu, potassium gluconate; ½Ca Glu, hemi-calcium gluconate; NMDG⁺, *N*-methyl-D-glucamine.

Table 2: Composition of $\text{HCO}_3^-/\text{CO}_2$ -buffered experimental solutions at room temperature (all concentrations in mM):

	Solution					
	6 Standard	7 Na ⁺ free	8 Cl ⁻ free	9 PROP	10 TMA	11 NH ₄ Cl
NaCl	120.5	-	-	100.5	110.5	100.5
NaHCO ₃	26.0	-	26.0	26.0	26.0	26.0
KCl	3.0	3.0	-	3.0	3.0	3.0
CaCl ₂	2.0	2.0	-	2.0	2.0	2.0
NaH ₂ PO ₄	1.5	-	1.5	1.5	1.5	1.5
MgSO ₄	1.5	1.5	1.5	1.5	1.5	1.5
D-glucose	10.0	10.0	10.0	10.0	10.0	10.0
NH ₄ Cl	-	-	-	-	-	20.0
Na Glu	-	-	120.5	-	-	-
K Glu	-	-	3.0	-	-	-
½Ca Glu	-	-	4.0	-	-	-
Choline HCO ₃	-	26.0	-	-	-	-
Choline Cl	-	120.5	-	-	-	-
PROP	-	-	-	20.0	-	-
TMA	-	-	-	-	10.0	-
final pH	7.32 ± 0.01 (n=14)	7.35 (n=1)	7.33 ± 0.01 (n=2)	7.30 (n=1)	7.31 (n=1)	7.32 (n=2)

All HCO_3^- -containing solutions were equilibrated with 5% CO_2 in balance air. pHs are reported as the mean ± S.E.M. Abbreviations: Na Glu, sodium gluconate; K Glu, potassium gluconate; ½Ca Glu, hemi-calcium gluconate; PROP, propionate; TMA, trimethylamine.

Table 3: Composition of $\text{HCO}_3^-/\text{CO}_2$ -buffered experimental solutions at 37°C
(all concentrations in mM):

	Solution				
	12 Standard	13 Na^+ free	14 Cl^- free	15 Na^+ and Cl^- free	16 NH_4Cl
NaCl	126.5	-	-	-	106.5
NaHCO_3	20.0	-	20.0	-	20.0
KCl	3.0	3.0	-	-	3.0
CaCl_2	2.0	2.0	-	-	2.0
NaH_2PO_4	1.5	-	1.5	-	1.5
MgSO_4	1.5	1.5	1.5	1.5	1.5
D-glucose	10.0	10.0	10.0	10.0	10.0
NH_4Cl	-	-	-	-	20.0
Na Glu	-	-	126.5	-	-
K Glu	-	-	3.0	3.0	-
$\frac{1}{2}\text{Ca Glu}$	-	-	4.0	4.0	-
Gluconic acid	-	-	-	126.5	-
Choline HCO_3	-	20.0	-	20.0	-
Choline Cl	-	126.5	-	-	-
Choline base	-	-	-	126.5	-
final pH	7.36 ± 0.01 (n=19)	7.38 ± 0.01 (n=4)	7.38 ± 0.01 (n=7)	7.38 (n=1)	7.35 ± 0.01 (n=7)

All HCO_3^- -containing solutions were equilibrated with 5% CO_2 in balanced air. Reported pHs are given as the mean \pm S.E.M. Abbreviations: Na Glu, sodium gluconate; K Glu, potassium gluconate; $\frac{1}{2}\text{Ca Glu}$, hemi-calcium gluconate.

Table 4: Composition of $\text{HCO}_3^-/\text{CO}_2$ -buffered experimental solutions at varying pHs at 37°C
(all concentrations in mM):

	Solution					
	17 pH 6.5 standard	18 pH 6.8 standard	19 pH 6.8 NH_4Cl	20 pH 7.0 standard	21 pH 7.8 standard	22 pH 8.0 standard
NaCl	143.5	140.7	120.7	137.5	101.5	61.5
NaHCO_3	3.0	5.8	5.8	9.0	45.0	85.0
KCl	3.0	3.0	3.0	3.0	3.0	3.0
CaCl_2	2.0	2.0	2.0	2.0	2.0	2.0
NaH_2PO_4	1.5	1.5	1.5	1.5	1.5	1.5
MgSO_4	1.5	1.5	1.5	1.5	1.5	1.5
D-glucose	10.0	10.0	10.0	10.0	10.0	10.0
NH_4Cl	-	-	20.0	-	-	-
final pH	6.56 (n=2)	6.79 ± 0.01 (n=3)	6.80 (n=1)	7.00 ± 0.01 (n=3)	7.75 (n=2)	8.02 (n=2)

All HCO_3^- -containing solutions were equilibrated with 5% CO_2 in balanced air. pH's are indicated as the mean ± S.E.M.

Figure 1. Relationship between the concentration of HCO_3^- and the resulting solution pH when equilibrated with 5% CO_2 in balance air at 37°C.

Following equilibration with 5% CO_2 , the pHs of solutions were measured at 37°C containing 3.0 mM, 5.8 mM, 9.0 mM, 20.0 mM, 45.0 mM, and 85.0 mM HCO_3^- (see Table 4 for solution recipes). Data was derived from a single experiment. The curve was formed from a logarithmic growth least squares regression fit to the data points having the equation:

$$\text{pH} = 6.03 + 1.03 \times \log[\text{HCO}_3^-]$$

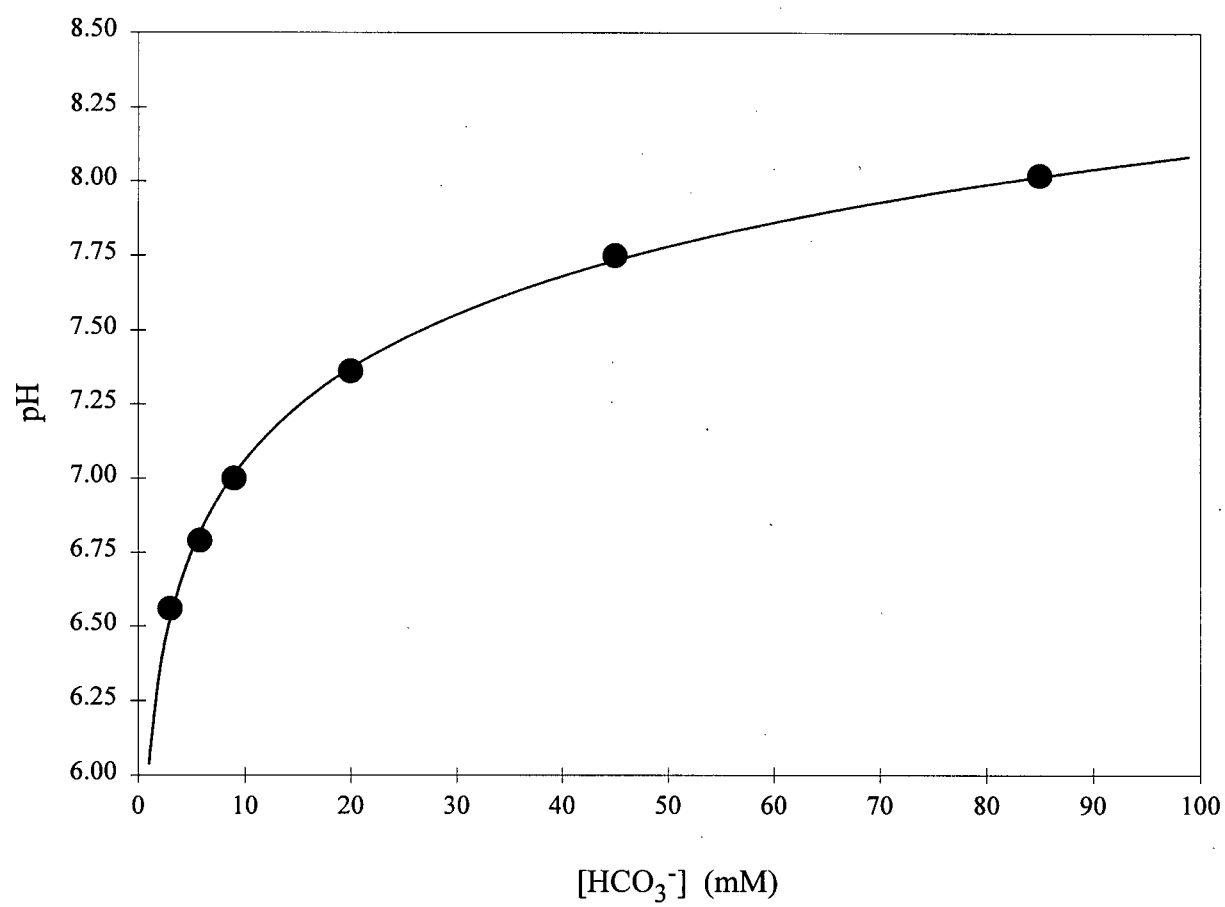
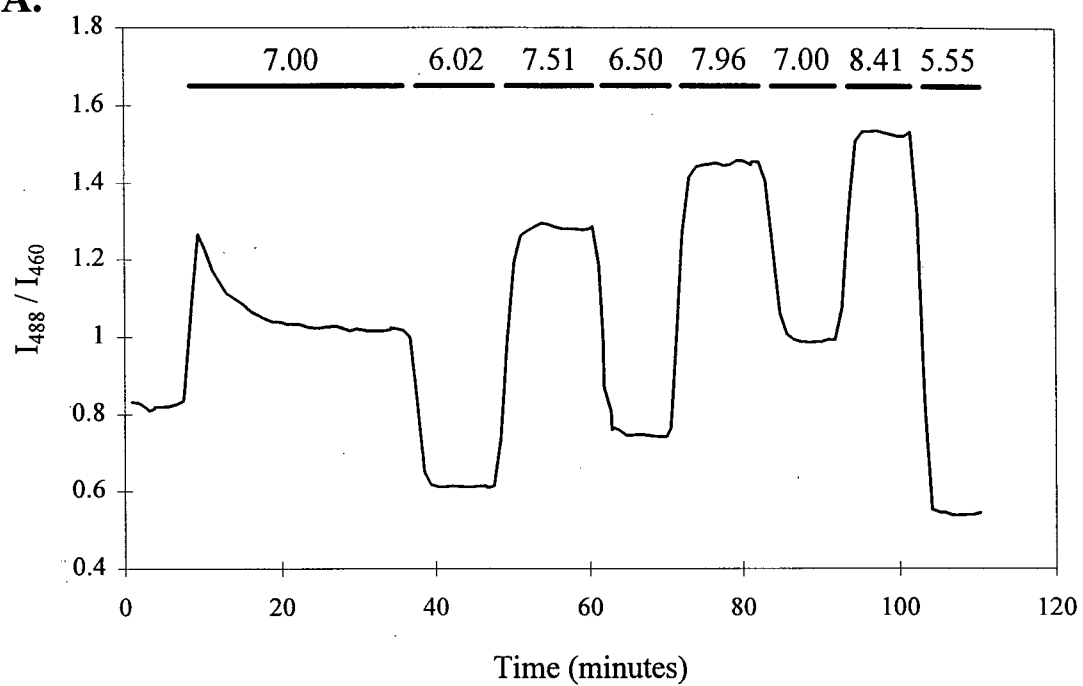
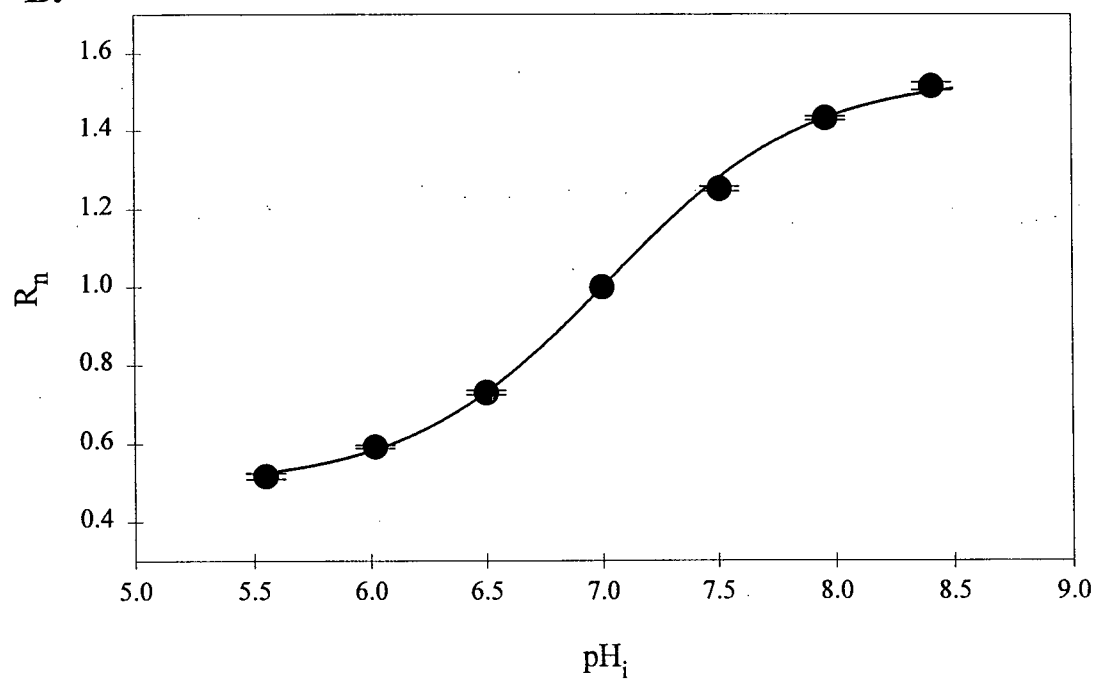


Figure 2. Sample calibration plot for BCECF.

A. Cells were exposed to HEPES-buffered solutions (*solution 5*, Table 1) containing 10 μ M nigericin at pH_o (and therefore pH_i) 5.55, 6.02, 6.50, 7.00, 7.51, 7.96, and 8.41. The duration of each exposure is indicated by the bars above the trace, which is a mean of data obtained from 29 cells recorded on a single coverslip. The resulting background subtracted ratios (I_{488}/I_{460}) were normalized to 1.00 at pH_i 7.00. **B.** Plot of pH_i against the resulting normalized ratio (R_n). Standard error bars are indicated ($n=3$ coverslips). The curve is a result of a non-linear least squares regression fit to Equation 16. For this particular calibration, the values of R_{max} , R_{min} , and pK_a were 1.542, 0.491, and 7.027, respectively.

A.**B.**

RESULTS

STEADY-STATE pH_i REGULATION

Regulation of pH_i at room temperature:

In HCO_3^- -free HEPES buffered medium at pH_o 7.32 (*solution 1*, Table 1), steady-state pH_i rested at 6.85 ± 0.04 ($n=25$) as shown in Table 5 and Figure 3A. At the same pH_o but in the presence of HCO_3^- , (*solution 6*, Table 2) the baseline pH_i resided at the substantially higher level of 7.15 ± 0.03 ($n=22$; Table 5; Figure 3B). This suggests a substantial contribution of HCO_3^- -dependent mechanisms to the maintenance of steady-state pH_i at room temperature. The equimolar replacement of constituent ions in the perfusion medium, or application of pharmacological agents, provided insight into this HCO_3^- -dependent mechanism (see Table 5). In the presence of HCO_3^- , the removal of extracellular Cl^- ($[Cl^-]_o$) (*solution 8*, Table 2) resulted in a reversible pH_i increase of 0.28 ± 0.04 pH units ($n=2$; Figure 4). As depicted in Figure 5, the application of 200 μM DIDS, an inhibitor of HCO_3^-/Cl^- exchange, reduced pH_i by 0.08 ± 0.04 pH units ($n=3$). Figure 5 also demonstrates that pH_i immediately returned to normal resting levels when DIDS was washed from the extracellular medium. According to these results, it would appear that Cl^- and HCO_3^- -dependent mechanisms may play a role regulating steady-state pH_i at room temperature.

To further investigate the role of HCO_3^- in maintaining steady-state pH_i at room temperature, the next series of experiments explored the modulation of pH_i during the transition from HCO_3^- -free (*solution 1*, Table 1) into HCO_3^- -containing (*solution 6*, Table 2) perfusion media at a constant pH_o . As shown in Figure 6A, such a manoeuvre was marked by an initial acidification due to the influx of CO_2 and its subsequent hydration to carbonic acid. This brief fall in pH_i was followed by a sustained alkalization, presumably due to the activation of HCO_3^- -dependent acid extrusion

mechanisms. This result is reflected in the more alkaline resting pH_i observed in experiments performed in the presence of HCO_3^- as compared with experiments conducted in the absence of HCO_3^- at room temperature (see Table 5; Figures 3A and B). As shown in Figure 6B, the tendency of pH_i to shift towards a more alkaline value during perfusion with HCO_3^- -containing medium was inhibited by 200 μM DIDS. On return to HCO_3^- - and DIDS-free medium, there was a transient increase in pH_i due to the efflux of CO_2 , after which pH_i fell to the normal resting levels observed under HEPES-buffered perfusion conditions. These results suggest the contribution of some form of $\text{HCO}_3^-/\text{Cl}^-$ exchange to the maintenance of steady-state pH_i at room temperature. A detailed analysis of Na^+ -dependent acid extrusion mechanisms was carried out at 37°C (see below). However, at room temperature and in the absence of HCO_3^- , the removal of extracellular Na^+ (*solution 2*, Table 1) resulted in an immediate intracellular acidification (see Figure 17), which indicates that a Na^+ -dependent, HCO_3^- -independent acid extruder contributes to the preservation of a stable resting pH_i .

Regulation of steady state pH_i at 37°C :

In nominally HCO_3^- -free HEPES buffered medium at 37°C (*solution 1*, Table 1; pH_o 7.34), steady-state pH_i was maintained at 7.23 ± 0.03 ($n=29$; see Figure 3C). At this temperature, changes to the ionic composition of the perfusing medium had a moderate influence on steady-state pH_i . These results are summarized Table 5. As shown in Figure 7, the removal of extracellular Na^+ ($[\text{Na}^+]_o$) from the HEPES-buffered medium (*solution 2*, Table 2) caused a 0.53 ± 0.05 pH unit fall in pH_i ($n=5$); the re-introduction of $[\text{Na}^+]_o$ caused a return of pH_i to steady-state levels. This result suggests the presence of Na^+ -dependent acid extrusion mechanisms which are operational under steady-state conditions. However, the removal of $[\text{Cl}^-]_o$ (*solution 3*, Table 3) did not significantly change the steady state pH_i ($n=3$; Figure 8), suggesting the absence of Cl^- -dependent pH_i regulating mechanisms operating under HCO_3^- -free conditions at 37°C .

Figure 9 shows that the application of 50 μM EIPA, a pharmacological inhibitor of Na^+/H^+ exchange in a wide variety of cell types (Clark and Limbird, 1991), did not alter the resting pH_i ($n=3$). Similarly, the application of EIPA after 5 minutes of $[\text{Na}^+]_o$ -free perfusion did not influence the acidification caused by $[\text{Na}^+]_o$ removal ($n=3$; Figure 10). Figure 10 also demonstrates that pH_i rebounded back to its steady-state value after $[\text{Na}^+]_o$ was returned to the perfusion solution, despite the continued presence of EIPA. MGCMA, another amiloride analogue (Amoroso *et al*, 1991), and HOE 694, a novel inhibitor of Na^+/H^+ exchange (Schmid *et al*, 1992; Wöll *et al*, 1993), were both applied at 100 μM but were also found to have no effect on steady-state pH_i at 37°C ($n=3$ for each compound; Figure 11). It therefore appears that the Na^+ -dependent acid extrusion mechanism present on these neurones is not sensitive to inhibition by known blockers of Na^+/H^+ exchange.

In HCO_3^- -containing perfusion medium at pH_o 7.36 (*solution 12*, Table 3), the steady-state pH_i was 7.13 ± 0.01 ($n=44$; Figure 3D), a value lower than in HCO_3^- -free, HEPES-buffered medium at the same temperature. Removing $[\text{Na}^+]_o$ from the perfusing solution under $\text{HCO}_3^-/\text{CO}_2$ buffering conditions (*solution 13*, Table 3) caused a 0.65 ± 0.04 pH unit fall in pH_i ($n=8$; Table 5). As shown in Figure 12, pH_i fell rapidly on exposure to $[\text{Na}^+]_o$ -free medium, reached a minimum in less than 10 minutes, and immediately returned to steady-state levels upon the re-introduction of $[\text{Na}^+]_o$. This result indicates the dominance of Na^+ -dependent acid extruders regulating steady-state pH_i at 37°C , possibly a Na^+/H^+ exchanger. However, application of 50 μM EIPA over a 10 minute period did not alter resting pH_i ($n=3$; Figure 13), which prevents a more precise description of this acid extrusion mechanism, other than its dependence on Na^+ and capacity to operate in the presence or absence of HCO_3^- . These results are consistent with previous observations showing the inability of 50 μM EIPA to influence steady-state pH_i in the absence of HCO_3^- at 37°C (see Figures 9 and 10).

As steady state pH_i at room temperature appeared to be dependent on $\text{HCO}_3^-/\text{Cl}^-$ exchange, further studies explored the sensitivity of pH_i at 37°C to the removal of constituent ions and the application of blockers of the cation exchanger. Shown in Figure 14A, replacing $[\text{Cl}^-]_o$ with gluconate in the presence of HCO_3^- (*solution 14*, Table 3) caused a gradual pH_i increase of 0.19 ± 0.01 pH units ($n=5$). This 0 $[\text{Cl}^-]_o$ -induced rise in pH_i at 37°C was similar to, though slightly smaller than, the increase in pH_i induced by the same manoeuvre at room temperature (see Figure 4). Upon substitution of $[\text{Cl}^-]_o$ back into the perfusing buffer, pH_i returned to its steady-state level. The introduction of 200 μM DIDS, applied in combination with 0 $[\text{Cl}^-]_o$ perfusion, abolished the 0 $[\text{Cl}^-]_o$ -induced pH_i rise ($n=3$; Figure 14A). Furthermore, the application of DIDS 5 minutes after the removal of $[\text{Cl}^-]_o$ prevented the sustained alkalization associated with the absence of $[\text{Cl}^-]_o$ and resulted in a decline of pH_i back towards steady state levels despite continued perfusion with Cl-free medium ($n=4$; Figure 14B). When $[\text{Cl}^-]_o$ was re-introduced to the perfusion solution in the continued presence of 200 μM DIDS, pH_i continued to fall, overshooting steady-state pH_i levels to rest ~ 0.05 pH units below normal levels. Once the DIDS was removed, pH_i slowly returned to baseline levels. Applied alone, 200 μM DIDS did not significantly alter steady-state pH_i at 37°C (Table 5, and Figure 15). This result differs from that observed in HCO_3^- -containing medium at room temperature in which steady-state pH_i was significantly reduced by 200 μM DIDS ($n=3$; Figure 5). These results suggest that at 37°C , though a DIDS-sensitive $\text{HCO}_3^-/\text{Cl}^-$ exchanger may be present, steady-state pH_i is primarily governed by the activity of the Na^+/H^+ exchanger.

In a manner similar to experiments performed at room temperature, the effects on pH_i caused by the transition from HCO_3^- -free (*solution 1*, Table 1) to HCO_3^- -containing (*solution 12*, Table 3) perfusion media at constant pH_o were investigated at 37°C . Interestingly, the net alkalization that occurred on the transition from a HCO_3^- -free to a HCO_3^- -containing medium at room temperature (see Figure 6A) was not observed at

37°C (n=13; Figure 16). In fact, the steady-state pH_i in $\text{HCO}_3^-/\text{CO}_2$ -buffered medium at this temperature was significantly lower than the observed level under HCO_3^- -free HEPES-buffered conditions (Table 5). In contrast to those experiments performed at room temperature (see Figure 6B), the application 200 μM DIDS at 37°C did not affect the pH_i response to the introduction of HCO_3^- -containing perfusion medium (Figure 16), again indicating the relative unimportance of $\text{HCO}_3^-/\text{Cl}^-$ exchange towards the maintenance of steady-state pH_i at this temperature.

Na^+ -dependent or -independent anion exchange:

By responding to changes in the extracellular concentrations of both HCO_3^- and Cl^- , especially at room temperature, the neurones employed in these experiments indicated their ability to regulate pH_i through anion exchange. To determine whether the suspected $\text{HCO}_3^-/\text{Cl}^-$ exchanger present on these neurones was dependent on extracellular Na^+ , an experiment was performed in the absence of HCO_3^- at room temperature in which $[\text{Na}^+]_o$ was removed initially from the perfusion solution (*solution 2*, Table 1). As illustrated in Figure 17, this caused pH_i to fall, but the subsequent introduction of HCO_3^- (*solution 7*, Table 2) resulted in a slow increase in pH_i despite the continued absence of $[\text{Na}^+]_o$ (n=3). Since pH_i recovered in the presence of HCO_3^- and in the absence $[\text{Na}^+]_o$, this result suggests that Na^+ -independent $\text{HCO}_3^-/\text{Cl}^-$ exchange was being utilized by the neurones to regulate pH_i back to resting levels. Using an alternative approach, extracellular Na^+ was again eliminated but now from $\text{HCO}_3^-/\text{CO}_2$ -buffered medium at 37°C (*solution 13*, Table 3). After letting pH_i fall to a plateau, perfusate devoid of $[\text{Cl}^-]_o$ and $[\text{Na}^+]_o$ (*solution 15*, Table 15) was introduced, which caused a 0.14 ± 0.03 increase in pH_i (n=3; Figure 18). This 0 $[\text{Cl}^-]_o$ -induced intracellular alkalinization in the absence of external Na^+ was similar to, though smaller than, the 0 $[\text{Cl}^-]_o$ -induced alkalinization observed in the corresponding experiment performed in the presence of $[\text{Na}^+]_o$ (see Figure 14A). In the absence of $[\text{Na}^+]_o$, the return of $[\text{Cl}^-]_o$ produced a brief acidification

followed by a gradual pH_i recovery towards steady-state levels. This slow recovery was probably the result of the activation of Na^+ -independent acid extrusion mechanisms. Overall, these results suggest that these neurones are able to regulate pH_i utilizing a Na^+ -independent form of the $\text{HCO}_3^-/\text{Cl}^-$ exchanger.

Modulation of pH_i by shifts in pH_o and the application of weak acids and bases:

The steady-state pH_i of the neurones perfused with media containing HCO_3^- equilibrated with 5% CO_2 in balance air at 37°C was strongly influenced by the pH of the extracellular environment. Increasing pH_o from 7.35 to 7.75 and then 8.02 caused pH_i to reach levels of 7.41 ± 0.01 and 7.54 ± 0.01 , respectively ($n=3$; Figure 19A). Reducing pH_o below 7.35 resulted in a decrease in pH_i below normal resting levels: when pH_o was lowered to 7.02 and 6.56, pH_i stabilized at 6.90 ± 0.07 and 6.53 ± 0.01 , respectively ($n=3$). As shown in Figure 19B, a linear regression analysis of the relationship between pH_o and pH_i yielded the following relationship:

$$\text{pH}_i = 1.990 + 0.699 \times \text{pH}_o \quad (\text{Equation 19})$$

The modulation of pH_o at room temperature in the presence of HCO_3^- had a similar effect on pH_i (data not shown). Under these conditions, the relationship representing the dependence of pH_i on pH_o was:

$$\text{pH}_i = 1.240 + 0.807 \times \text{pH}_o \quad (\text{Equation 20})$$

These results suggest that pH_i is steeply dependent on pH_o and that pH_i is not regulated back to normal steady-state values until pH_o is normalized.

The extracellular application of weak acids or bases at constant pH_o has been shown to alter pH_i (Sharp and Thomas, 1981; Roos and Boron, 1981). Accordingly, propionate and trimethylamine (TMA) were applied to hippocampal neurones at room temperature in $\text{HCO}_3^-/\text{CO}_2$ -buffered medium in order to investigate their ability to modulate pH_i at a constant pH_o . In exposing the neurones to 20 mM propionate (solution 9, Table 2), the undissociated form of the acid readily crossed the cell membrane,

whereas the dissociated form of the acid, due to its negative charge, remained relatively membrane impermeant. Once across the membrane the acid dissociated according to its pK_a to release protons, thus acidifying the cell's interior (Figure 20A). Since the amount of acid entering the cells was minimal when compared to the total extracellular propionate concentration, pH_i was lowered while pH_o was maintained at 7.32. The initial pH_i decrease was 0.21 ± 0.05 pH units ($n=3$), after which pH_i gradually increased towards normal steady-state levels due either to the slow permeation of the dissociated form of the acid through the membrane or the activation of acid extrusion mechanisms. The latter is the most likely explanation because the removal of propionate caused a brief intracellular alkalinization followed by gradual return to normal steady-state pH_i levels. Figure 20B illustrates the opposite change in pH_i at room temperature resulting from the application of 10 mM TMA, a weak organic base (*solution 10*, Table 2). The application of extracellular TMA caused a immediate intracellular alkalinization of 0.38 ± 0.04 pH units which gradually returned towards baseline ($n=3$). Once removed, the intracellular milieu was briefly acidified followed by a pH_i recovery to resting baseline levels.

Table 5: Steady-state pH_i in HCO_3^- -free and HCO_3^- -containing media at room temperature and at 37°C , and the change in pH_i caused by exposure to the experimental solutions indicated.

	Temp	pH_i	ΔpH_i	n
HEPES buffer: (<i>solution 1</i>)	room	6.85 ± 0.04		25
$\text{HCO}_3^-/\text{CO}_2$ buffer: (<i>solution 6</i>)	room	7.15 ± 0.03		22
0 $[\text{Cl}^-]_o$ (<i>solution 8</i>)	room		0.28 ± 0.04	2
200 μM DIDS (in <i>solution 6</i>)	room		-0.08 ± 0.04	3
HEPES buffer: (<i>solution 1</i>)	37°C	7.23 ± 0.03		29
0 $[\text{Na}^+]_o$ (<i>solution 2</i>)	37°C		-0.53 ± 0.05	5
0 $[\text{Cl}^-]_o$ (<i>solution 3</i>)	37°C		0.00 ± 0.02	3
50 μM EIPA (in <i>solution 1</i>)	37°C		0.01 ± 0.01	3
$\text{HCO}_3^-/\text{CO}_2$ buffer: (<i>solution 12</i>)	37°C	7.13 ± 0.01		44
0 $[\text{Na}^+]_o$ (<i>solution 13</i>)	37°C		-0.65 ± 0.04	8
0 $[\text{Cl}^-]_o$ (<i>solution 14</i>)	37°C		0.19 ± 0.01	5
50 μM EIPA (in <i>solution 12</i>)	37°C		0.01 ± 0.02	3
200 μM DIDS (in <i>solution 12</i>)	37°C		-0.01 ± 0.01	3
0 $[\text{Cl}^-]_o$ + 200 μM DIDS (<i>solution 14</i>)	37°C		0.01 ± 0.01	2

Solution recipes are referred to in parentheses (see Tables 1 to 3). The experimental temperature (Temp) was either room temperature ($18 - 22^\circ\text{C}$) or 37°C . pH_i is the steady-state pH_i under the listed buffering conditions, and ΔpH_i is the change in pH_i (in pH units) caused by exposure to the indicated experimental solutions. Values are reported as the mean of n coverslips (i.e. cell populations) studied, \pm S.E.M.

Figure 3. Distribution of steady-state pH_i .

A. Distribution of steady-state pH_i at room temperature in the absence of HCO_3^- (*solution 1*, pH 7.32). **B.** Distribution of steady-state pH_i at room temperature in the presence of HCO_3^- (*solution 6*, pH 7.32). **C.** Distribution of steady-state pH_i at 37°C in the absence of HCO_3^- (*solution 1*, pH 7.34). **D.** Distribution of steady-state pH_i at 37°C in the presence of HCO_3^- (*solution 12*, pH 7.36). The mean steady-state pH_i under each of the four conditions is indicated (\pm S.E.M.), where n equals the total number of coverslips (i.e. cell populations) studied. The solid lines represent the least squares Gaussian fit to the data.

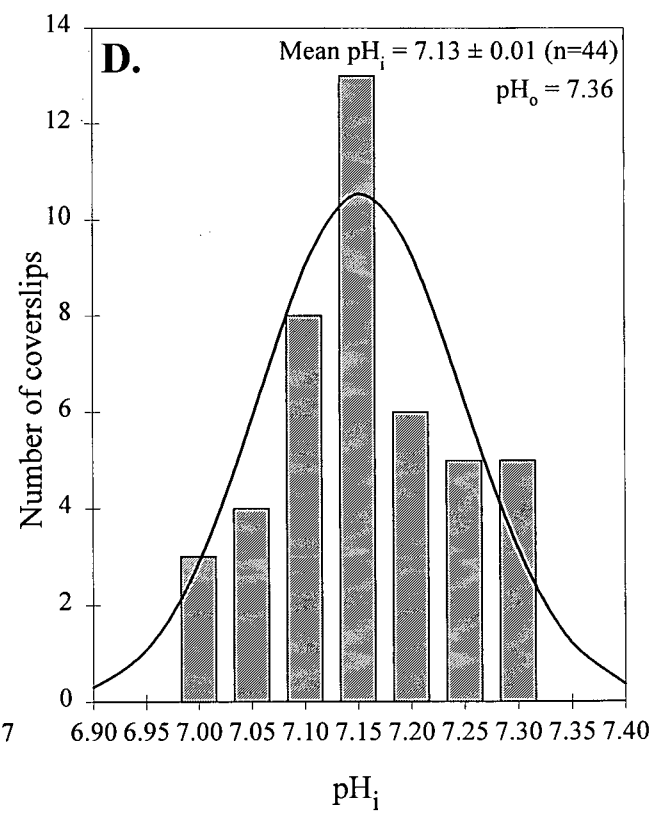
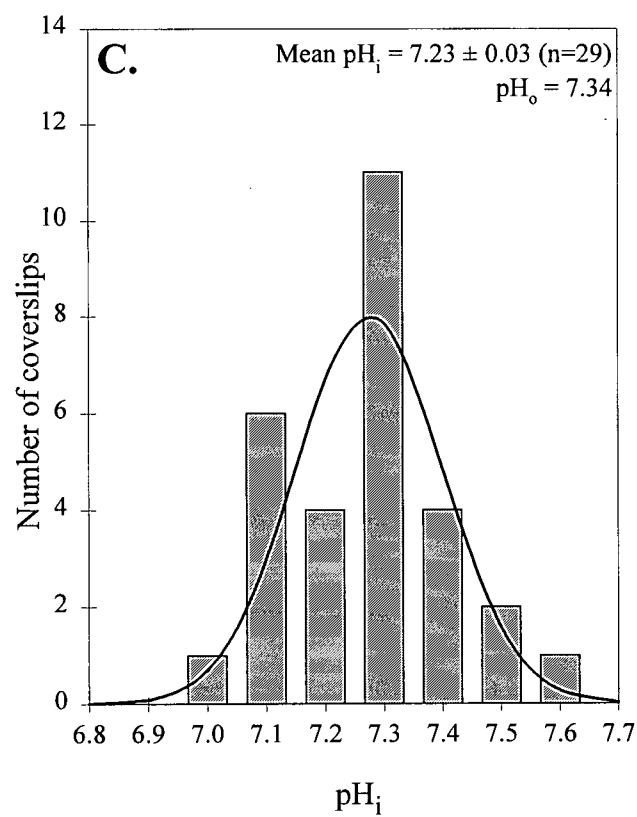
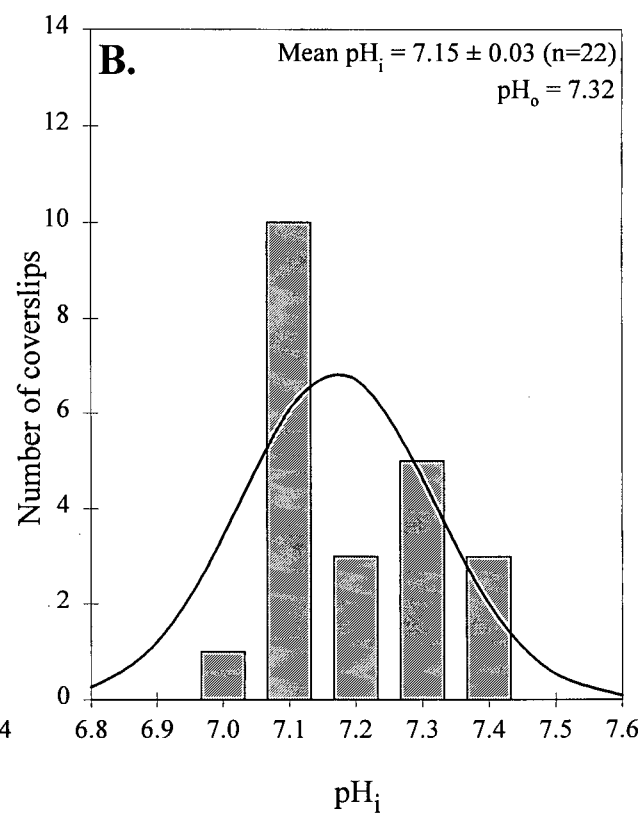
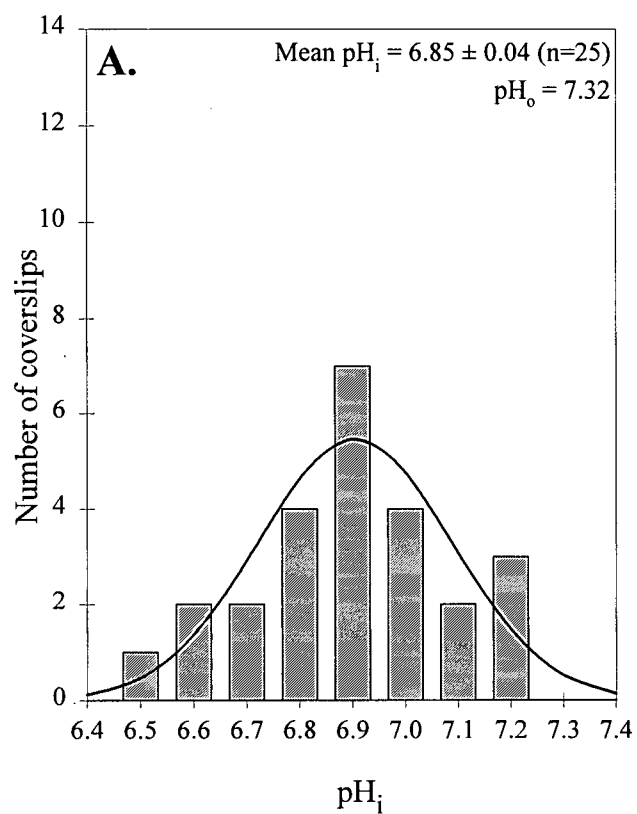


Figure 4. Effect of 0 $[\text{Cl}^-]_o$ on steady-state pH_i in the presence of HCO_3^- at room temperature.

The removal of $[\text{Cl}^-]_o$ (*solution 8*) at a constant pH_o (7.31) for the period indicated by the bar above the trace resulted in an ~ 0.3 pH unit increase in resting pH_i ($n=2$). pH_i returned to normal levels with the re-introduction of $[\text{Cl}^-]_o$. Shown also is a one point calibration with 10 μM nigericin at pH 7.00. The trace is a mean of data simultaneously obtained from 20 cells recorded on a single coverslip.

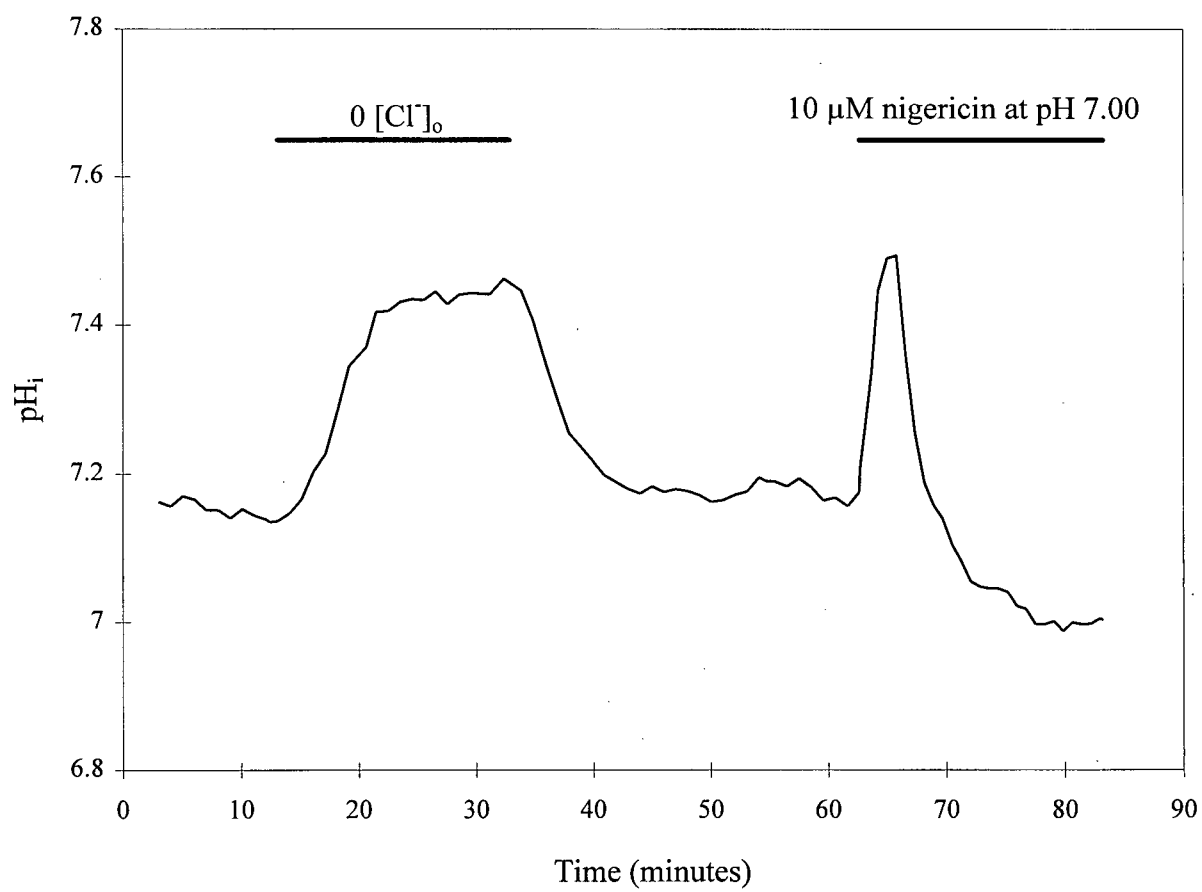


Figure 5. Effect of DIDS on steady-state pH_i in the presence of HCO_3^- at room temperature.

The addition of 200 μM DIDS to *solution 6* for the period indicated by the bar above the trace caused an ~ 0.1 pH unit intracellular acidification ($n=3$), while pH_o was maintained at 7.32. pH_i was restored to normal levels on removal of DIDS. The trace is a mean of data obtained from 30 cells recorded on a single coverslip.

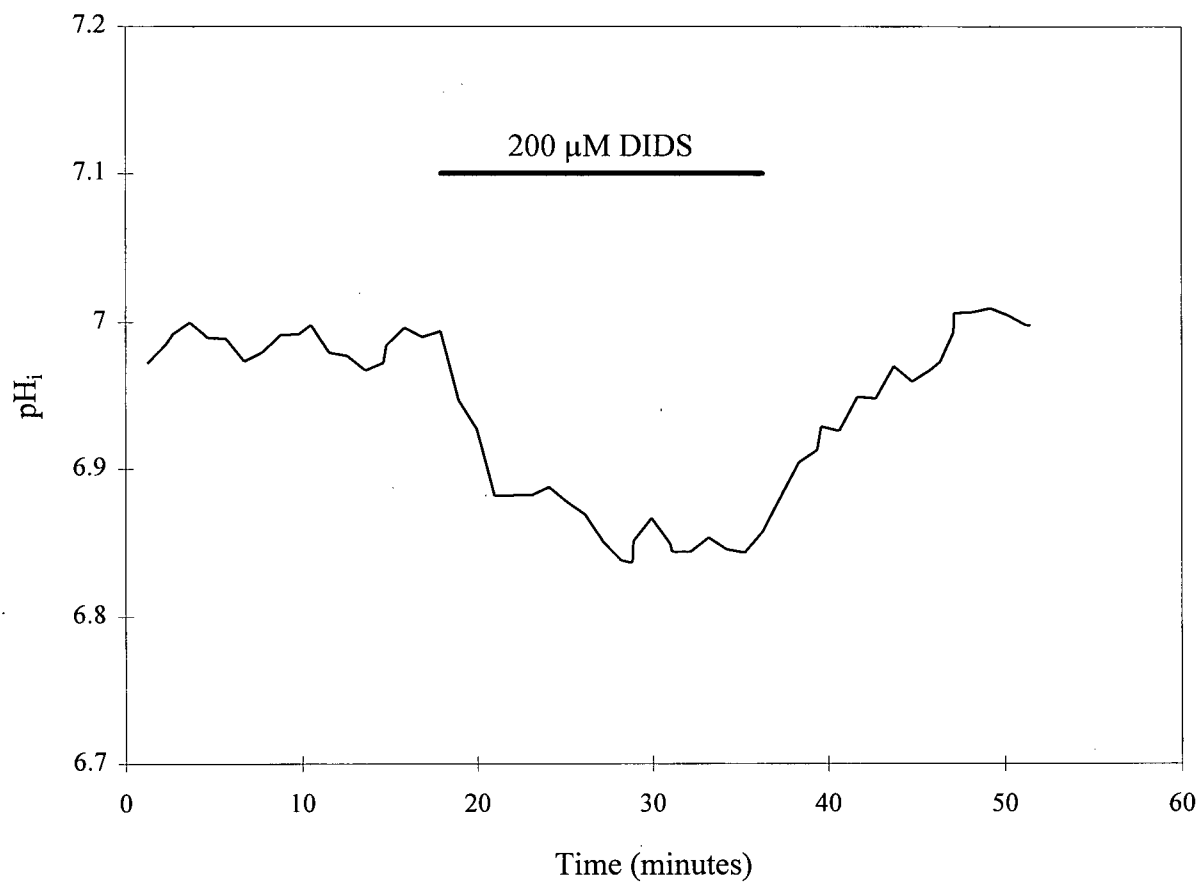


Figure 6. Steady-state pH_i in the presence and absence of $\text{HCO}_3^-/\text{CO}_2$ at room temperature.

A. The transition from HEPES-buffered medium (*solution 1*, pH_o 7.32) to $\text{HCO}_3^-/\text{CO}_2$ -buffered medium (*solution 6*, pH_o 7.32) at room temperature caused a brief acidification, presumably caused by CO_2 influx, followed by a net alkalization of ~ 0.3 pH units ($n=7$). The transition back into HEPES-buffered medium was marked by a momentary alkalization due to CO_2 efflux, followed by a fall in pH_i to the normal resting levels found in the absence of HCO_3^- . **B.** The net alkalization caused by the transition into $\text{HCO}_3^-/\text{CO}_2$ -buffered medium was abolished by the presence 200 μM DIDS ($n=5$). Rather, there was an acidification followed by a slow recovery. Each trace, recorded from separate coverslips, is data obtained from 10 cells simultaneously.

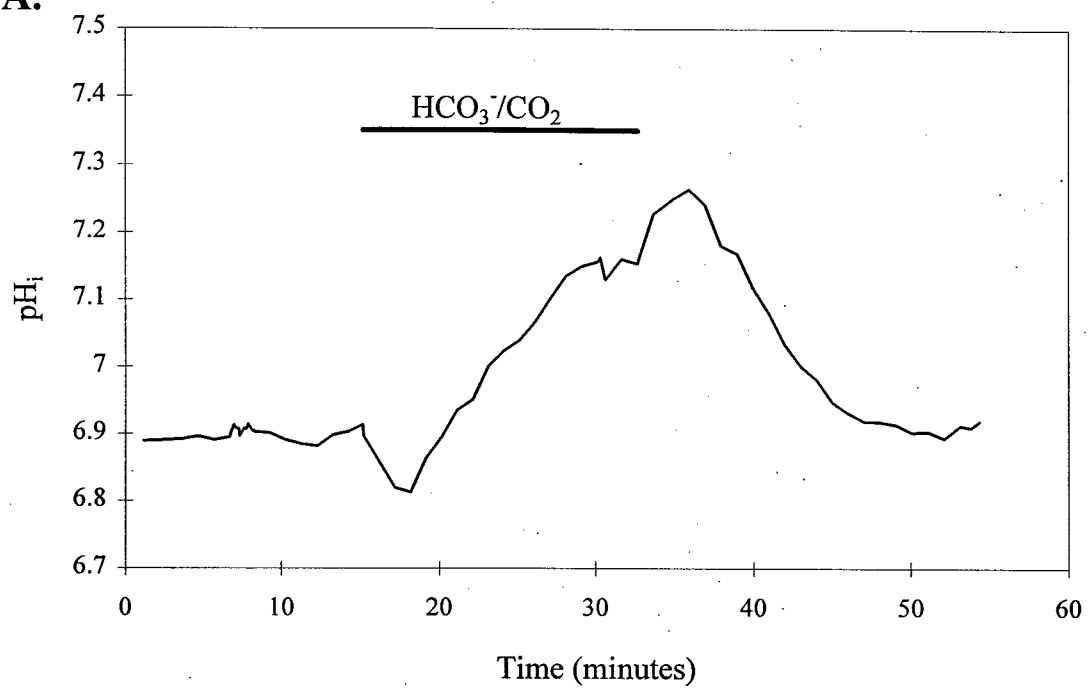
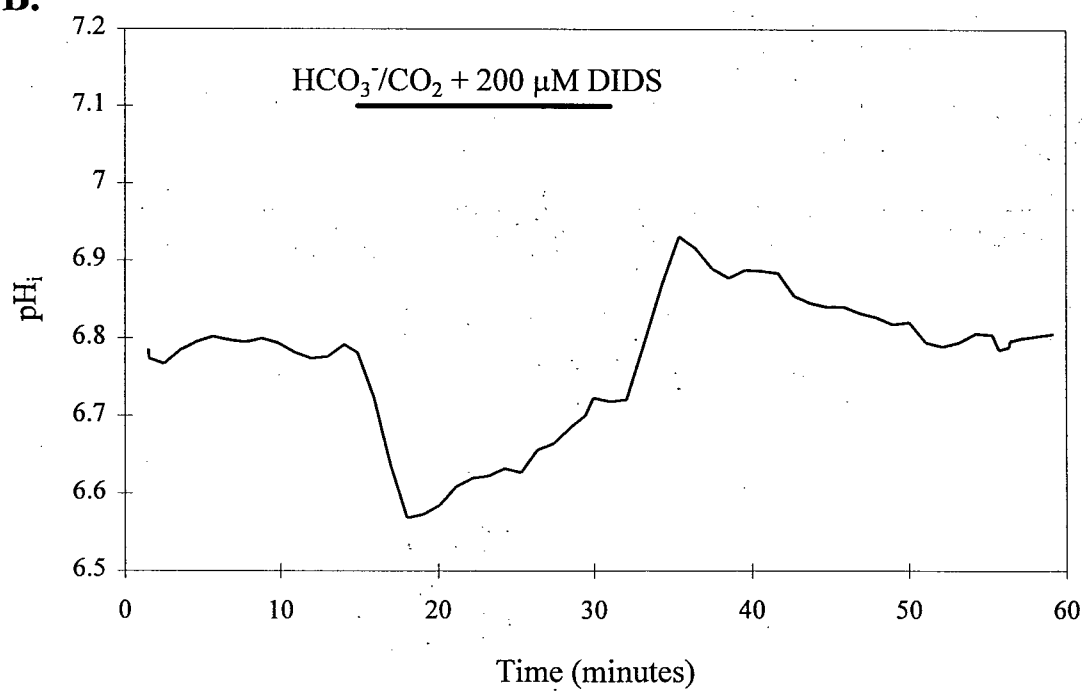
A.**B.**

Figure 7. Effect of 0 $[\text{Na}^+]_o$ on steady-state pH_i in the absence of HCO_3^- at 37°C.

The replacement of extracellular Na^+ with NMDG^+ (*solution 2*) at pH_o 7.35 caused an ~ 0.5 pH unit fall in pH_i ($n=5$). The re-introduction of Na^+ produced a rapid return to steady-state pH_i levels. Shown also is a one point calibration with 10 μM nigericin at pH 7.00. The trace is a mean of data obtained from 6 cells recorded on a single coverslip.

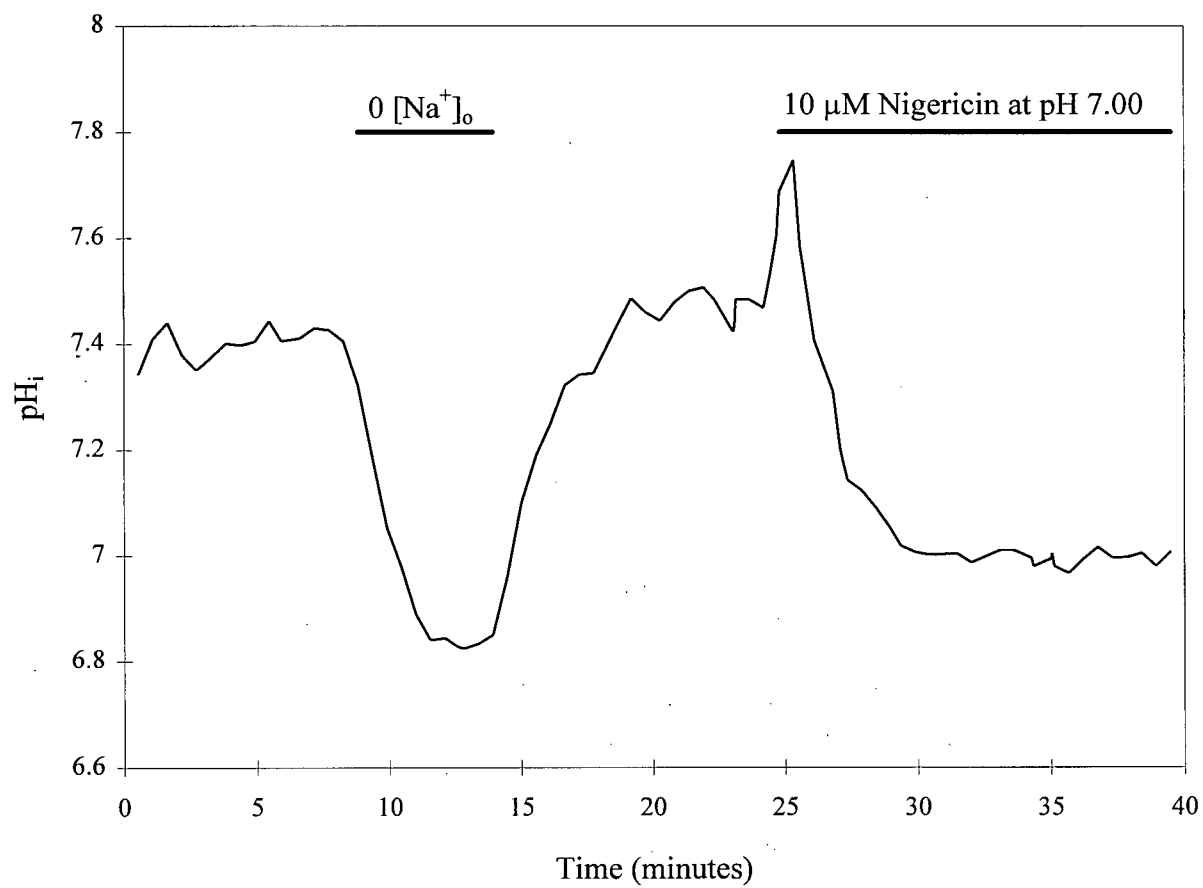


Figure 8. Effect of 0 $[\text{Cl}^-]_o$ on steady-state pH_i in the absence of HCO_3^- at 37°C.

The replacement of extracellular Cl^- with gluconate (*solution 3*) at pH_o 7.33 for the period indicated by the bar above the trace did not change resting pH_i levels ($n=3$). The trace is a mean of data obtained from 26 cells recorded on a single coverslip. Compare with Figure 4.

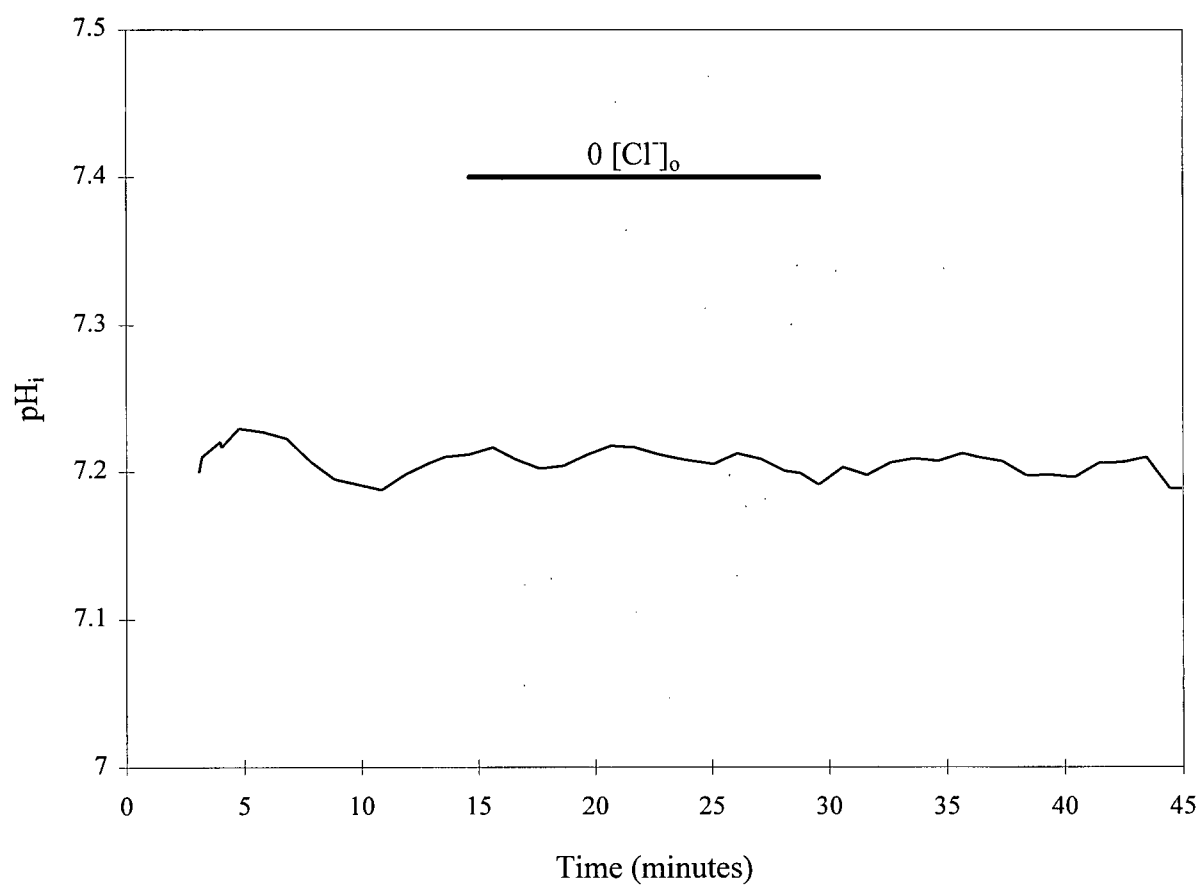


Figure 9. Effect of EIPA on steady-state pH_i in the absence of HCO_3^- at 37°C .

The application of $50\ \mu\text{M}$ EIPA to *solution 1* at pH_o 7.35 for the period indicated by the solid bar did not significantly alter resting pH_i levels ($n=3$). The trace is a mean of data simultaneously obtained from 6 cells recorded on a single coverslip.

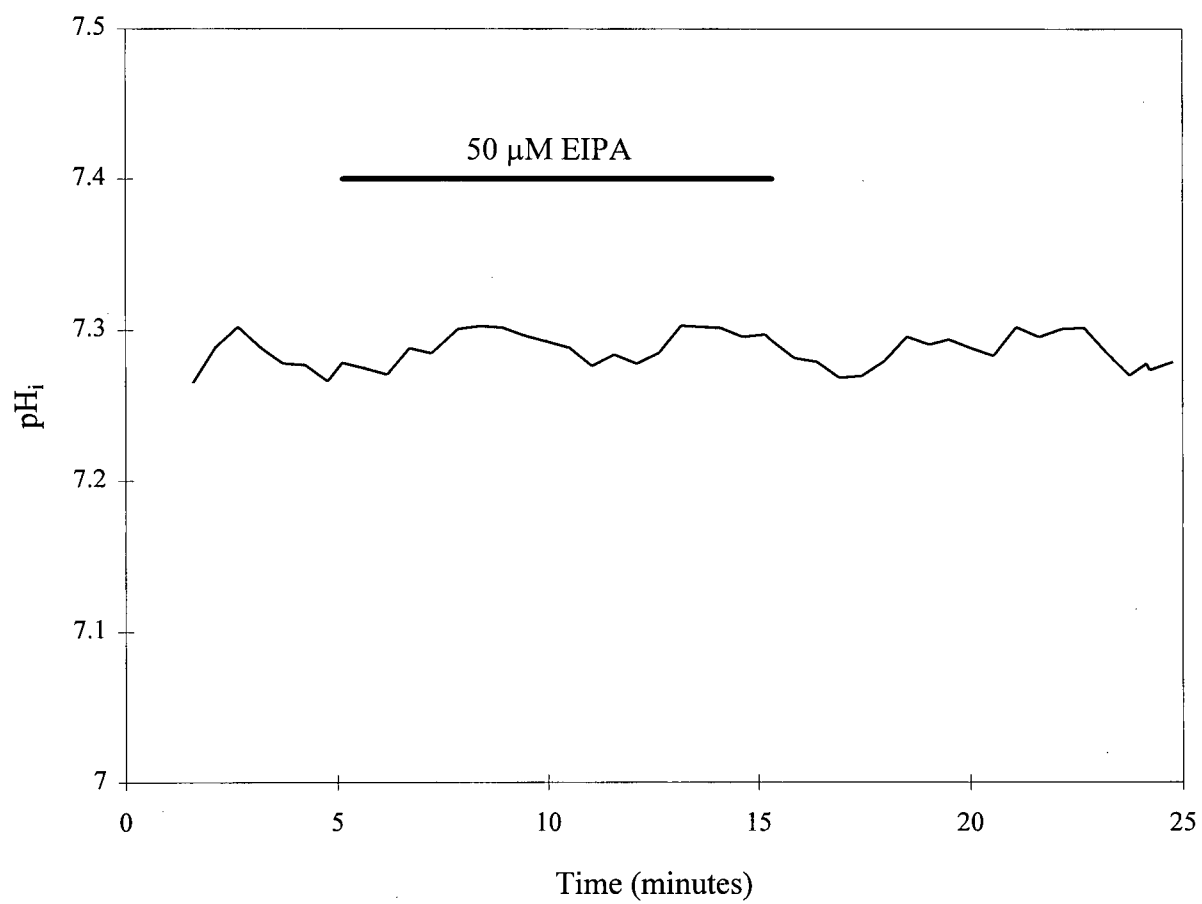


Figure 10. Combined effect of 0 $[\text{Na}^+]_o$ and EIPA on steady-state pH_i in the absence of HCO_3^- at 37°C.

The application of 50 μM EIPA 5 minutes after the removal of extracellular Na^+ (*solution 2*) did not reverse the fall in pH_i caused by 0 $[\text{Na}^+]_o$, nor the return to resting pH_i levels after the re-introduction of $[\text{Na}^+]_o$ ($n=3$). Throughout the experiment, pH_o was maintained at 7.33. The trace is a mean of data obtained from 23 cells recorded on a single coverslip.

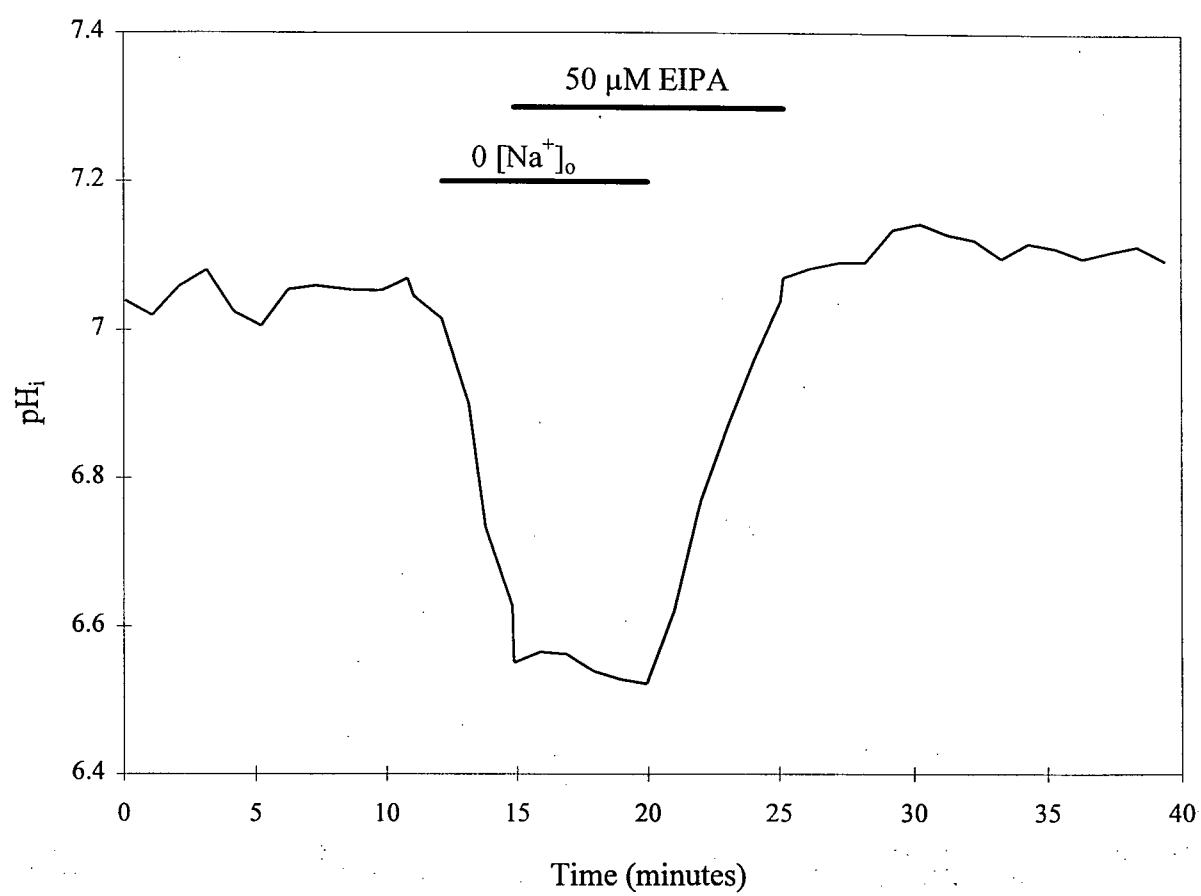


Figure 11. Effect of MGCMA and HOE 694 on steady-state pH_i in the absence of HCO_3^- at 37°C .

A. The application of $100\ \mu\text{M}$ MGCMA at $\text{pH}_o\ 7.36$ did not significantly change steady-state pH_i ($n=3$). **B.** Similarly, the application of $100\ \mu\text{M}$ HOE 694 ($\text{pH}_o\ 7.38$) had no effect on normal resting pH_i levels ($n=3$). Trace A is a mean of data obtained from 8 cells, whereas trace B is a mean of data obtained from 13 cells, each recorded on separate coverslips.

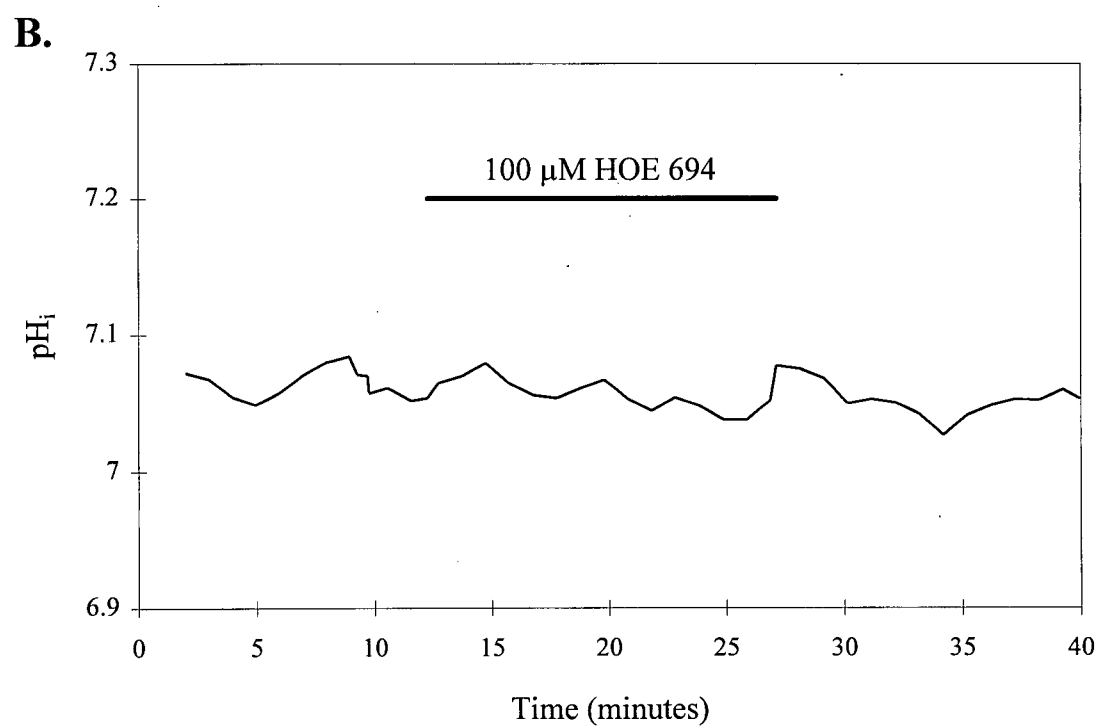
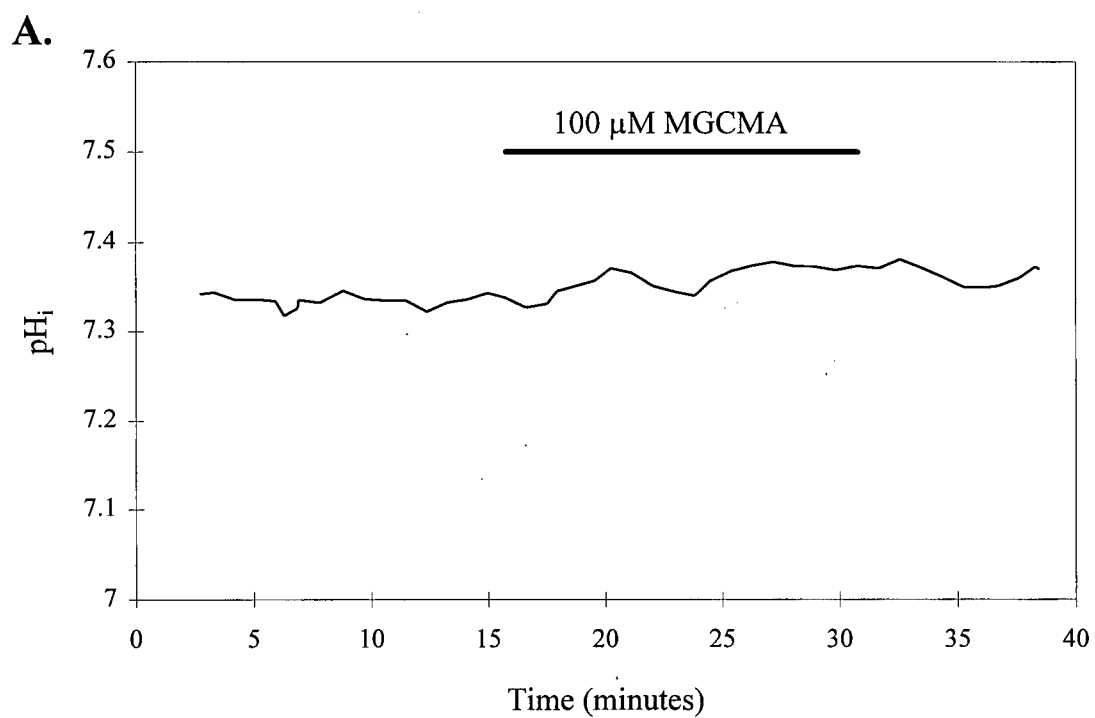


Figure 12. Effect of 0 $[\text{Na}^+]_o$ on steady-state pH_i in the presence of HCO_3^- at 37°C.

The removal of extracellular Na^+ (*solution 13*, pH_o 7.35) produced an ~ 0.60 pH unit fall in pH_i ($n=8$). pH_i rebounded to normal resting levels with the re-introduction of extracellular Na^+ . Also shown is a one point calibration with 10 μM nigericin at pH 7.00. The trace is a mean of data obtained from 35 cells recorded on a single coverslip.

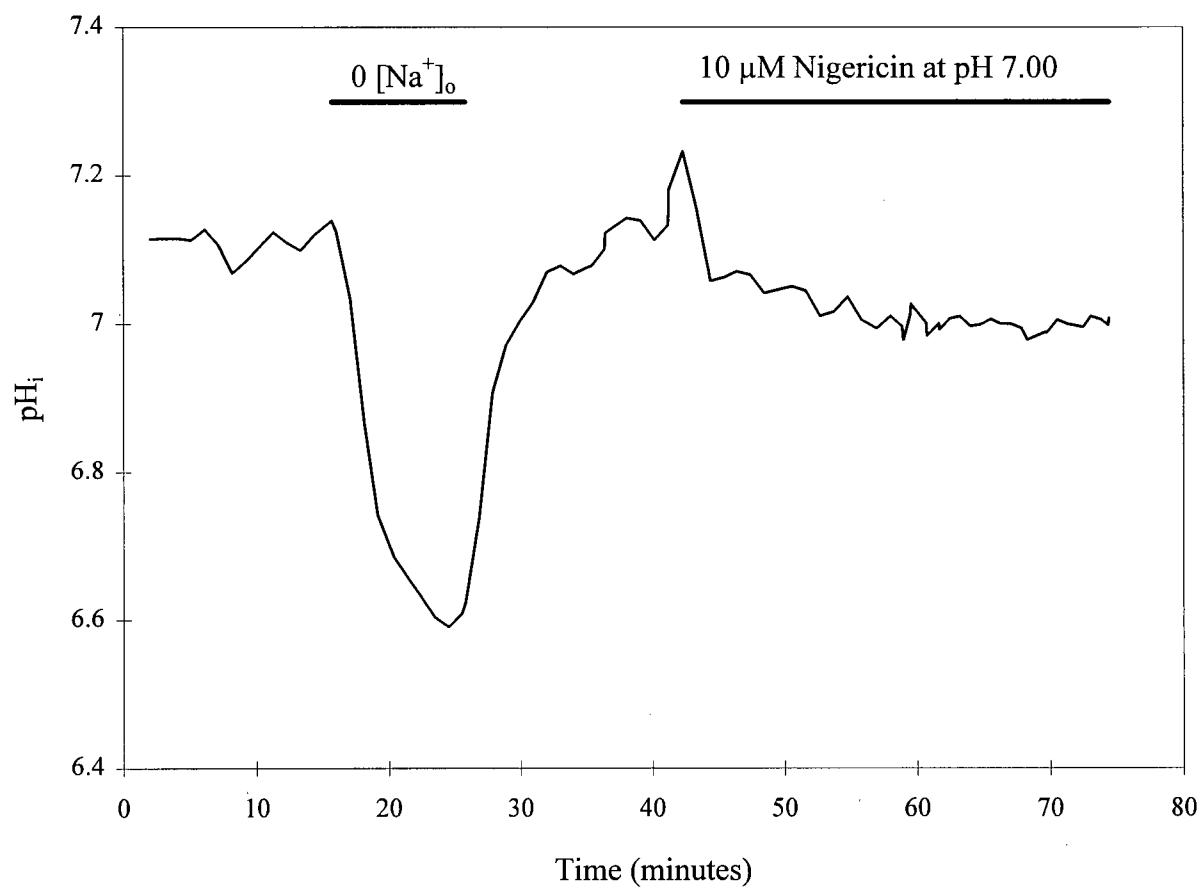


Figure 13. Effect of EIPA on steady-state pH_i in the presence of HCO_3^- at 37°C .

The addition of $50\ \mu\text{M}$ EIPA to *solution 12* at pH_o 7.32 did not significantly alter resting pH_i levels ($n=3$). This result was also observed in the absence of HCO_3^- as shown in Figure 9. The trace is a mean of data simultaneously obtained from 30 cells recorded on a single coverslip.

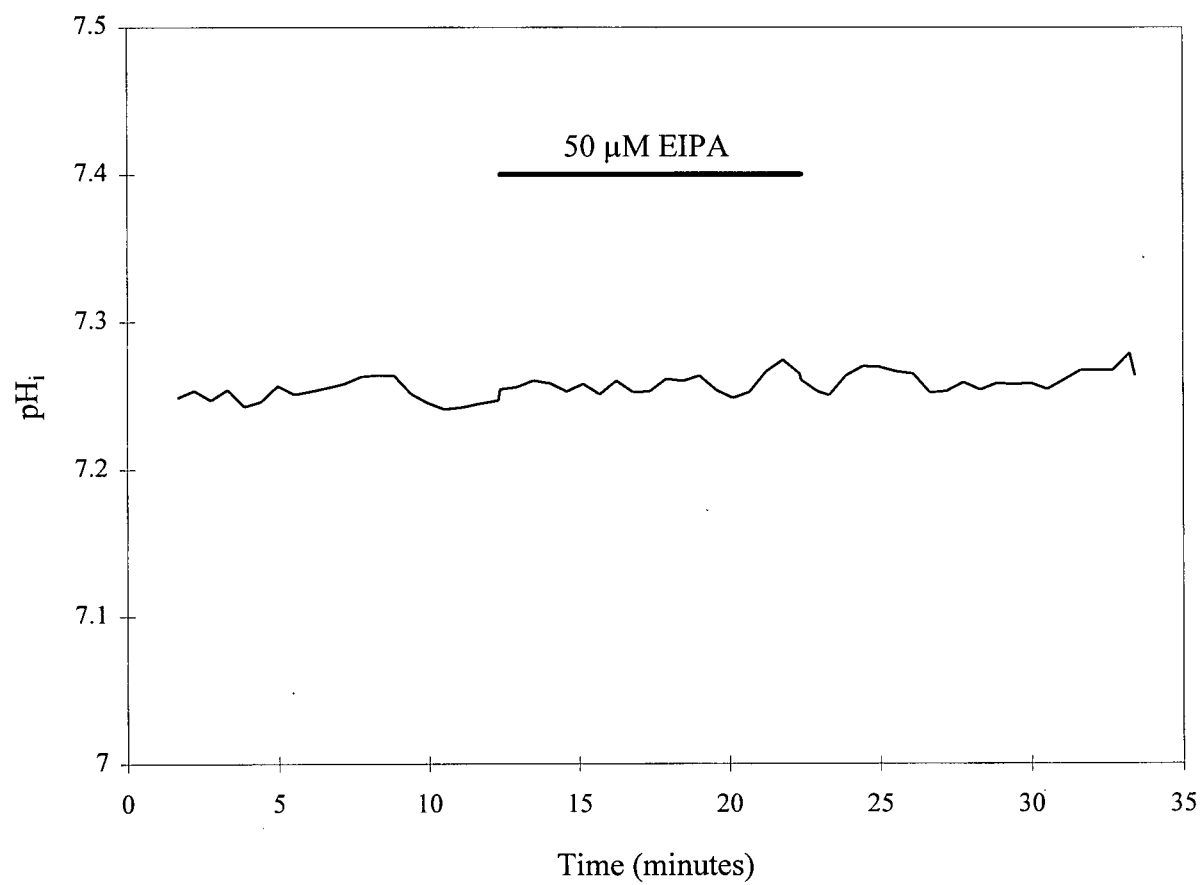


Figure 14. Effect of 0 [Cl⁻]_o, and the combined effect of 0 [Cl⁻]_o plus DIDS on steady-state pH_i in the presence of HCO₃⁻ at 37°C.

A. The removal of extracellular Cl⁻ (*solution 14*) at pH_o 7.36 produced an ~0.20 pH unit intracellular alkalinization (n=5). This 0 [Cl⁻]_o-induced pH_i increase was completely inhibited by 200 μM DIDS (n=3). This trace is a mean of data obtained from 16 cells recorded on a single coverslip. **B.** At pH_o 7.36, the addition of 200 μM DIDS 5 minutes after the removal of extracellular Cl⁻ returned pH_i to normal resting levels, with a small overshoot to acidic values (n=4). This trace is a mean of data obtained from 37 cells recorded on a different coverslip to A.

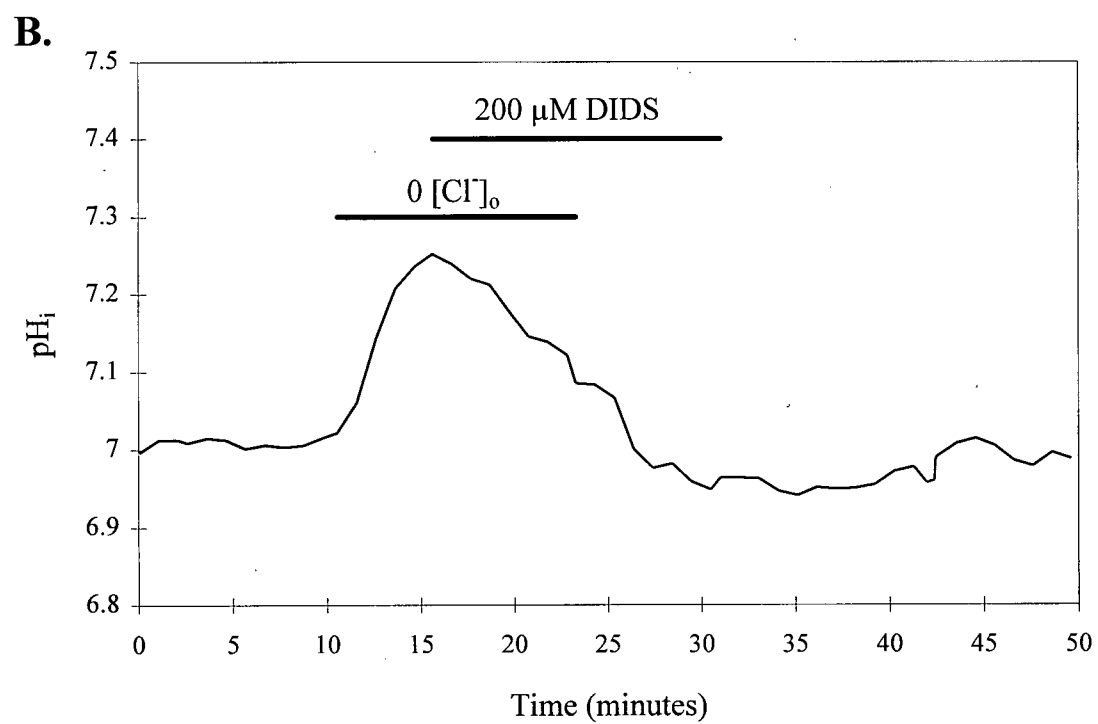
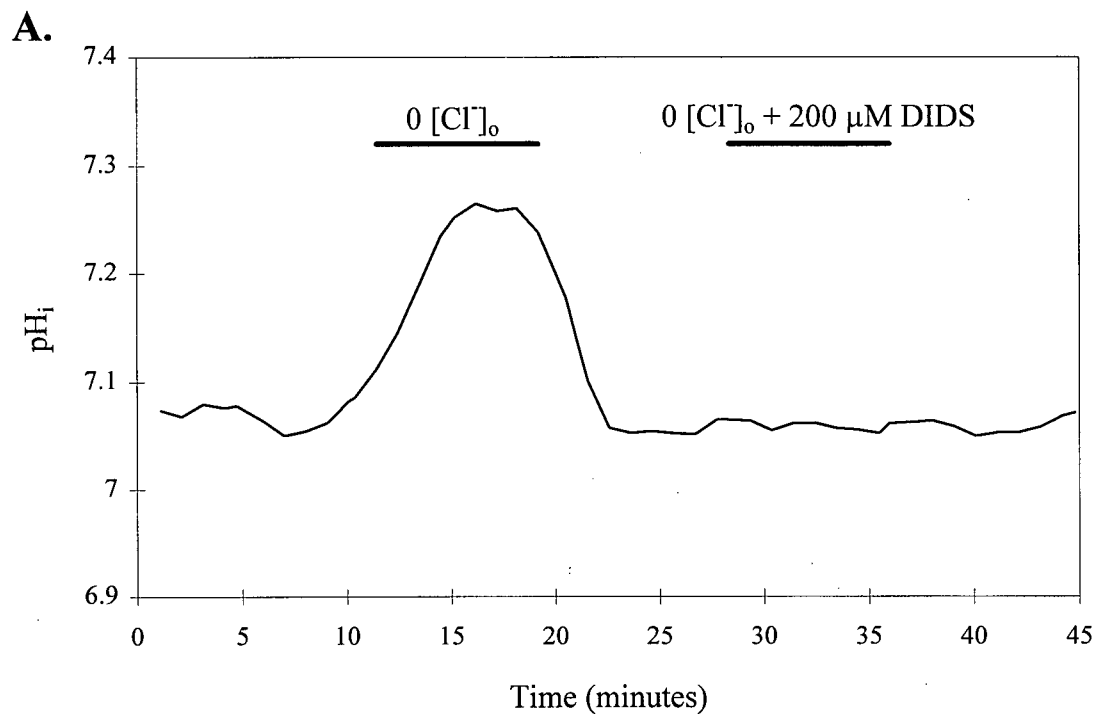


Figure 15. Effect of DIDS on steady-state pH_i in the presence of HCO_3^- at 37°C .

The application of $200\ \mu\text{M}$ DIDS for the period indicated by the bar above the trace in the presence of HCO_3^- at 37°C ($\text{pH}_o\ 7.33$) did not significantly alter steady-state pH_i ($n=3$). This result differs from that observed at room temperature (see Figure 5), in which DIDS reduced pH_i by ~ 0.10 pH units. This trace is a mean of data obtained from 44 cells recorded on the same coverslip.

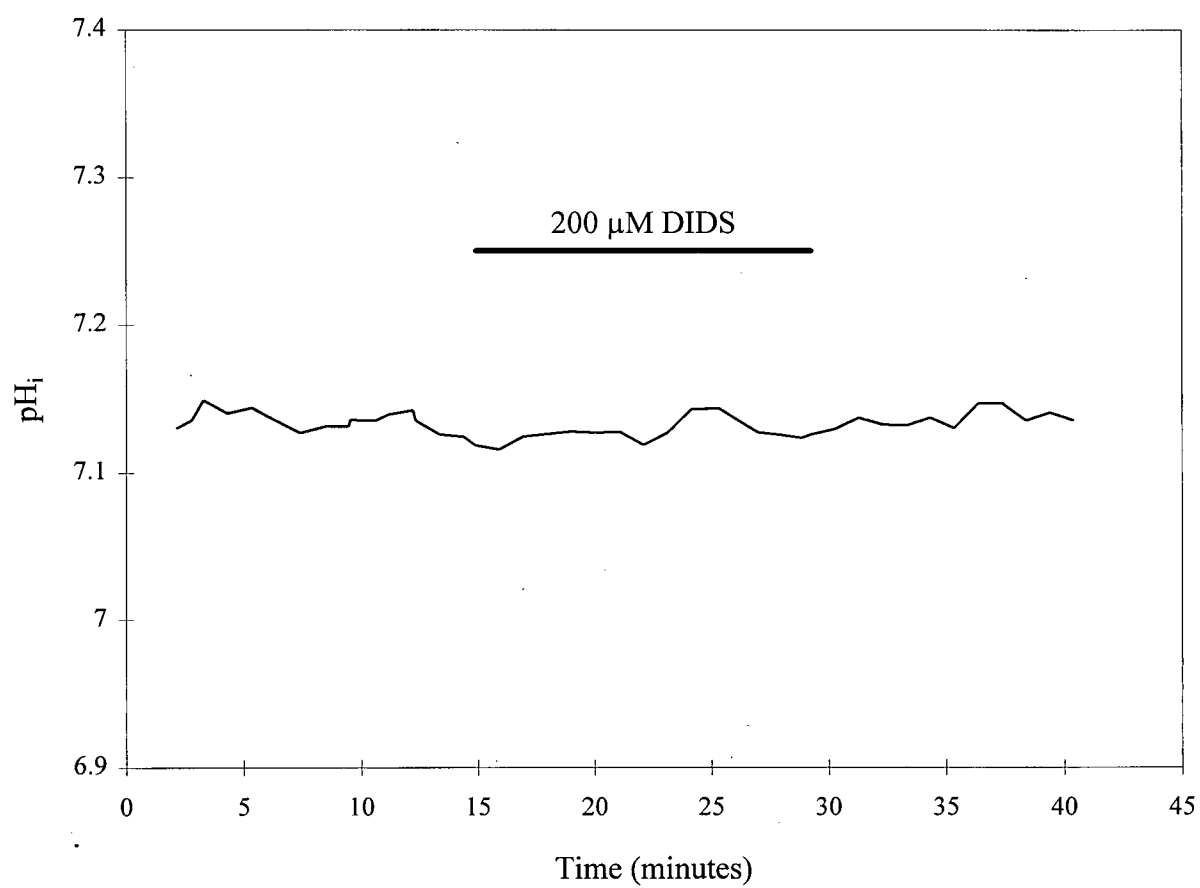


Figure 16. Steady state pH_i in the presence and absence of $\text{HCO}_3^-/\text{CO}_2$ at 37°C .

The transition from HEPES-buffered medium (*solution 1*, pH_o 7.35) to $\text{HCO}_3^-/\text{CO}_2$ -buffered medium (*solution 12*, pH_o 7.35) at 37°C caused an intracellular acidification such that the resulting pH_i in the presence of HCO_3^- remained ~ 0.1 pH units lower than resting pH_i in the absence of HCO_3^- ($n=13$). With the re-introduction of HEPES-buffered medium, pH_i briefly increased followed by a decline to the normal resting levels found in the absence of HCO_3^- . The presence of $200\text{ }\mu\text{M}$ DIDS did not influence the manner in which pH_i responded to the transition from HCO_3^- -free to HCO_3^- -containing perfusion media at 37°C ($n=3$). The trace is a mean of data obtained from 16 cells recorded on the same coverslip. Compare with Figures 6A and B.

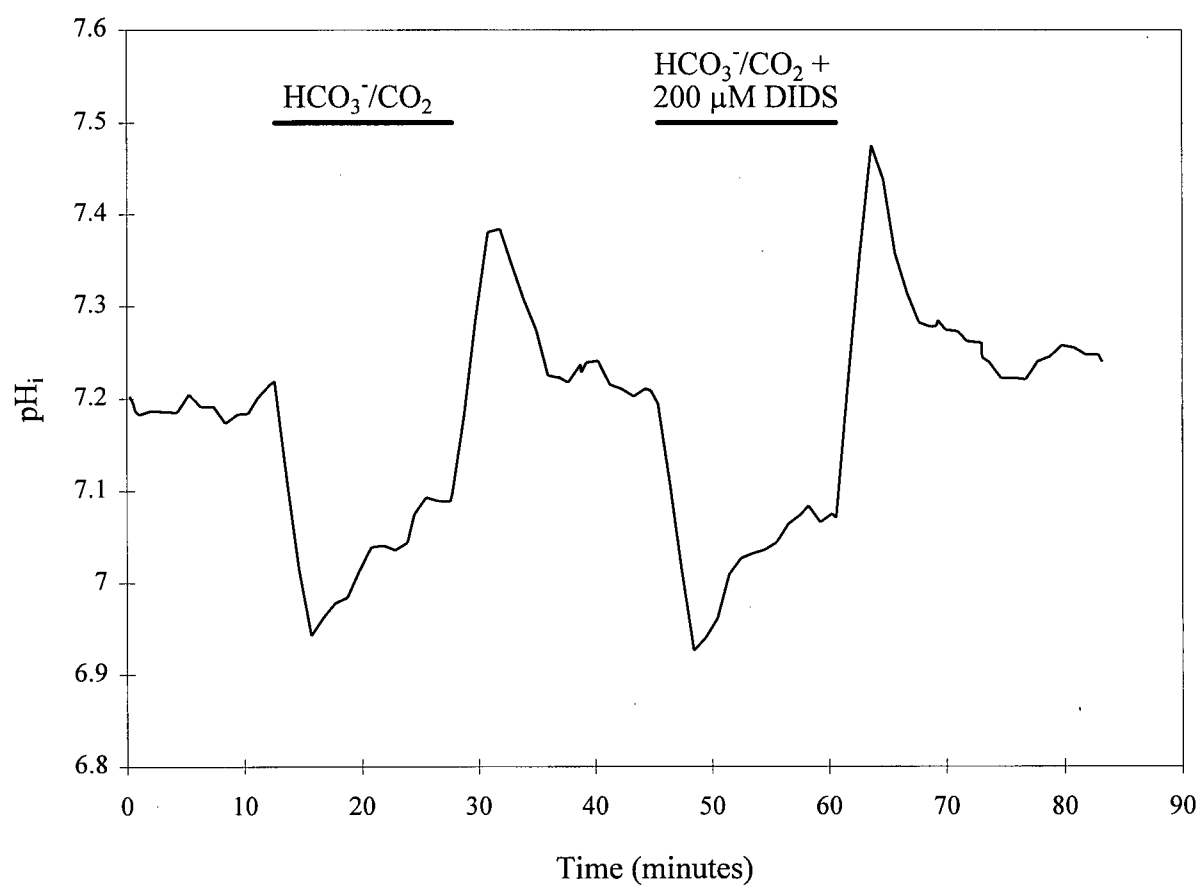


Figure 17. Effect of $\text{HCO}_3^-/\text{CO}_2$ on steady-state pH_i during 0 $[\text{Na}^+]_o$ perfusion at room temperature.

$[\text{Na}^+]_o$ was removed from the HCO_3^- -free buffered media (*solution 2*) at pH_o 7.35, resulting in an immediate fall in pH_i . The addition of HCO_3^- during the period of continued 0 $[\text{Na}^+]_o$ (*solution 7*) perfusion caused pH_i to gradually recover ($n=3$). pH_i immediately returned to normal levels when $[\text{Na}^+]_o$ was re-introduced to the perfusion medium. The trace is a mean of data obtained from 34 cells recorded on a single coverslip.

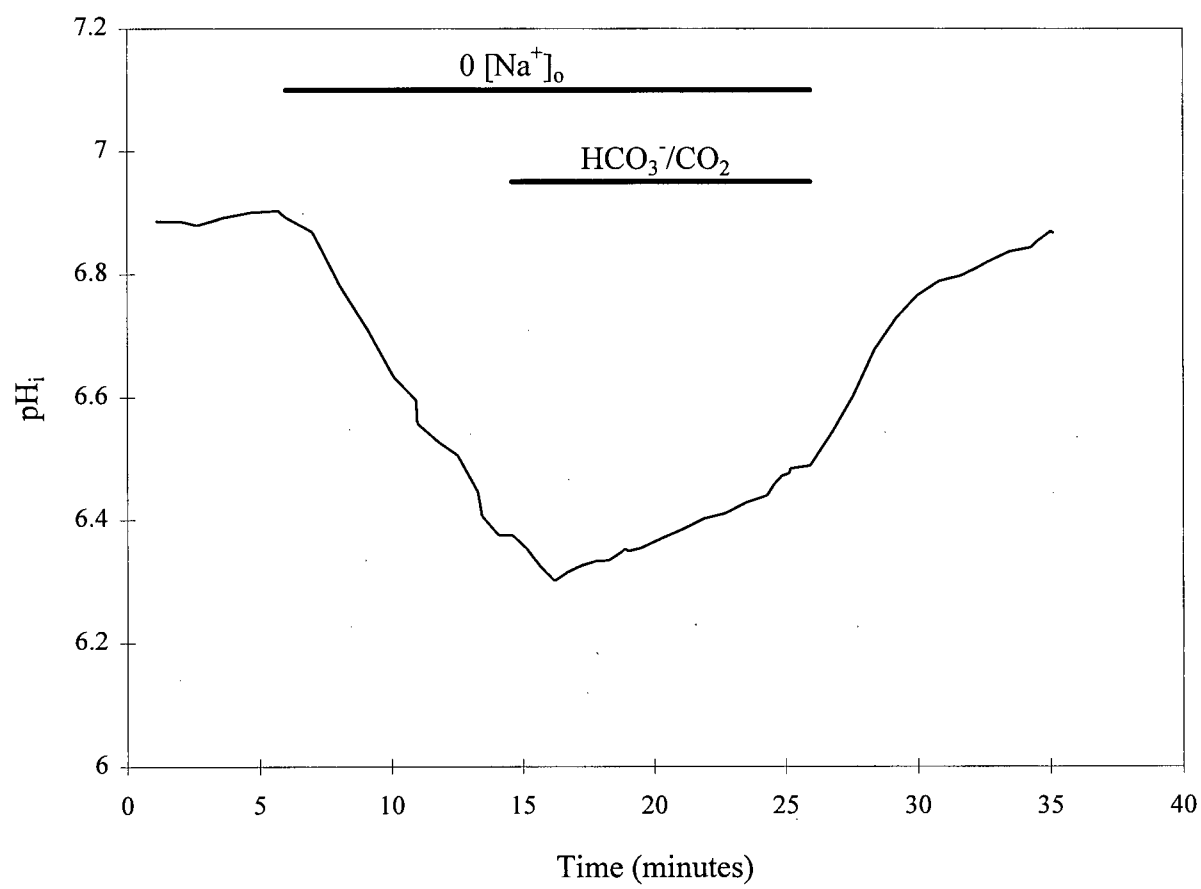


Figure 18. Effect of 0 $[\text{Cl}^-]_o$ during 0 $[\text{Na}^+]_o$ perfusion on steady-state pH_i in the presence of HCO_3^- at 37°C.

The removal of external Na^+ from the $\text{HCO}_3^-/\text{CO}_2$ -buffered medium at 37°C (*solution 13*, pH_o 7.37) caused a similar fall in pH_i to that shown in Figure 12. The additional removal of extracellular Cl^- during a sustained period of perfusion with 0 $[\text{Na}^+]_o$ (*solution 15*) caused an ~ 0.15 pH unit increase in pH_i ($n=3$). The re-introduction of $[\text{Cl}^-]_o$ caused pH_i to fall back to a level observed prior to its removal, followed by a gradual increase in pH_i probably due to the activity of Na^+ -independent acid extrusion mechanisms (see Figure 17). pH_i quickly recovered to normal levels when Na^+ was again added to the perfusion medium. The trace is a mean of data obtained from 8 cells recorded on a single coverslip.

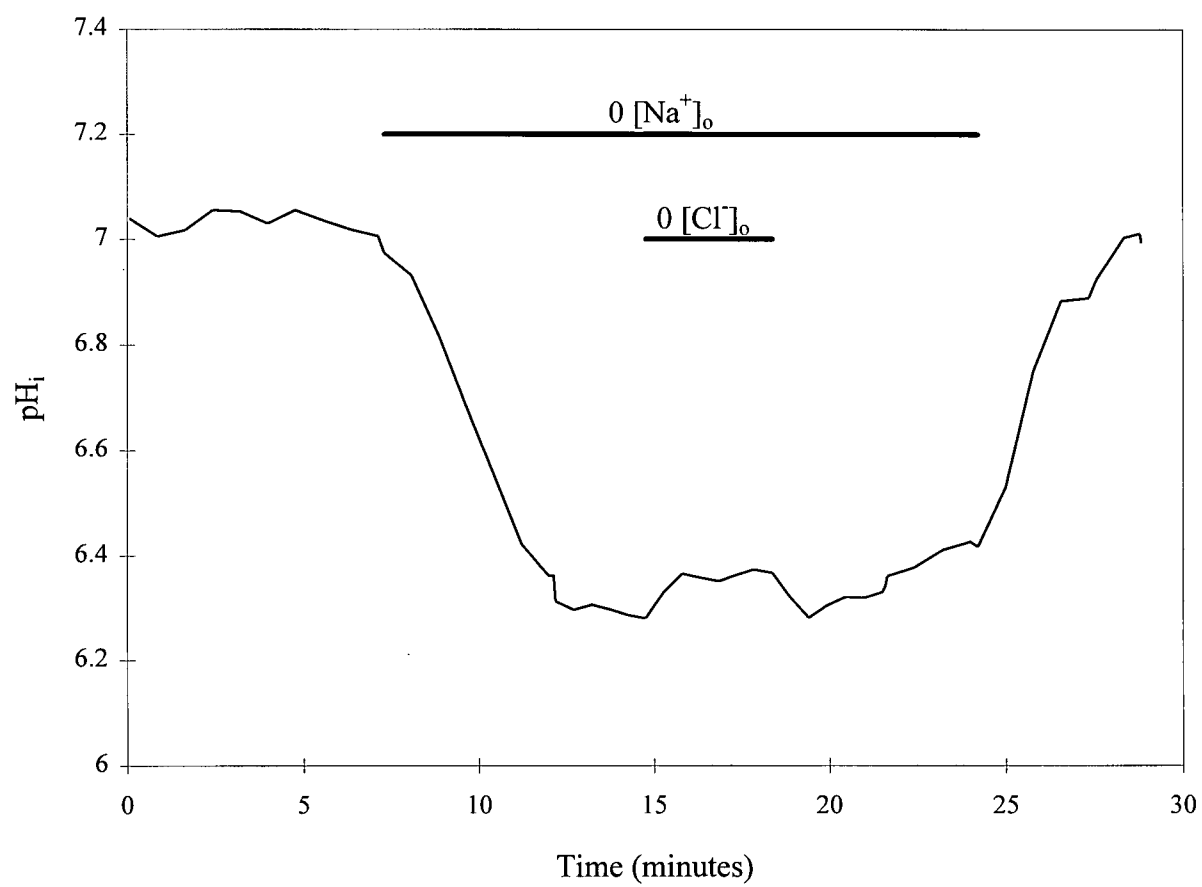


Figure 19. Effect of changes in pH_o on steady-state pH_i in the presence of HCO_3^- at 37°C .

A. Increasing pH_o from a normal level of 7.35 (*solution 12*) to 7.75 (*solution 21*) and 8.02 (*solution 22*) caused a similar though smaller increase in pH_i . Decreasing pH_o to 7.02 (*solution 20*) and 6.56 (*solution 17*) caused pH_i to fall to acidic levels. This trace is a mean of data obtained from 35 cells on a single coverslip. **B.** Linear regression analysis of the dependence of pH_i on pH_o . The equation describing this relationship is:

$$\text{pH}_i = 1.99 + 0.699 \times \text{pH}_o \quad (R^2 = 0.978, n=3 \text{ coverslips})$$

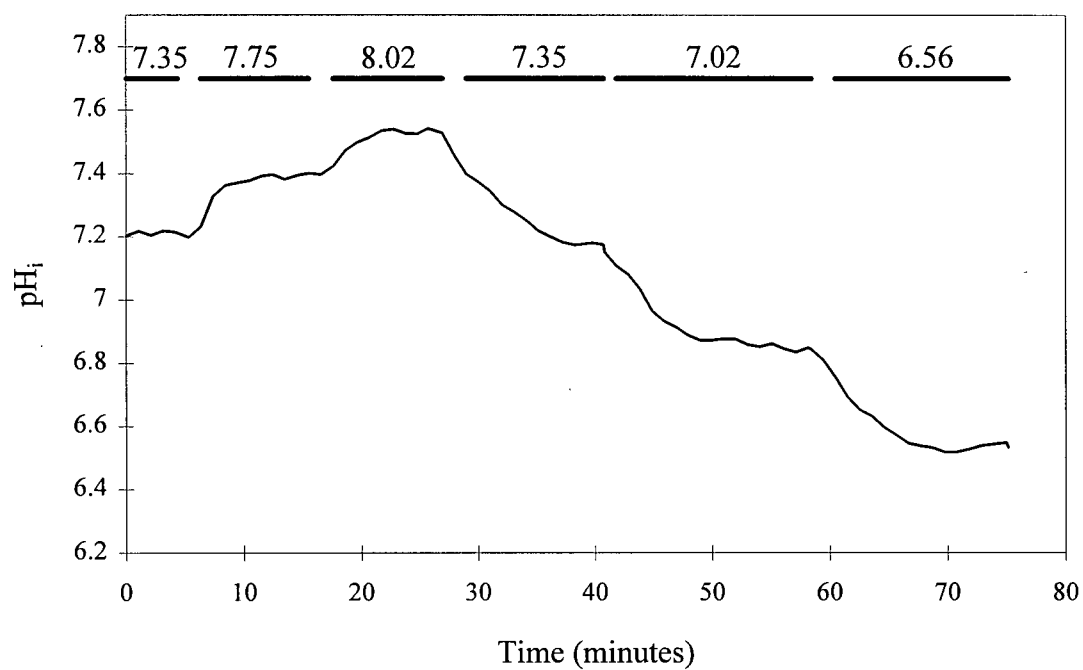
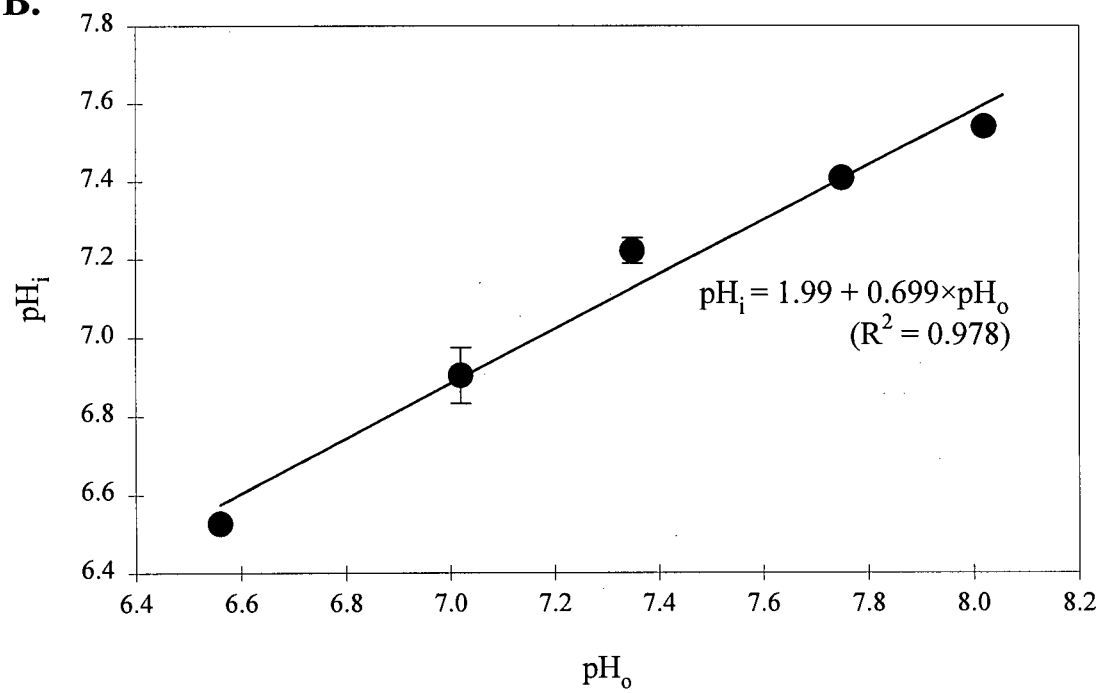
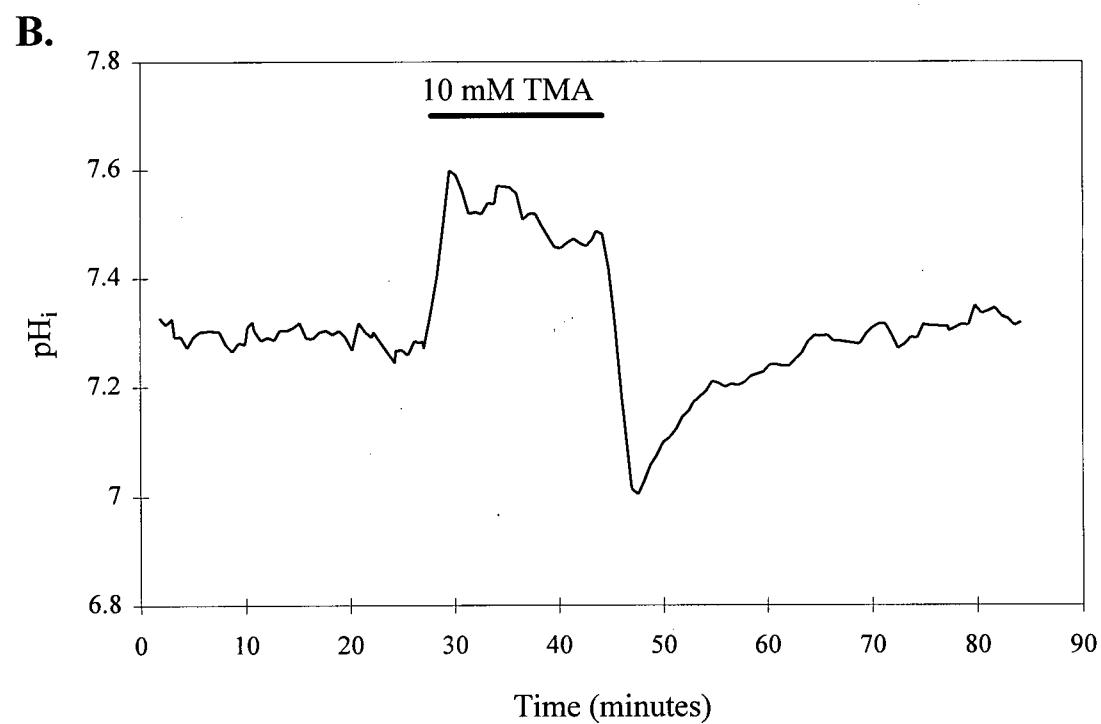
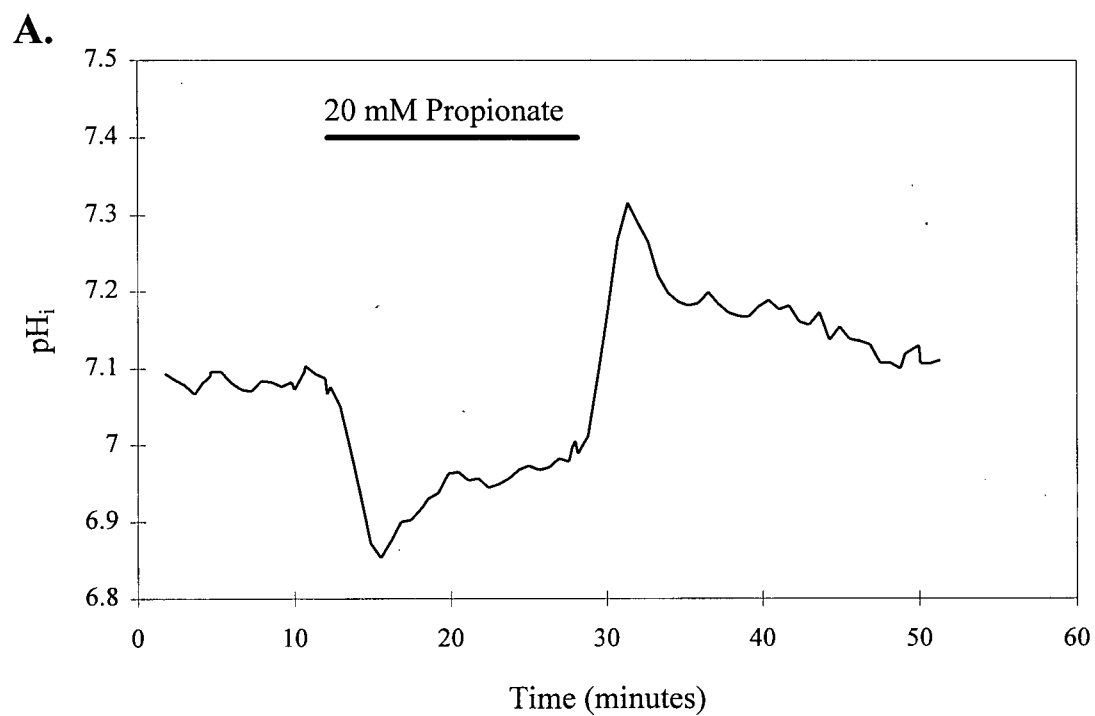
A.**B.**

Figure 20. Effect of propionate and TMA on steady-state pH_i in the presence of HCO_3^- at room temperature.

A. The application of 20 mM propionate (*solution 9*) at a constant pH_o (7.30) caused an immediate intracellular acidification of ~ 0.20 pH units ($n=3$) followed by a gradual recovery to baseline levels. The removal of propionate from the extracellular medium caused pH_i to rapidly increase after which it recovered to normal resting levels. **B.** The application of 10 mM TMA (*solution 10*) at a constant pH_o (7.31) caused an immediate intracellular alkalinization of ~ 0.40 pH units ($n=3$) followed by a slow recovery to baseline levels. The removal of TMA caused an immediate intracellular acidification followed by a return to steady-state pH_i levels. Recorded on separate coverslips, trace A is a mean of data obtained from 12 cells, whereas trace B is a mean of data obtained from 20 cells.



pH_i RECOVERY FROM AN IMPOSED ACID LOAD

The investigation of pH_i regulatory mechanisms was expanded by inducing an intracellular acidification, while maintaining a constant pH_o, and studying the subsequent recovery. The examination of acid load recoveries provides additional information on mechanisms regulating pH_i, since excessive intracellular protons will activate acid extrusion mechanisms (Roos and Boron, 1981). Acid transients were produced using the NH₄⁺-prepulse technique (Boron and De Weer, 1976), in which the neurones were exposed to NH₄⁺ through the addition of 20 mM NH₄Cl to the perfusion solution (*solution 4*, Table 1; *solution 11*, Table 2; *solution 16*, Table 3). As shown in Figure 21, this exposure causes an immediate intracellular alkalinization due to the passive influx of NH₃, the dissociated form of NH₄⁺, and its impending hydration to form NH₄⁺ and OH⁻. The membrane exhibits a slight permeability to NH₄⁺, and thus the initial pH_i rise is slowly dampened by the influx of extracellular NH₄⁺ driven by an inwardly-directed electrochemical gradient (Boron and De Weer, 1976). The removal of the external NH₄Cl, 3 minutes after its original application, results in an exodus of the highly permeable NH₃, leaving behind significant concentrations of NH₄⁺, trapped in the cells by the opposing electrical gradient generated by the membrane potential. The dissociation of intracellular NH₄⁺ into NH₃ liberates protons, thus forcing pH_i to fall below its initial resting value. The recovery from this imposed acidification back to steady-state pH_i levels is an established means of analyzing the mechanisms involved in pH_i regulation, as first demonstrated by Messeter and Siesjö (1971).

Data generated from the acid load experiments are summarized in Table 6. The initial rate of pH_i recovery to resting levels was quantified 10 seconds after the peak acidification. The instantaneous recovery rates were also determined at t₅₀ and t₈₀, which are defined as the time at which pH_i recovered to 50% and 80% of its pre-acid load level, respectively. pH_i at t₅₀ was calculated by taking the resting pH_i before the application of

NH_4^+ (the "preload pH_i "), and then subtracting 50% of the resulting net change in pH_i (the "net pH_i decrease"). The net pH_i decrease was calculated by subtracting the minimum pH_i reached during the acidification from the preload pH_i . Similarly, pH_i at t_{80} was determined by subtracting 20% of the NH_4^+ -induced net pH_i decrease from the preload pH_i . As an indicator of intracellular buffering power, the increase in pH_i (the " pH_i increase") caused by the 3 minute exposure to NH_4^+ was also measured by taking the difference between the preload pH_i and the pH_i immediately prior to the removal of extracellular NH_4^+ (see Table 6). At room temperature, the mean pH_i increases after the 3 minute exposure to NH_4^+ were 0.52 ± 0.05 pH units ($n=6$) and 0.38 ± 0.01 pH units ($n=7$) in the absence and presence of HCO_3^- , respectively. These values markedly decreased when studies were performed at 37°C . In cells exposed to a solution buffered with HEPES, the 3 minute application of NH_4^+ elicited a 0.27 ± 0.03 pH unit rise ($n=12$), whereas pH_i increased by only 0.11 ± 0.01 pH units ($n=16$) during the NH_4^+ exposure in solutions buffered with $\text{HCO}_3^-/\text{CO}_2$. These results suggest that both an increase in temperature and the presence of HCO_3^- lead to an enhanced intracellular buffering capacity (see Roos and Boron, 1981).

In any given experiment, the rate of pH_i recovery was greatest at the acid peak and then declined, in a linear fashion, as pH_i recovered to normal levels. This phenomenon is graphically depicted in Figure 22A. These data, though obtained from a single experiment, represent the trend found in all neurones under all buffering conditions. The rate of pH_i recovery was not related to the preload pH_i nor the minimum pH_i reached during acidification in 14 randomly selected experiments (Figure 23B). Likewise, as illustrated in Figure 23C, the net decrease in pH_i caused by the NH_4^+ prepulse was not a factor in evaluating the rate of pH_i restoration. In accordance with these observations, it was not necessary to replicate exact acid load conditions throughout these acid load recovery studies.

Recovery from an acid load at room temperature:

Neurons perfused at room temperature in the absence of HCO_3^- (*solution 1*, Table 1) recovered from an NH_4^+ -induced acidification at an maximum initial rate of 1.31×10^{-3} pH units/second ($n=6$; Table 6, row *a*). Figure 23 shows that the addition of HCO_3^- (*solution 6*, Table 2) during the recovery portion of the experiment caused a significant increase in the acid extrusion rate throughout the entire course of the restoration. Under these conditions, the initial rate of pH_i recovery from an induced acidification was 2.55×10^{-3} pH units/second ($n=7$; Table 6, row *b*). As expected from data presented earlier regarding the regulation of steady-state pH_i at room temperature (see Figure 6A), Figure 23 also illustrates that the restoration of pH_i from an acid load in the presence of HCO_3^- continued to a higher resting pH_i than the prevailing steady-state level found when the neurons were being perfused with HEPES buffered medium.

Initial experiments performed at room temperature in the presence of HCO_3^- were conducted to assess the contribution of the $\text{HCO}_3^-/\text{Cl}^-$ exchanger to the rate of pH_i recovery following an acid load. Figure 24 illustrates that the application of 200 μM DIDS during recovery caused a significant reduction in the rate of acid efflux ($n=3$), as expected given the contribution of $\text{HCO}_3^-/\text{Cl}^-$ exchange towards the maintenance of steady-state pH_i at room temperature. The initial rate fell from 2.55×10^{-3} pH units/second to 0.95×10^{-3} pH units/second (Table 6, row *d*). The t_{50} rate in the presence of 200 μM DIDS was also notably reduced from a control level of 1.38×10^{-3} pH units/second (Table 6, row *b*) to 0.63×10^{-3} pH units/second (Table 6, row *d*). A qualitatively similar effect was observed in the t_{80} rate (Table 6, row *d*). As DIDS is an inhibitor of $\text{HCO}_3^-/\text{Cl}^-$ exchange (Thomas, 1976a), then the depletion of $[\text{Cl}^-]_i$ during pH_i recovery should similarly alter the rate of acid extrusion. Figure 25A depicts the ability of the neurons to recover from an acid load while being perfused with a $[\text{Cl}^-]_o$ -free solution (*solution 8*, Table 2). Under these conditions, the initial rate of recovery in fact increased to 3.14×10^{-3} pH units/second ($n=3$; Table 6, row *c*), which may indicate a

0 $[\text{Cl}^-]_o$ -induced acceleration of the $\text{HCO}_3^-/\text{Cl}^-$ exchanger. This result also suggests that the duration of 0 $[\text{Cl}^-]_o$ perfusion was not long enough to sufficiently deplete intracellular Cl^- stores, which would have likely produced a similar decrease in the pH_i recovery rate as that caused by the application of DIDS (see Table 6, row *d*). The former possibility is supported by the experiment shown in Figure 25B in which the rapid recovery seen on removing extracellular Cl^- was hindered when the neurones were simultaneously exposed to 200 μM DIDS ($n=2$). This manoeuvre reduced the initial recovery rate to 1.18×10^{-3} pH units/second (Table 6, row *e*) compared to an initial rate of 3.14×10^{-3} pH units/second in the absence of DIDS (Table 6, row *c*). Overall, these results suggest that $\text{HCO}_3^-/\text{Cl}^-$ exchange is utilized by these neurones at room temperature to recover from induced intracellular acidifications. The inability of 200 μM DIDS to completely block pH_i restoration (see Figure 24) indicates that other acid transporters, such as a Na^+ -dependent, HCO_3^- -independent acid extrusion mechanism, contribute to the regulation of pH_i at room temperature. The participation of this latter mechanism in the recovery of pH_i after an imposed acidification is described in detail at 37°C (see below).

Recovery from an acid load at 37°C :

At 37°C and in the absence of HCO_3^- (*solution 1*, Table 1), the neurones recovered from the acidifying NH_4^+ prepulse at an initial rate of 5.56×10^{-3} pH units/second ($n=12$; Table 6, row *f*; Figure 26). This is higher than the initial rate of recovery under identical buffering conditions at room temperature (see Table 6, row *a*). Corresponding values for the t_{50} and t_{80} rates were also higher at 37°C than at room temperature (Table 6). pH_i restoration was abolished when $[\text{Na}^+]_o$ was removed from the perfusate (*solution 2*, Table 1) during the recovery portion of the experiment ($n=2$; Figure 27), as expected given the contribution of Na^+ -dependent mechanisms to the maintenance of steady-state pH_i (see above). However, studied on 6 cell populations, the application of 50 μM EIPA did not influence the ability of the neurones to recover from

the induced intracellular acidification (Figure 28; Table 6, row *h*). Two other compounds were tested for their ability to inhibit pH_i recovery from an induced acid load via blockade of the putative Na^+/H^+ exchanger present on these neurones. The application of 100 μM MGCMA ($n=3$) or 100 μM HOE 694 ($n=3$) failed to affect the rate of steady-state pH_i restoration from an NH_4^+ -induced acidification (data not shown). Similarly, as illustrated in Figure 29, 200 μM DIDS did not influence the rate of pH_i recovery in neurones in the absence of HCO_3^- ($n=3$). As this control experiment was conducted in the absence of HCO_3^- , which is a constituent ion of the DIDS-sensitive anion exchanger, it demonstrates that the application of DIDS does not cause spurious effects on pH_i recovery. Though the instantaneous initial rate, t_{50} rate, and t_{80} rate for the recovery from an acid load in the presence of DIDS seemed to decline in comparison to control values (Table 6, row *i*), such differences were not statistically significant under paired and unpaired *t*-test calculations ($P > 0.05$). The similarity between acid load recoveries in the presence or absence of 200 μM DIDS is better depicted by the actual time required for 50% and 80% pH_i restoration (Table 6, row *i* versus row *f*). The fact that DIDS had no effect on pH_i recovery in the absence of HCO_3^- supports the premise that stilbene derivatives only inhibit HCO_3^- -dependent acid transporters (Thomas, 1976a; Russell and Boron, 1976). Overall, these results suggest that in the absence of HCO_3^- at 37°C, hippocampal neurones recover from an induced acidification utilizing a Na^+ -dependent, EIPA-insensitive acid extrusion mechanism.

Interestingly, as shown in Figure 26, the addition of HCO_3^- to the perfusing medium (*solution 12*, Table 3) throughout the entire course of pH_i restoration did not alter the rate of acid load recovery at 37°C. The initial rate of pH_i restoration in the presence of HCO_3^- at 37°C was 4.77×10^{-3} pH units/second ($n=16$; Table 6, row *j*). In addition, the ability of the neurones to recover from an imposed acidification while being perfused with a $\text{HCO}_3^-/\text{CO}_2$ buffered solution was nearly halted by the removal of extracellular Na^+ ($n=3$; Figure 30). These results reflect the lack of influence of a HCO_3^-

/Cl⁻ exchanger and the possible dominance of a Na⁺-dependent, HCO₃⁻-independent mechanism governing pH_i regulation in these cells at 37°C. However, in the absence of [Na⁺]_o (*solution 13*, Table 3) a small amount of pH_i recovery occurred (see Figure 30), presumably caused by pH_i regulatory mechanisms not requiring extracellular Na⁺. Illustrated in Figure 31, the rate of pH_i recovery was unaffected by the presence of 50 μM EIPA (n=3; Table 6, row *l*), a result similar to that obtained at room temperature. The inability of EIPA to influence pH_i has been previously demonstrated under steady-state conditions (see Figures 9 and 13).

In contrast to a similar study performed at room temperature (see Table 6, row *c*; Figure 25), acid load recovery at 37°C was not affected by the removal of Cl⁻ from the extracellular perfusate (*solution 14*, Table 3). Illustrated in Figure 32 and Table 6 (row *m*), this result may reflect a diminished cellular dependence on HCO₃⁻/Cl⁻ exchange towards the regulation of pH_i at 37°C, as already suggested by results from the steady-state pH_i experiments. In the absence of [Cl⁻]_o, pH_i did however recover to a slightly higher level than was present before the induced acidification, a result that is reflected by previous observations regarding 0 [Cl⁻]-induced increases in resting pH_i at this temperature (see Figure 14A). Though the activity of the HCO₃⁻/Cl⁻ exchanger may not be pronounced at 37°C, the application of 200 μM DIDS inhibited recovery from an imposed acid load on 5 out of 9 coverslips examined (Figure 33A). When affected by DIDS, the initial rate of pH_i recovery was reduced to 1.02×10^{-3} pH units/second with corresponding reductions in the t₅₀ and t₈₀ rates (Table 6, row *o*). Illustrated in Figure 33B, acid load recovery in the remaining 4 cell populations (one of which was a sister culture of a population that did respond to the drug) was not influenced by the presence of 200 μM DIDS (Table 6, row *n*). The point and duration of DIDS application during the pH_i restoration did not appear to influence the ability of this anion exchange blocker to inhibit acid load recoveries. These results suggest a variable contribution of HCO₃⁻/Cl⁻ exchange to pH_i recovery from an NH₄⁺-induced acid load at 37°C.

To determine whether the sensitivity to DIDS was perhaps dependent on the level of intracellular acidification induced by the NH_4^+ prepulse, the preload pH_i was reduced by lowering the pH of the HCO_3^- -containing perfusion medium to 6.8 at 37°C (*solution 18*, Table 4). After exposure to the NH_4^+ -prepulse at pH_o 6.8 (*solution 19*, Table 4), pH_i typically fell to a level of 6.4 (Figure 34), a value that was approximately 0.25 pH units lower than was typically achieved when pH_o rested at 7.36. The initial, t_{50} , and t_{80} rates of recovery were accelerated under these conditions ($n=3$; Table 6, row *p*), but 200 μM DIDS did not inhibit the rate of pH_i restoration when pH_o was maintained at 6.8 ($n=2$; Table 6, row *q*). This result indicates that the rate of pH_i recovery is sensitive to pH_o in a manner that is independent of the activity of $\text{HCO}_3^-/\text{Cl}^-$ exchange.

In summary, the experiments outlined above have demonstrated that the activities of the acid extrusion mechanisms present on cultured foetal hippocampal pyramidal neurones are dependent on temperature. At room temperature, both a Na^+ -dependent, HCO_3^- -independent acid extrusion mechanism (possibly a Na^+/H^+ exchanger) and a $\text{HCO}_3^-/\text{Cl}^-$ exchanger have been shown to be involved in restoring pH_i back to resting levels following an imposed acid load. Presumably, this anion exchanger is the same Na^+ -independent $\text{HCO}_3^-/\text{Cl}^-$ counter-transporter regulating steady-state pH_i at room temperature. However, at 37°C , the dominant mechanism that acts to return pH_i to baseline values after an applied acidification appears to be a Na^+ -dependent, HCO_3^- -independent acid extruder. These results are in agreement with those obtained under steady-state conditions, in which Na^+ -independent $\text{HCO}_3^-/\text{Cl}^-$ exchange was similarly observed to be appreciably active only at room temperature.

Figure 21. Sample acid load with NH_4Cl .

The addition of 20 mM NH_4Cl to the perfusion medium for the period indicated by the bar above the trace produces an initial alkalinization due to the influx of membrane permeable NH_3 , and its subsequent hydration into NH_4^+ and OH^- . This rise in pH_i quickly plateaus due to the gradual influx extracellular NH_4^+ . The removal of extracellular NH_4Cl results in an immediate fall in pH_i to acidic levels, caused by the fast efflux of NH_3 ; the remaining NH_4^+ dissociates to release H^+ ions. After peak acidification is reached, pH_i recovers to pre-acid load levels. This sample trace is mean of data obtained from 6 cells recorded on a single coverslip at room temperature in the absence of HCO_3^- (*solutions 1 and 4*, pH_o 7.36).

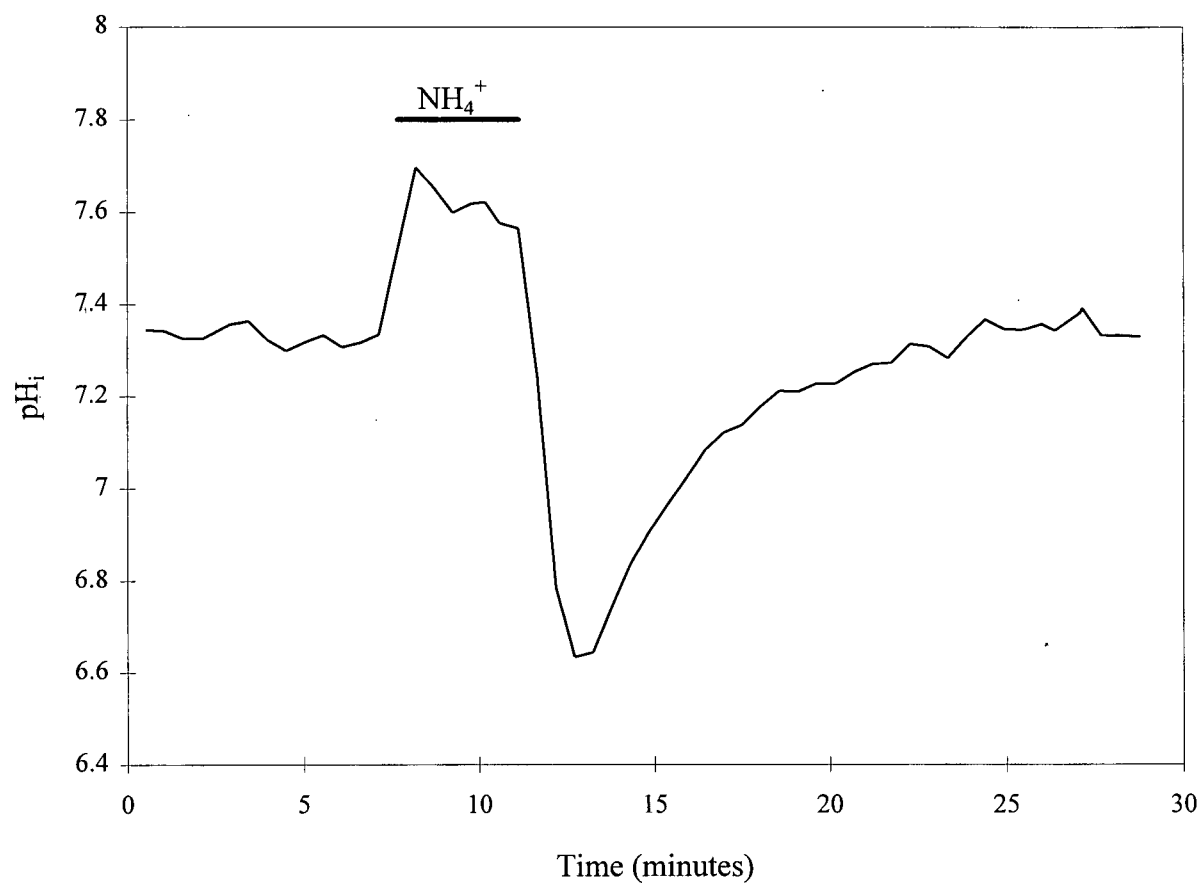


Table 6: pH_i recoveries from an NH_4^+ -induced intracellular acidification.

Solution	Temp	pH_i increase (pH units)	Net pH_i decrease (pH units)	Initial rate ($\times 10^{-3}$ pH units/second)	t_{50} rate ($\times 10^{-3}$ pH units/second)	t_{80} rate ($\times 10^{-3}$ pH units/second)	t_{50} (seconds)	t_{80} (seconds)	n
<i>a</i> HEPES	room	0.52 ± 0.05	0.68 ± 0.04	1.31 ± 0.33	0.73 ± 0.16	0.35 ± 0.05	376 ± 56	824 ± 119	6
<i>b</i> $\text{HCO}_3^-/\text{CO}_2$	room	0.38 ± 0.01	0.70 ± 0.12	2.55 ± 0.17	1.38 ± 0.09	0.60 ± 0.05	173 ± 25	388 ± 52	7
<i>c</i> 0 $[\text{Cl}^-]_0$	room		0.43 ± 0.07	3.14 ± 0.14	1.83 ± 0.12	0.95 ± 0.08	89 ± 7	185 ± 14	3
<i>d</i> 200 μM DIDS	room		0.42 ± 0.01	0.95 ± 0.04	0.63 ± 0.03	0.33 ± 0.03	181 ± 25	456 ± 49	3
<i>e</i> 0 $[\text{Cl}^-]_0$ + DIDS	room		0.43 ± 0.04	1.18 ± 0.38	0.70 ± 0.25	0.30 ± 0.14	187 ± 49	494 ± 156	2
<i>f</i> HEPES	37°C	0.27 ± 0.03	0.66 ± 0.03	5.56 ± 1.04	3.43 ± 0.66	1.90 ± 0.35	109 ± 18	211 ± 32	12
<i>g</i> 0 $[\text{Na}^+]_0$	37°C		0.61 ± 0.10	-	-	-	-	-	2
<i>h</i> 50 μM EIPA	37°C		0.66 ± 0.03	5.64 ± 0.45	3.51 ± 0.29	2.12 ± 0.16	83 ± 11	157 ± 17	6
<i>i</i> 200 μM DIDS	37°C		0.64 ± 0.07	3.93 ± 0.53	2.29 ± 0.20	1.05 ± 0.13	95 ± 8	216 ± 10	3
<i>j</i> $\text{HCO}_3^-/\text{CO}_2$	37°C	0.11 ± 0.01	0.51 ± 0.03	4.77 ± 0.58	2.76 ± 0.32	1.22 ± 0.14	75 ± 7	170 ± 18	16
<i>k</i> 0 $[\text{Na}^+]_0$	37°C		0.63 ± 0.04	-	-	-	-	-	3
<i>l</i> 50 μM EIPA	37°C		0.50 ± 0.08	4.82 ± 0.16	2.66 ± 0.81	1.26 ± 0.36	78 ± 10	165 ± 23	3
<i>m</i> 0 $[\text{Cl}^-]_0$	37°C		0.43 ± 0.03	4.46 ± 0.65	2.83 ± 0.38	1.52 ± 0.21	64 ± 12	134 ± 24	7
<i>n</i> DIDS (-)	37°C		0.44 ± 0.03	4.90 ± 1.19	2.91 ± 0.72	1.06 ± 0.26	57 ± 15	139 ± 32	4
<i>o</i> DIDS (+)	37°C		0.40 ± 0.03	1.02 ± 0.19	0.73 ± 0.12	0.50 ± 0.08	231 ± 59	455 ± 90	5
<i>p</i> pH_0 6.8	37°C		0.53 ± 0.09	7.12 ± 1.98	4.58 ± 1.30	2.18 ± 0.54	60 ± 32	127 ± 66	3
<i>q</i> pH_0 6.8 + DIDS	37°C		0.46 ± 0.06	9.68 ± 0.62	6.59 ± 0.98	3.31 ± 0.79	27 ± 7	58 ± 16	2

Rates of pH_i recovery were determined at room temperature (room) and at 37°C under the various conditions listed. Solutions were prepared according to recipes shown in Tables 1 to 4. Values are reported as the mean of n coverslips (i.e. cell populations), \pm S.E.M. Indicated rates are the instantaneous change in pH_i per unit time ($d\text{pH}_i/dt$), determined from the derivatives of exponential fit curves for the pH_i versus time record. DIDS (-) data refers to those pH_i recoveries that were not effected by 200 μM DIDS; DIDS (+) data refers to those pH_i recoveries that were inhibited by 200 μM DIDS.

Figure 22. Initial rate of acid load recovery as a function of pH_i , preload pH_i , minimum pH_i , and net pH_i decrease.

A. Based on a single experiment at 37°C in the absence of HCO_3^- , though indicative of all recoveries, the initial instantaneous rate of recovery was maximal at the minimum pH_i reached during the acid load. The rate of recovery decreased to 0 in a linear fashion as pH_i returned to the preload level. **B.** The initial rates of recovery from 14 randomly chosen experiments (9 in the presence and 5 in the absence of HCO_3^- at 37°C) as a function of the preload pH_i (\circ), and the minimum pH_i reached during the acid load (\bullet). **C.** The initial rates of recovery of the same 14 experiments shown in B as a function of the net pH_i decrease, which is the difference between the preload pH_i and the minimum pH_i reached during the acid load.

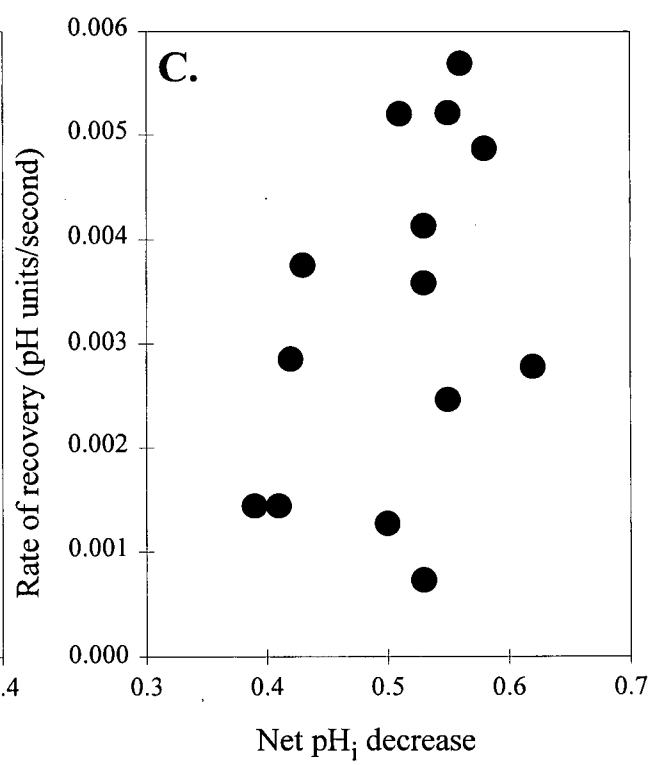
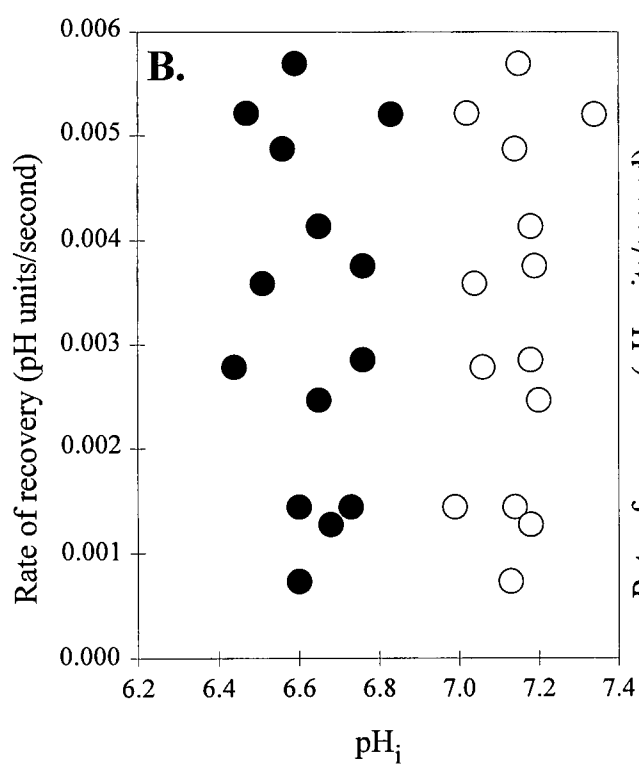
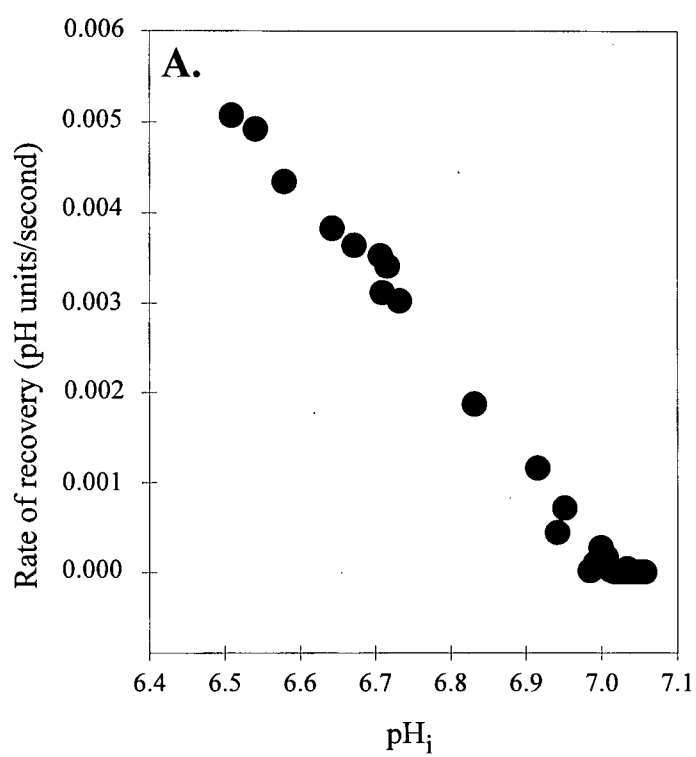


Figure 23. pH_i recovery from an acid load in the absence and presence of HCO_3^- at room temperature.

In the absence of $\text{HCO}_3^-/\text{CO}_2$ buffer at room temperature (*solution 1* at pH_o 7.33), pH_i recovered from an NH_4^+ -induced acid load at an initial rate of 1.31×10^{-3} pH units/second ($n=6$). Recovery from an acid load was faster in the presence of HCO_3^- (*solution 12*). Under the latter conditions, the initial rate of recovery was 2.55×10^{-3} pH units/second ($n=7$). The trace is a mean of data simultaneously obtained from 26 cells recorded on a single coverslip.

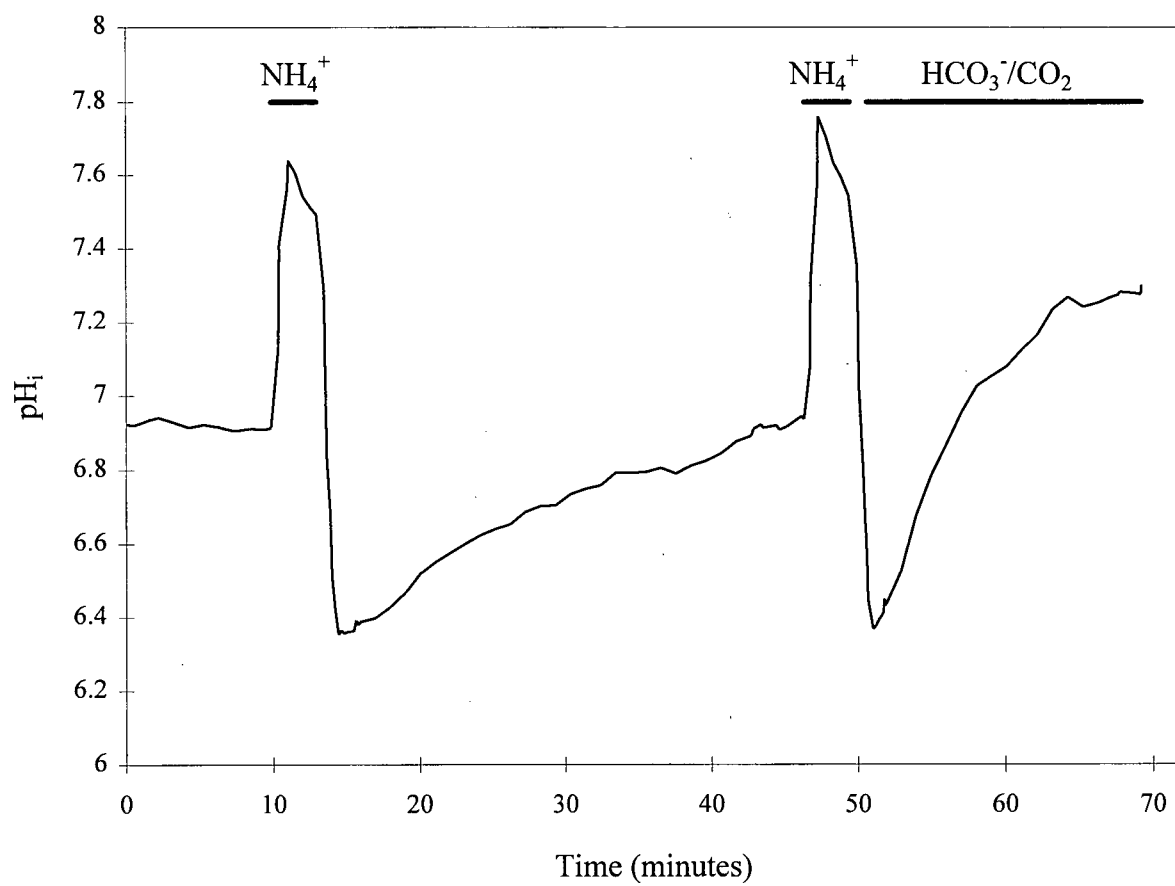


Figure 24. Effect of DIDS on pH_i recovery from an acid load in the presence of HCO_3^- at room temperature.

At pH_o 7.32, the application of 200 μM DIDS, a pharmacological inhibitor of $\text{HCO}_3^-/\text{Cl}^-$ exchange, slowed the pH_i recovery from an induced intracellular acidification when applied during the period indicated by the bar above the trace ($n=3$). In the presence of DIDS, the initial rate of pH_i recovery was 0.95×10^{-3} pH units/second. The trace is a mean of data obtained from 22 cells recorded on a single coverslip.

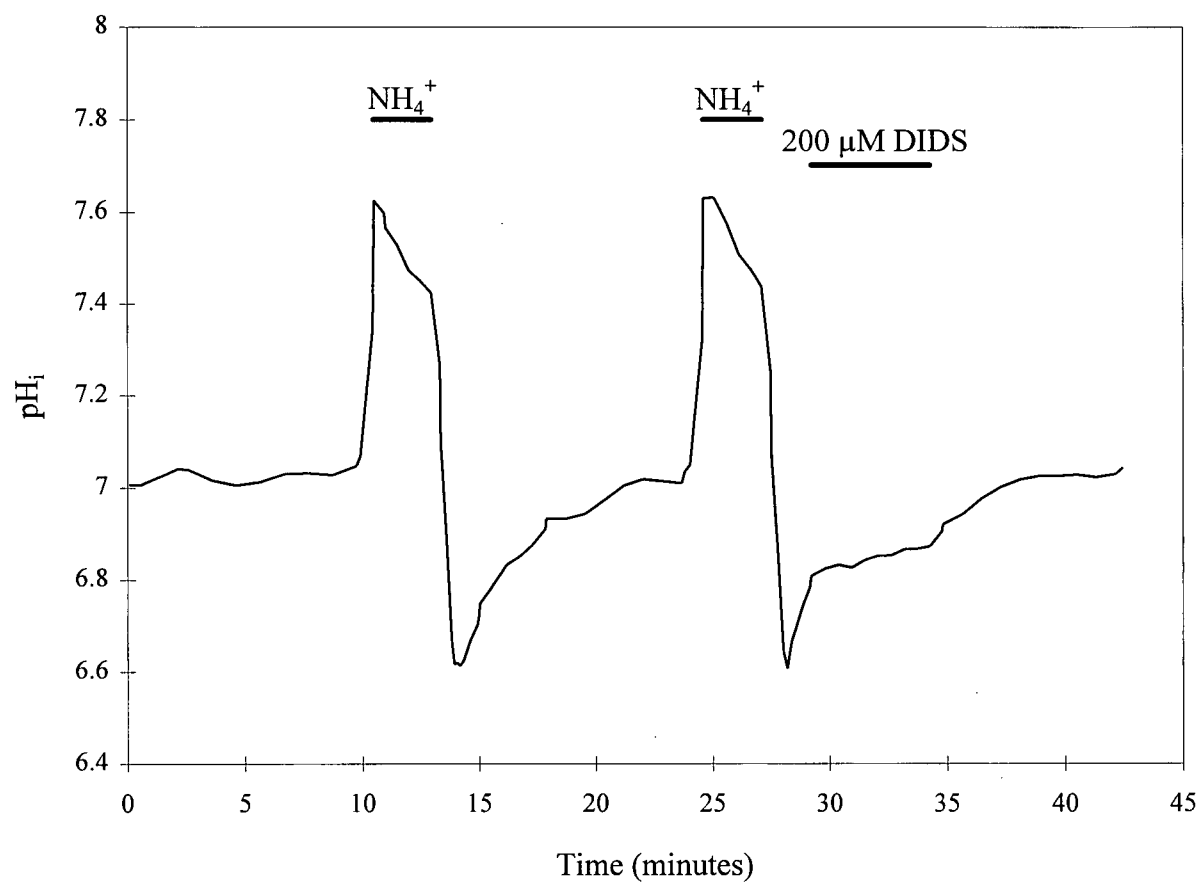


Figure 25. Effect of 0 $[\text{Cl}^-]_o$ on pH_i recovery from an acid load in the presence of HCO_3^- at room temperature.

A. At pH_o 7.33, the removal of extracellular Cl^- at room temperature (*solution 8*) enhanced the rate pH_i recovery from an acid load ($n=3$). Under $[\text{Cl}^-]_o$ -free conditions, the initial rate of recovery increased to 3.14×10^{-3} pH units/second from 2.55×10^{-3} pH units/second in the presence of $[\text{Cl}^-]_o$. **B.** The increase in the recovery rate caused by exposure to 0 $[\text{Cl}^-]_o$ was blocked by the simultaneous application of 200 μM DIDS. In the absence of $[\text{Cl}^-]_o$ and the presence of DIDS, the initial rate of pH_i recovery was 1.18×10^{-3} pH units/second ($n=2$). Trace A is mean of data obtained from 26 cells, whereas trace B is a mean of data obtained from 34 cells, each recorded on a separate coverslip.

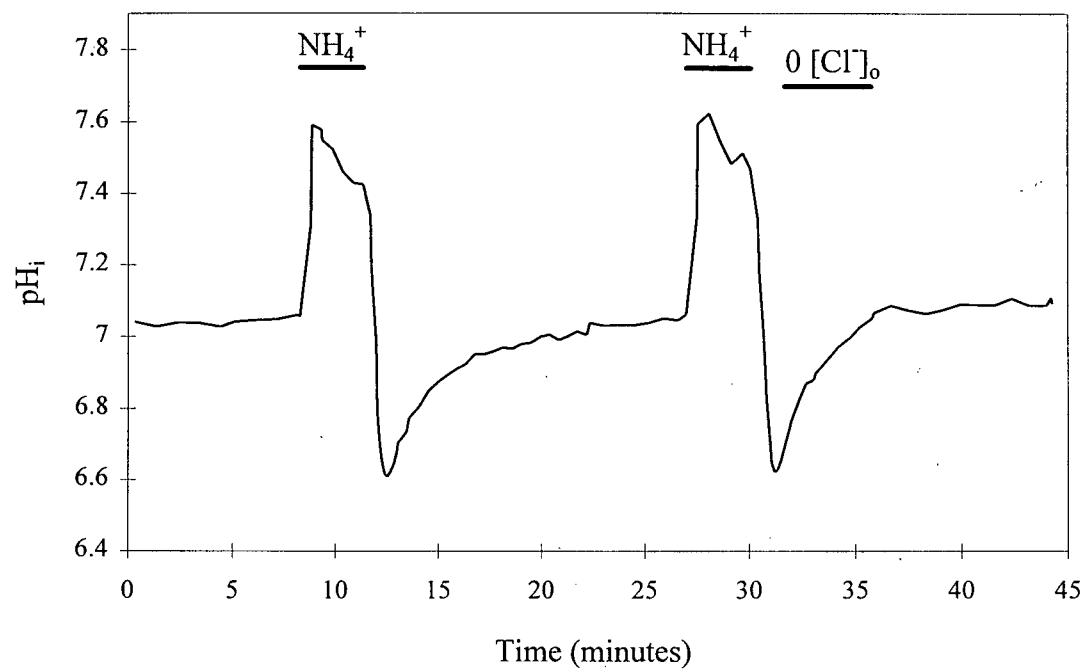
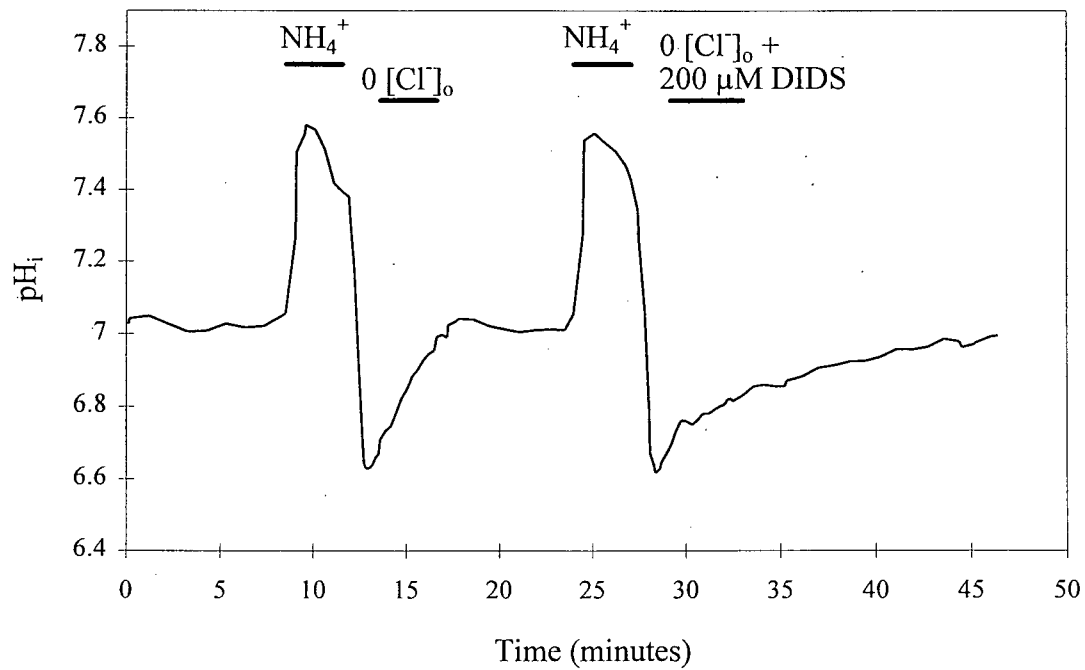
A.**B.**

Figure 26. pH_i recovery from an acid load in the absence and presence of HCO_3^- at 37°C .

In the absence of HCO_3^- at 37°C (*solution 1* at pH_o 7.36), pH_i recovered from an NH_4^+ -induced intracellular acid load at an initial rate of 5.56×10^{-3} pH units/second ($n=12$). The presence of HCO_3^- (*solution 12*) did not significantly alter the restoration rate at this temperature; cells buffered by $\text{HCO}_3^-/\text{CO}_2$ recovered from an imposed acidification with an initial rate of 4.77×10^{-3} pH units/second ($n=16$). The trace is a mean of data obtained from 7 cells recorded on a single coverslip. Compare with Figure 23, which is a similar experiment performed at room temperature.

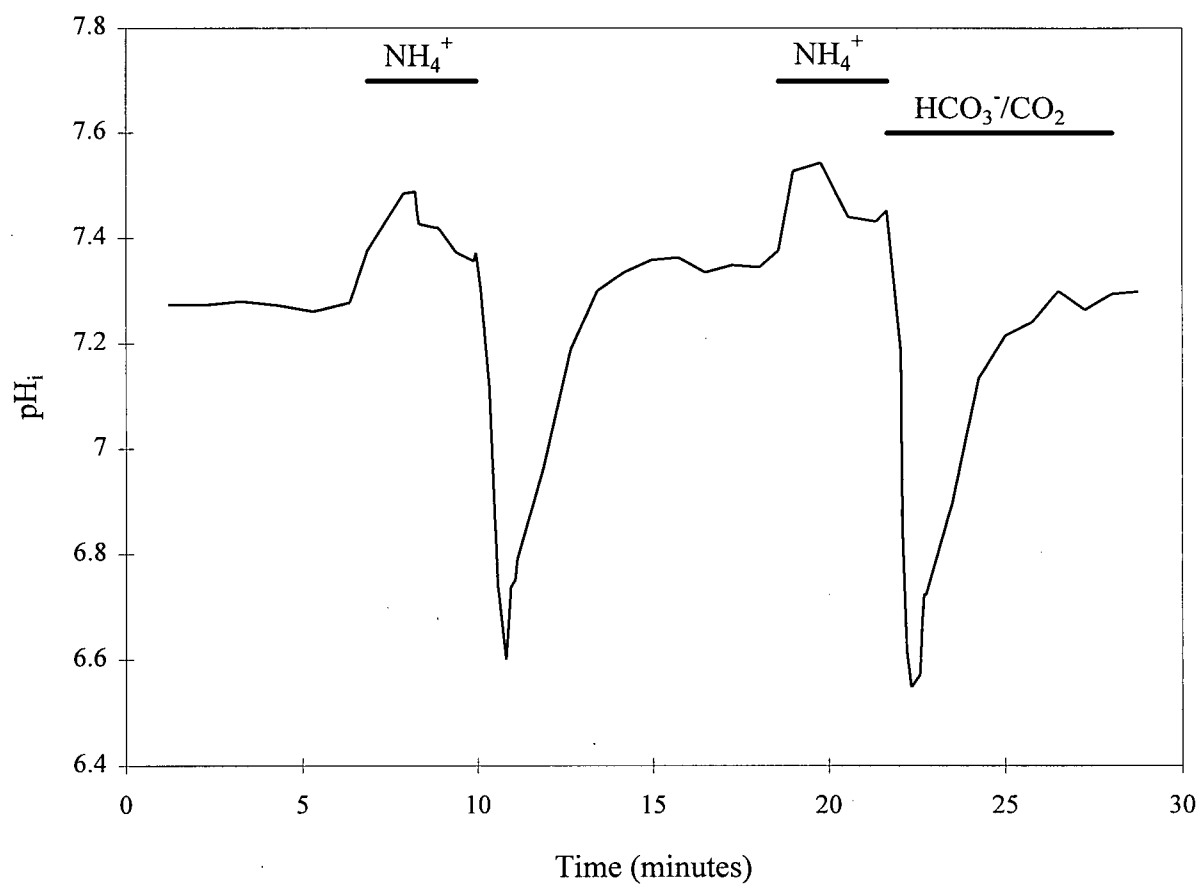


Figure 27. Effect of 0 $[\text{Na}^+]_o$ on pH_i recovery from an acid load in the absence of HCO_3^- at 37°C.

The removal of extracellular Na^+ in the absence of HCO_3^- (*solution 2* at pH_o 7.32) completely halted the ability of pH_i to recover from an induced acid load ($n=2$). Once $[\text{Na}^+]_o$ was re-introduced to the perfusion medium, pH_i resumed its recovery to normal resting levels. The trace is a mean of data obtained from 10 cells recorded on a single coverslip.

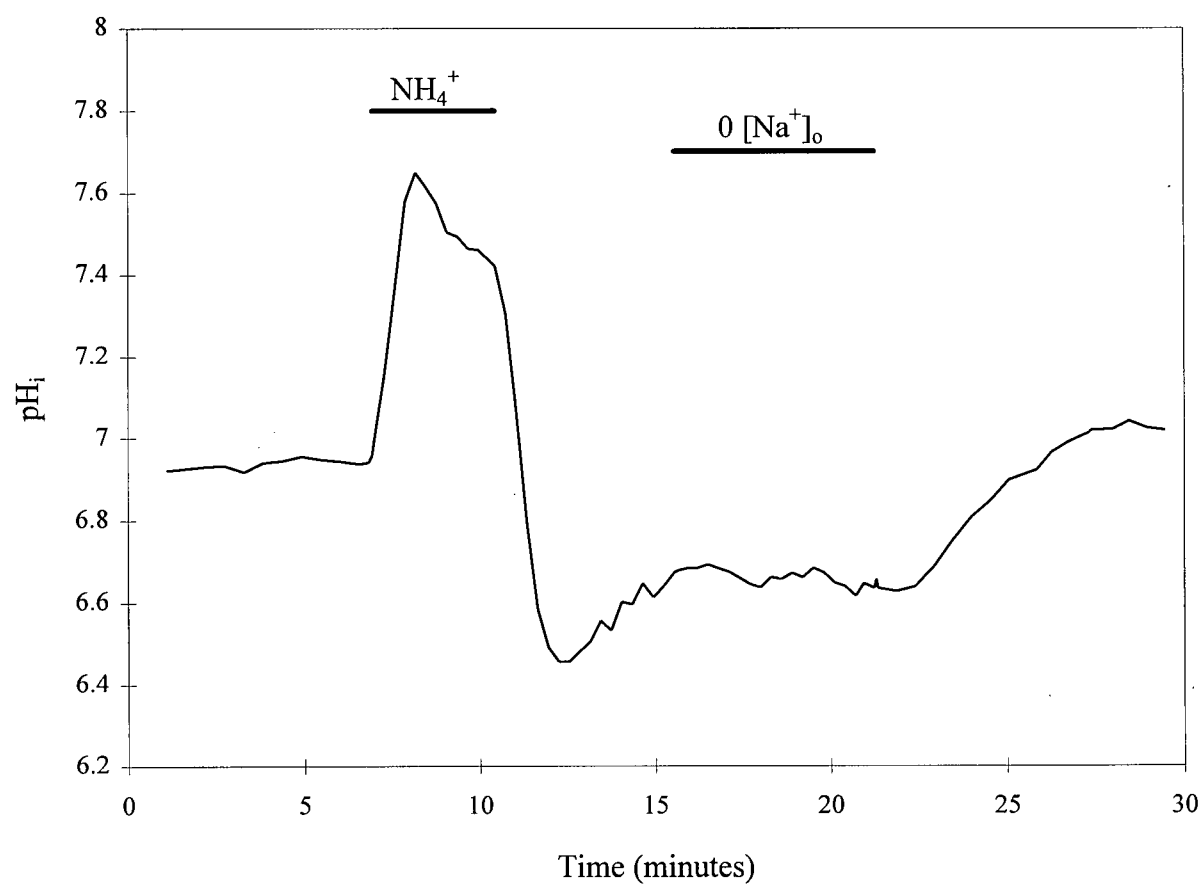


Figure 28. Effect of EIPA on pH_i recovery from an acid load in the absence of HCO_3^- at 37°C.

The addition of 50 μM EIPA to the HEPES buffered perfusion medium (*solution 1*) at 37°C (pH_o 7.35) did not affect the rate of pH_i recovery during the restoration of pH_i to normal levels after an induced intracellular acidification ($n=6$). The trace is a mean of data obtained from 30 cells recorded on a single coverslip.

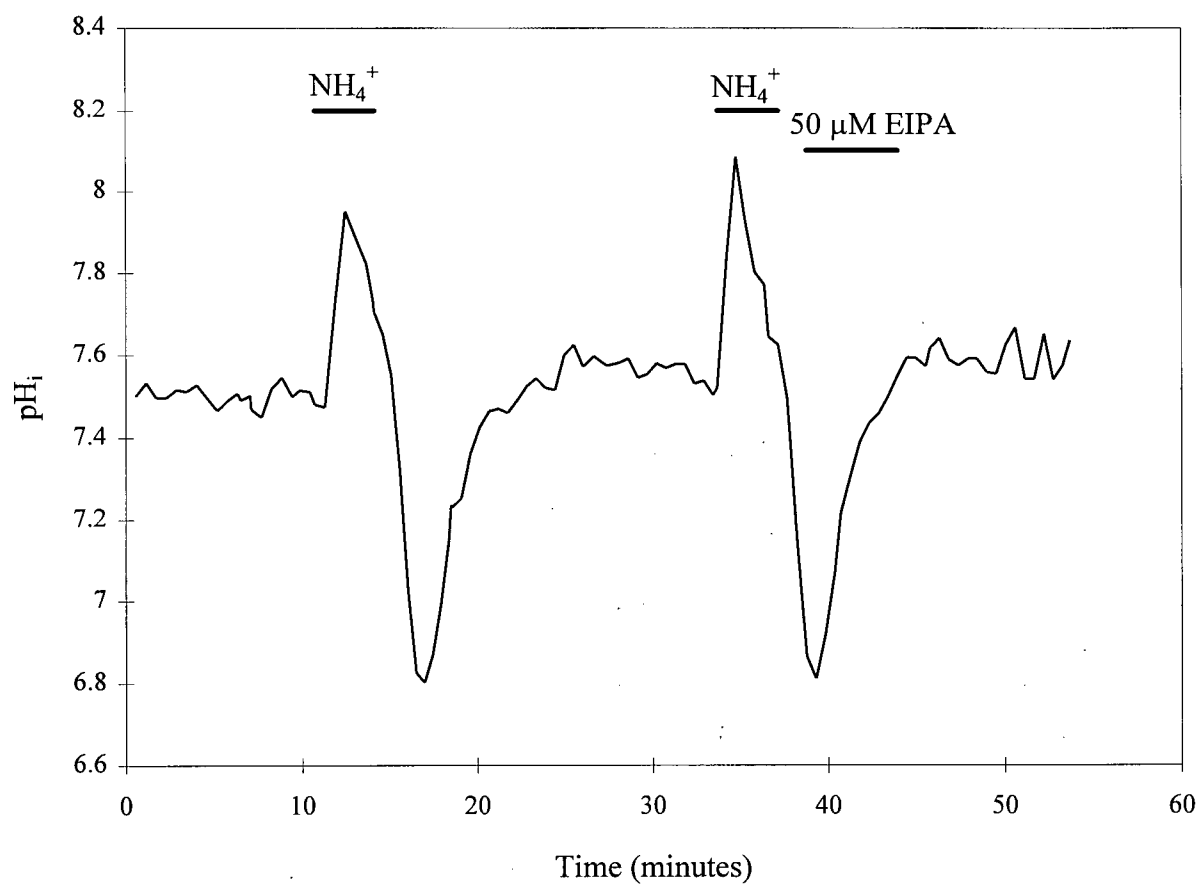


Figure 29. Effect of DIDS on pH_i recovery from an acid load in the absence of HCO_3^- at 37°C .

The application of $200\ \mu\text{M}$ DIDS during the restoration of pH_i did not significantly affect the rate of pH_i recovery in neurones perfused in the absence of HCO_3^- at 37°C (pH_o 7.37). The trace is a mean of data obtained from 23 cells recorded from 1 of the 3 cell populations studied.

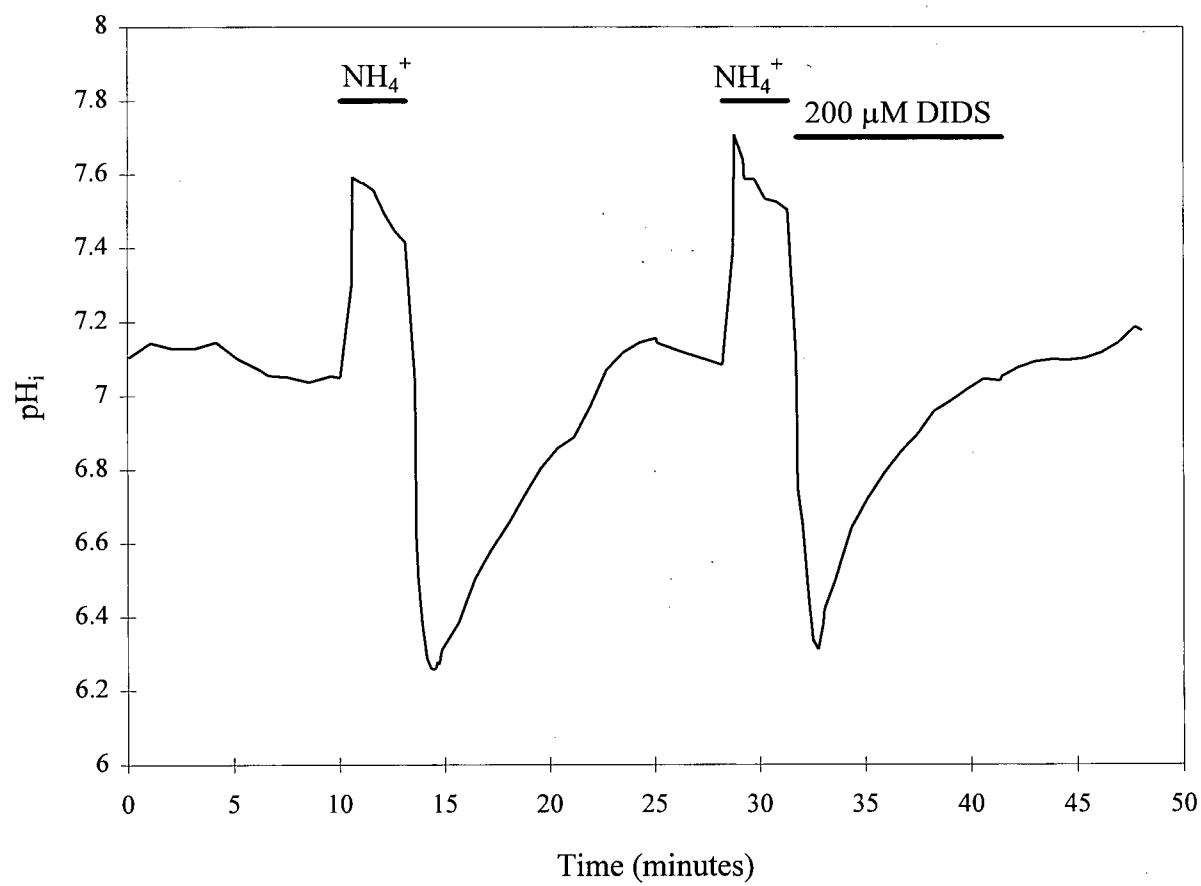


Figure 30. Effect of 0 $[\text{Na}^+]_o$ on pH_i recovery from an acid load in the presence of HCO_3^- at 37°C.

At pH_o 7.36, the removal of extracellular Na^+ in the presence of HCO_3^- at 37°C (*solution 13*) at the point of peak acidification caused a near complete inhibition of pH_i recovery ($n=3$). However, some pH_i recovery did occur despite the absence of $[\text{Na}^+]_o$, possibly due to the activity of Na^+ -independent recovery mechanisms. The re-addition of $[\text{Na}^+]_o$ resulted in a rapid restoration of pH_i to steady-state levels. The trace is a mean of data obtained from 37 cells recorded on a single coverslip.

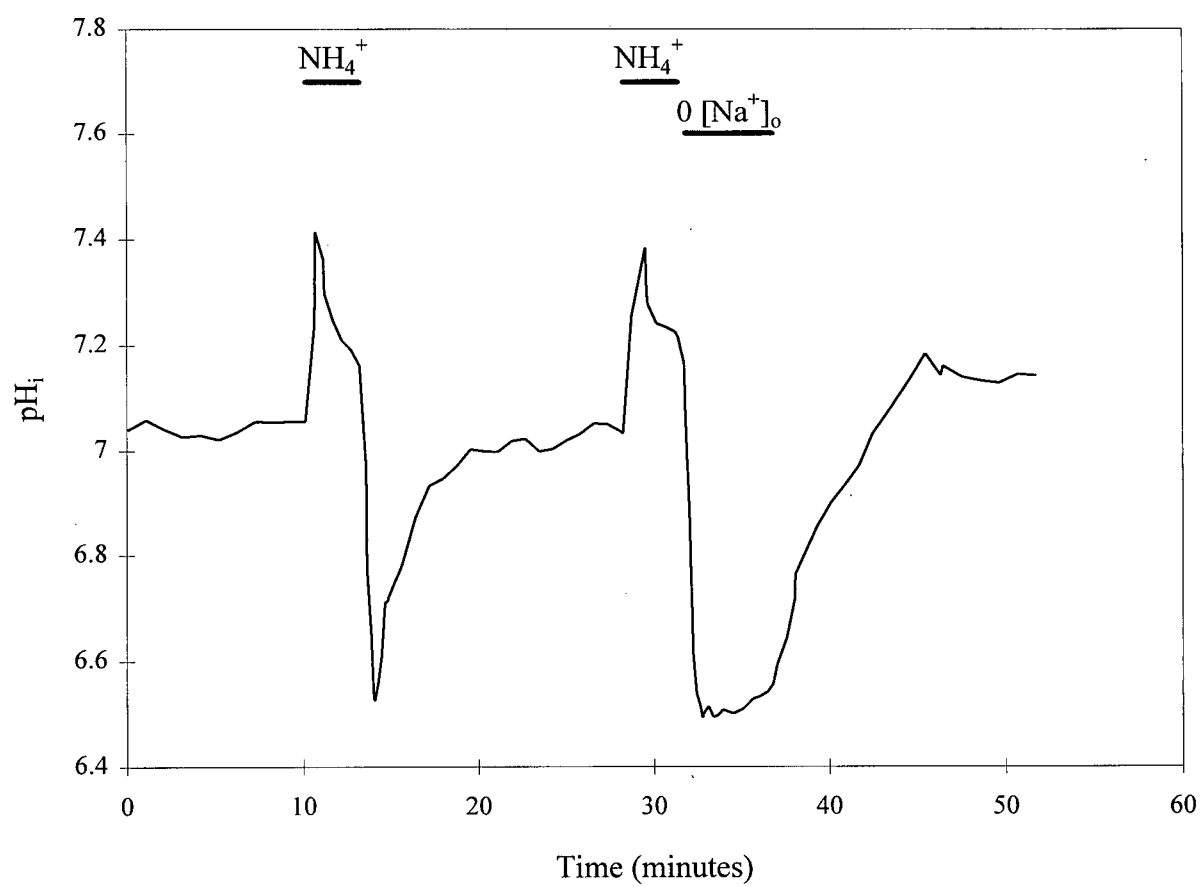


Figure 31. Effect of EIPA on pH_i recovery from an acid load in the presence of HCO_3^- at 37°C .

In neurones exposed to solutions containing $\text{HCO}_3^-/\text{CO}_2$ at 37°C (pH_o 7.34), the addition of $50\text{ }\mu\text{M}$ EIPA during the period of pH_i restoration did not alter the rate of pH_i recovery from an induced acidification ($n=3$). The trace is a mean of data obtained from 25 cells recorded on a single coverslip.

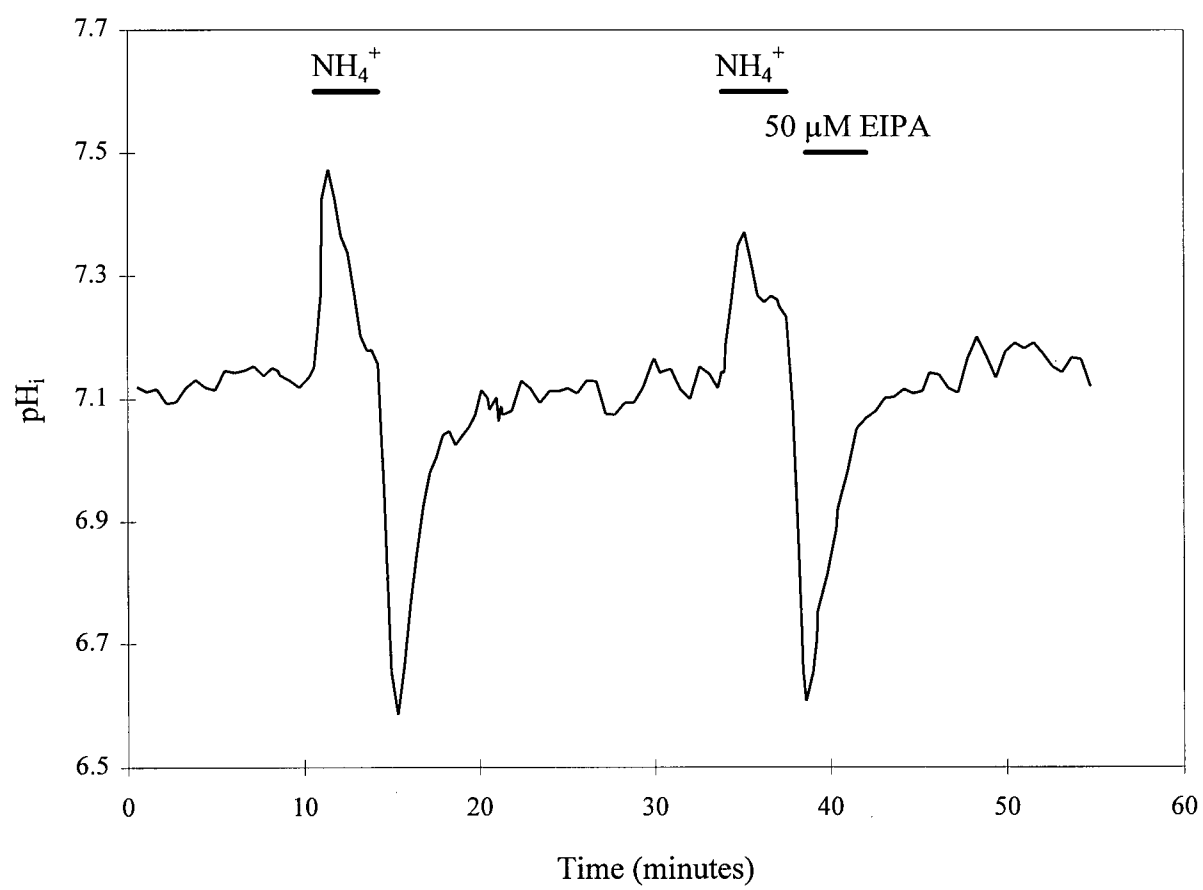


Figure 32. Effect of 0 $[\text{Cl}^-]_o$ on pH_i recovery from an acid load in the presence of HCO_3^- at 37°C .

The removal of extracellular Cl^- in the presence of HCO_3^- at 37°C (*solution 14*) did not increase the rate of recovery from an induced acidification ($n=7$). Though pH_o was held constant at 7.37, pH_i did recover to a slightly higher resting value in the absence of $[\text{Cl}^-]_o$, but returned to normal steady-state levels when $[\text{Cl}^-]_o$ was re-introduced to the perfusion medium. The trace is a mean of data obtained from 28 cells recorded on a single coverslip. Compare with Figure 25, which shows the effect of exposure to 0 $[\text{Cl}^-]_o$ on pH_i recovery in the presence of HCO_3^- at room temperature.

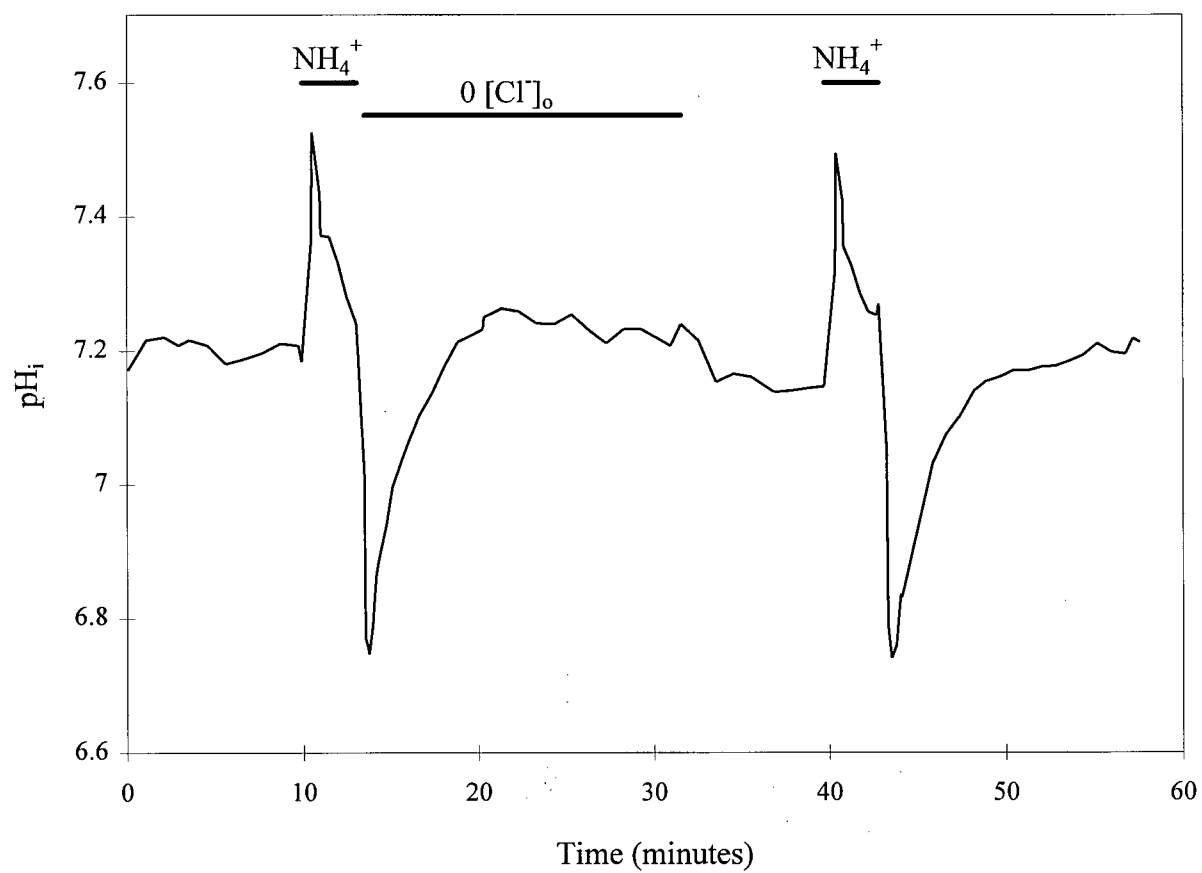


Figure 33. Effect of DIDS on pH_i recovery from an acid load in the presence of HCO_3^- at 37°C .

The application of DIDS had a variable effect on the rate of recovery from an induced acidification in the presence of HCO_3^- at 37°C (pH_o 7.37). **A.** The rate of recovery was inhibited by 200 μM DIDS in 5 out of 9 coverslips studied. pH_i restoration was significantly slowed as soon as DIDS was added to the extracellular solution. The initial pH_i recovery rate on those cell populations affected by DIDS was 1.02×10^{-3} pH units/second. The removal of DIDS resulted in an increase in the recovery rate until steady-state pH_i levels were attained. This trace is a mean of data obtained from 49 cells recorded on a single coverslip. **B.** On the remaining 4 coverslips, the application of 200 μM DIDS failed to slow the restoration towards resting pH_i levels. This trace is a mean of data obtained from 28 cells recorded on a separate coverslip to the one used in trace A. Compare with the same experiment performed at room temperature (Figure 24).

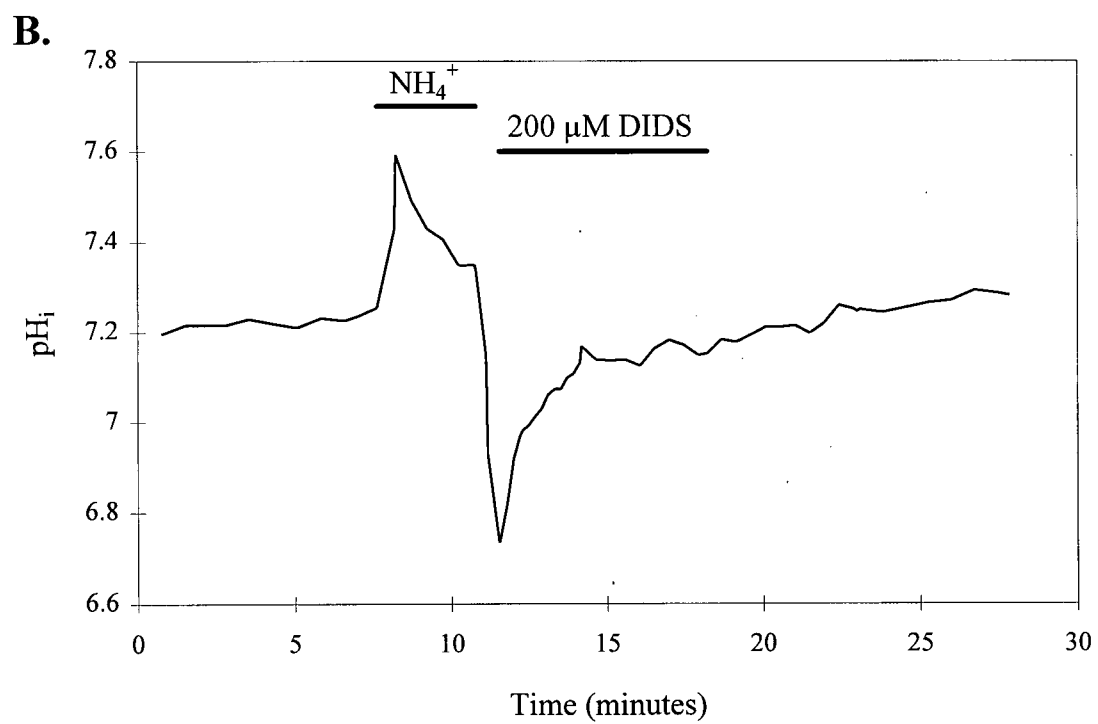
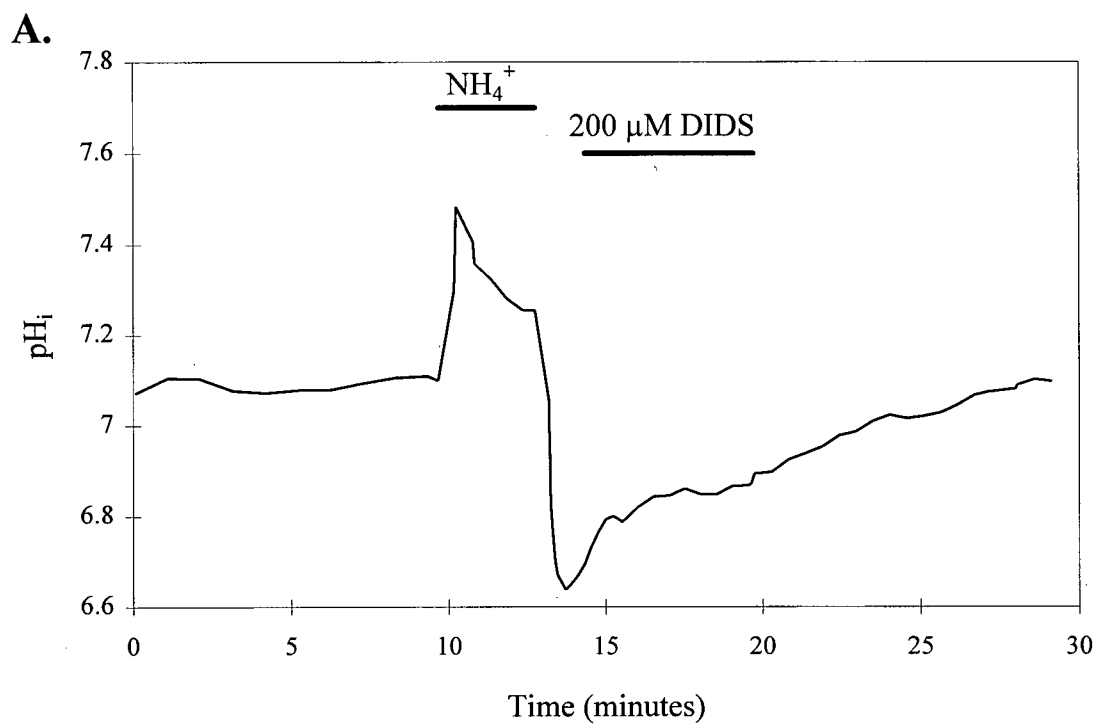
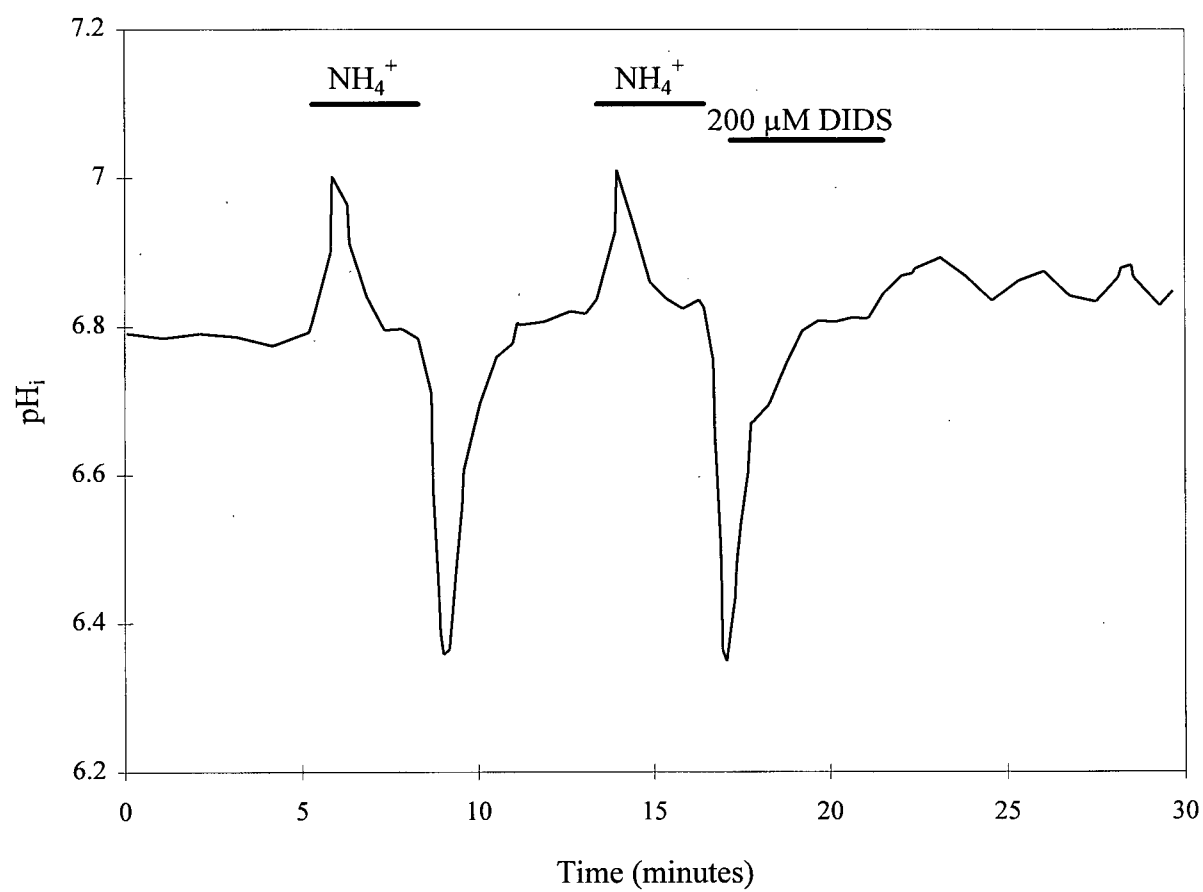


Figure 34. Effect of DIDS on pH_i recovery from an enhanced acid load in the presence of HCO_3^- at 37°C .

The pH of the perfusion medium was lowered to 6.80 (*solutions 18 and 19*) in order to reduce the resting pH_i (see Figure 19). This manoeuvre also lowered the minimum pH_i reached during the induced intracellular acidification. Under drug-free conditions at pH_o 6.8 (first acid load), the initial rate of pH_i recovery was 7.12×10^{-3} pH units/second ($n=3$). The presence of 200 μM DIDS during pH_i restoration failed to slow the rate of recovery ($n=2$). The trace is a mean of data obtained from 8 cells recorded on a single coverslip.



DISCUSSION

pH_i regulation, studied in various cell types, has been the source of considerable investigation. The predominant mechanisms regulating pH_i in the limited number of vertebrate neurone types studied to date appear to be a Na⁺/H⁺ exchanger, a Na⁺-independent HCO₃⁻/Cl⁻ exchanger, and a Na⁺-dependent HCO₃⁻/Cl⁻ exchanger (see, for example, Ou-yang *et al*, 1993; Raley-Susman *et al*, 1991; Schwiening and Boron, 1994). Other mechanisms have been described (e.g. Martínez-Zaguilán *et al*, 1994), though these appear to play a minor role. Very few studies, however, have comparatively examined the regulation of pH_i at room temperature and 37°C. The results presented in this thesis uncover some striking differences in pH_i regulation caused by temperature. Accordingly, this discussion will not only examine the mechanisms regulating the intracellular proton environment in cultured rat hippocampal neurones at 37°C and at room temperature, but will also address possible reasons underlying the differences in pH_i regulation at these two temperatures.

Regulation of pH_i at 37°C:

Steady-state pH_i resulting from the perfusion of the neurones at 37°C with HCO₃⁻-free HEPES buffered medium (pH_o 7.34) was 7.23. Resting pH_i in the nominal absence of HCO₃⁻ at 37°C (pH_o 7.35 to 7.4) has been reported to reside at 7.03 in cultured rat sympathetic neurones (Tolkovsky and Richards, 1987), 7.00 in cultured rat hippocampal neurones (Raley-Susman *et al*, 1991), 7.00 in cultured rat cortical neurones (Ou-yang *et al*, 1993), and 6.74 in freshly isolated CA1 pyramidal neurones from rat hippocampi (Schwiening and Boron, 1994). However, Gaillard and Dupont (1990) have shown that steady-state pH_i is 7.37 in cultured rat cerebellar Purkinje cells perfused with HEPES-buffered solutions (pH_o 7.4). Therefore, the value of resting pH_i determined in

the present experiments under HCO_3^- -free conditions is well within the reported range for vertebrate neurones.

The neurones employed in this study were able to sustain a stable pH_i during exposure to HEPES buffered (i.e. $\text{HCO}_3^-/\text{CO}_2$ -free) medium, thus indicating a significant contribution of HCO_3^- -independent mechanisms towards the maintenance of normal pH_i levels at 37°C . Under HCO_3^- -free conditions, the removal of extracellular Na^+ produced a marked and sustained acidification, which was reversed by the re-addition of $[\text{Na}^+]_o$ to the perfusion medium. These observations indicate the presence of a Na^+ -dependent acid extrusion mechanism operating independently of HCO_3^- . A probable candidate for this mechanism is the Na^+/H^+ exchanger, which removes intracellular protons in exchange for extracellular Na^+ . In the absence of $[\text{Na}^+]_o$ this antiporter is not able to function, causing an accumulation of intracellular acid equivalents. A small portion of these equivalents may originate outside of the membrane and leak through to the cytoplasm down an electrochemical gradient, but most are likely generated from normal cellular metabolism. The acidification resulting from the removal of $[\text{Na}^+]_o$ could also be explained by a reversal of the Na^+/H^+ antiporter, although it was not possible to test this in view of the lack of a pharmacological inhibitor.

To confirm the presence of the Na^+/H^+ exchanger on these neurones, a useful test would have been to inhibit its activity utilizing known pharmacological blockers. Unfortunately, the application of various Na^+/H^+ exchange inhibitors, including 2 potent amiloride analogues and one novel inhibitor, failed to alter steady-state pH_i in the absence of HCO_3^- at 37°C . EIPA, applied at a concentration of $50\text{ }\mu\text{M}$, did not influence resting pH_i , nor did it inhibit the recovery of pH_i after a $0\text{ }[\text{Na}^+]_o$ -induced acidification. Similarly, $100\text{ }\mu\text{M}$ MGCMA, which has been shown to inhibit the Na^+/H^+ antiporter in rat striatal synaptosomes (Amoroso *et al*, 1991), and $100\text{ }\mu\text{M}$ HOE 694, a novel inhibitor of Na^+/H^+ exchange first studied on brain capillary endothelial cells (Schmid *et al*, 1992), were both incapable of producing a change in baseline pH_i . To examine whether the

presence of HCO_3^- was required for the manipulation of pH_i by EIPA, the cation exchange inhibitor was applied to neurones perfused with $\text{HCO}_3^-/\text{CO}_2$ -buffered medium. Again, the application of 50 μM EIPA did not induce a change in pH_i . The insensitivity of the Na^+ -dependent acid extrusion mechanism present in hippocampal pyramidal neurones to amiloride and its analogues has recently been reported in two additional studies. Raley-Susman *et al* (1991) and Schwiening and Boron (1994) have observed that amiloride, or additional analogues tested, were unable to modulate the activity of the suspected Na^+/H^+ exchanger present on the cells used in their experiments. In contrast, it has been demonstrated that the regulation of pH_i is completely sensitive to amiloride in cultured rat Purkinje cells (Gaillard and Dupont, 1990) and sympathetic neurones (Tolkovsky and Richards, 1987), and partially sensitive to amiloride in cultured rat cortical neurones (Ou-yang *et al*, 1993). Other cation exchange inhibitors, such as harmaline (Aronson and Bounds, 1981), were not examined due to interference with the fluorescence signal emitted by the BCECF-loaded neurones. Although initially reported to inhibit Na^+/H^+ exchange in cultured hippocampal pyramidal cell loaded with BCECF (Raley-Susman *et al*, 1991), this finding has been questioned by others (e.g. Ou-yang *et al*, 1993; Schwiening and Boron, 1994) due to this technical limitation.

An analysis of the kinetic properties of cation counter-transport on various cell types has revealed that Li^+ is a substrate for the operation of the Na^+/H^+ antiporter (Aronson, 1985). The substitution of $[\text{Na}^+]_o$ with $[\text{Li}^+]_o$ has therefore been utilized as an alternative means of suggesting the presence of Na^+/H^+ exchange on cells insensitive to amiloride (Raley-Susman *et al*, 1991). The latter authors demonstrated that the replacement of $[\text{Na}^+]_o$ with $[\text{Li}^+]_o$ did not significantly alter the ability of cultured hippocampal neurones to regulate pH_i , which indicates that the Na^+ -dependent acid extrusion mechanism present was likely the Na^+/H^+ exchanger, despite its insensitivity to amiloride. Indeed, preliminary results on the neurones employed in this study indicate that the replacement of $[\text{Na}^+]_o$ with $[\text{Li}^+]_o$ does not jeopardize the maintenance of a stable

resting pH_i in HCO_3^- -free medium at 37°C . Accordingly, the Na^+ -dependent, HCO_3^- -independent acid extrusion mechanism regulating pH_i on these neurones may be an amiloride-insensitive variant of the Na^+/H^+ exchanger, similar to that proposed by Raley-Susman *et al* (1991), and Schwiening and Boron (1994).

Four isoforms of the Na^+/H^+ exchanger (NHE) have recently been distinguished (Mrkic *et al*, 1993) based on their amiloride sensitivity and tissue localization. The NHE-1 form, present on the basolateral surfaces of intestinal and kidney epithelia, is sensitive to amiloride (Sardet *et al*, 1989). Relative amiloride sensitivity has also been observed with the NHE-2 isoform, which has been localized in the intestine, kidney, and adrenal gland (Tse *et al*, 1991). An NHE-3 subtype, which is *hyper-resistant* to amiloride and EIPA (Tse *et al*, 1993), is predominantly expressed in the kidney and intestine, though it has been detected in minute concentrations in the heart and brain (Orlowski *et al*, 1992). Finally, an NHE-4 isoform has been detected by Orlowski *et al* (1992) in many mammalian tissues, including the brain, though its sensitivity to amiloride and its analogues has not been documented. It is not known which of these four NHE isoforms, if any, may be present on the cultured hippocampal neurones employed in the present experiments, though their resistance to EIPA, MGCMA, and HOE 694 is apparent.

Steady-state pH_i resulting from the perfusion of these neurones with $\text{HCO}_3^-/\text{CO}_2$ -buffered medium at 37°C (pH_o 7.36) was 7.13. This value compares well with that reported in previous studies on mammalian central neurones maintained under similar conditions. At 37°C and in the presence of HCO_3^- , it has been reported that pH_i rests at 7.16 in cultured rat cerebellar granule cells (Pocock and Richards, 1989), 7.18 in mixed neuronal cultures from various rat brain regions (Richards and Pocock, 1989), 7.06 in cultured rat cerebellar Purkinje cells (Gaillard and Dupont, 1990), 7.17 in cultured rat hippocampal neurones (Raley-Susman *et al*, 1991), 7.09 in cultured rat cortical neurones (Ou-yang *et al*, 1993), and 7.03 in acutely dissociated adult rat hippocampal CA1 pyramidal neurones (Schwiening and Boron, 1994). In the neurones employed in this

study, baseline pH_i was 0.10 pH units lower in the presence of HCO_3^- than in the absence of HCO_3^- at 37°C . Indeed, the transition from HCO_3^- -free to HCO_3^- -containing perfusion medium at 37°C did not induce the net alkalization observed in the same experiment performed at room temperature (see below). Though a number of studies on vertebrate neurones have demonstrated that resting pH_i is higher in the presence than in the absence of HCO_3^- at 37°C (Raley-Susman *et al*, 1991; Ou-yang *et al*, 1993; Schwiening and Boron, 1994), others have indicated the opposite. Gaillard and Dupont (1990), for example, reported that steady-state pH_i in rat Purkinje cells buffered by $\text{HCO}_3^-/\text{CO}_2$ resides 0.21 pH units below the resting pH_i in HCO_3^- -free (HEPES-buffered) medium. Similarly, Richards and Pocock (1989), in their examination of rat brain neurones, indicate that the *removal* of external HCO_3^- causes an intracellular alkalization. Accordingly, the level of steady-state pH_i in the neurones used in this investigation observed in the presence of HCO_3^- -containing external media are not unlike those reported in other studies on vertebrate central neurones.

The removal of extracellular Na^+ in the presence of HCO_3^- initiated a rapid and sustained intracellular acidification, a result similar to that obtained in the absence of HCO_3^- (see above). The re-addition of $[\text{Na}^+]_o$ relieved this acid-load, and an immediate recovery to steady-state pH_i levels was observed. These observations indicate that, even in the presence of HCO_3^- , the maintenance of steady-state pH_i at 37°C is largely dependent on $[\text{Na}^+]_o$. In neurones buffered by $\text{HCO}_3^-/\text{CO}_2$ -containing solutions, the removal of extracellular Cl^- caused a 0.19 pH unit and a 0.14 pH unit intracellular alkalization in the presence and absence of $[\text{Na}^+]_o$, respectively. By removing $[\text{Cl}^-]_o$, the gradient for Cl^- across the membrane would be increased and may result in a directional reversal of the $\text{HCO}_3^-/\text{Cl}^-$ exchanger (see Gaillard and Dupont, 1990). This would cause an influx of extracellular HCO_3^- which would produce the observed intracellular alkalization. In the presence of $[\text{Na}^+]_o$, this 0 $[\text{Cl}^-]_o$ -induced alkalization was abolished by 200 μM DIDS, which adds weight to the possibility that a $\text{HCO}_3^-/\text{Cl}^-$

exchanger is present on these neurones. Furthermore, this anion exchanger may predominantly function in a Na^+ -independent manner since the amplitude of the 0 $[\text{Cl}^-]_o$ -induced pH_i rise had a similar magnitude whether $[\text{Na}^+]_o$ was present or not.

It is possible that, at 37°C , Na^+ -independent $\text{HCO}_3^-/\text{Cl}^-$ exchange may operate to maintain steady-state pH_i at a level slightly below that which is observed in the absence of HCO_3^- . However, the application of 200 μM DIDS did not affect baseline pH_i in neurones perfused in the presence of HCO_3^- , nor did it influence the manner in which pH_i responded to the transition from HCO_3^- -free to HCO_3^- -containing perfusion media. The inability of DIDS to affect pH_i in these situations does not support the presence of an *active* Na^+ -independent $\text{HCO}_3^-/\text{Cl}^-$ exchanger at 37°C . As resting pH_i can be altered by fluctuations in $[\text{Cl}^-]_o$, it is possible that some other Cl^- -dependent mechanism assists in preserving the steady-state pH_i in these cells. In fact, recent evidence suggests that a DIDS-sensitive Cl^-/H^+ co-transporter is involved in pH_i regulation in rat brain synaptosomes (Martínez-Zaguilán *et al*, 1994). However, the likelihood of this co-transporter being present on hippocampal neurones is remote, since the exposure to 0 $[\text{Cl}^-]_o$ in the absence of HCO_3^- at 37°C did not cause any change in steady-state pH_i . Moreover, in the presence of HCO_3^- , any 0 $[\text{Cl}^-]_o$ -induced alkalization was blocked by the simultaneous application of DIDS, which suggests that anion exchange is in fact present on these neurones, though likely contributes little to the maintenance of steady-state pH_i at 37°C .

A clearer indication of the manner in which cultured hippocampal neurones regulate pH_i at 37°C was achieved through the analysis of acid load recovery experiments. The addition and subsequent removal of 20 mM NH_4Cl from the extracellular perfusion medium provided a convenient means of lowering pH_i . The rate of pH_i restoration towards its resting level was therefore examined as a means of expanding the characterization of pH_i regulating mechanisms and, in addition, was employed to provide information on activity rates. Acid extrusion rates are often reported

as the rate of change of the intracellular proton concentration as a function of time. These net H^+ fluxes (J_{H^+}) are usually calculated as the product the total intracellular buffering capacity (β_T) and the rate of pH_i change during recovery from an imposed acidification (see Boyarski *et al*, 1988a). For reasons explained below, absolute buffering capacities were not determined in the present experiments. Accordingly, this discussion of acid load recovery rates will be limited to the rate of pH_i change measured in pH units per second.

In HCO_3^- -free HEPES buffered medium at $37^\circ C$, the removal of $[Na^+]_o$ during acid load recovery completely blocked pH_i restoration. The inability of pH_i to recover in 0 $[Na^+]_o$ suggests that pH_i is highly regulated by the activity of a Na^+ -dependent, HCO_3^- -independent acid extrusion mechanism. The most likely candidate for such a mechanism, as discussed above, is the Na^+/H^+ exchanger. EIPA, whether in the absence or presence of external HCO_3^- , did not inhibit the recovery from an imposed intracellular acidosis, which is consistent with previous results demonstrating the insensitivity of steady-state pH_i in these neurones to amiloride analogues.

The rate of pH_i recovery from an imposed acid load was not significantly different in the presence or absence of HCO_3^- at $37^\circ C$ (see Figure 35). However, in the absence of HCO_3^- , pH_i did recover from the induced acidification to a more alkaline pH, which likely reflects the fact that steady-state pH_i is higher under HCO_3^- -free conditions at $37^\circ C$. The similarity between acid load recovery rates in the presence and absence of HCO_3^- suggests that these neurones are not dependent on the anion exchanger to recover from acidic changes in pH_i at $37^\circ C$, possibly due to an increase in the neuronal buffering capacity (see below). However, in solutions buffered by HCO_3^-/CO_2 , the removal of $[Na^+]_o$ did not completely inhibit the ability of these neurones to recover from an NH_4^+ -induced acidification. Though small, the observed recovery of pH_i in the absence of $[Na^+]_o$ indicates an additional Na^+ -independent pH_i regulator operating at $37^\circ C$. Since this Na^+ -independent recovery was not present in similar experiments conducted in the

absence of external HCO_3^- , this mechanism likely requires HCO_3^- to function effectively. Possibilities include Na^+ -independent $\text{HCO}_3^-/\text{Cl}^-$ exchange, which has been shown to be present though relatively inactive at 37°C , or HCO_3^- -dependent intracellular buffering. In fact, it appears that both of these factors may be involved in pH_i recovery from acidic levels at 37°C . In 5 of 9 neuronal populations studied, DIDS significantly slowed recovery rates from an imposed acid load, which reveals a dependence of pH_i restoration on the Na^+ -independent $\text{HCO}_3^-/\text{Cl}^-$ exchanger. As this transporter has previously been shown to remain relatively quiescent under steady-state conditions at 37°C , these 5 experiments uncover a possible relationship between the activity of the anion exchanger and the level of pH_i . Such a relationship between pH_i and the rate of acid extrusion has been demonstrated by Ou-yang *et al* (1993) on neurones isolated from the cortex of the rat brain. However, the remaining 4 neuronal populations exposed to DIDS during recovery from an acid load did not exhibit a reduction in pH_i recovery rates. Furthermore, the removal of $[\text{Cl}^-]_o$ during recovery did not alter the rate of pH_i restoration at 37°C . Taken as a whole, these results suggest that, at 37°C , the activity of the Na^+ -independent $\text{HCO}_3^-/\text{Cl}^-$ exchanger present on these neurones may be overshadowed by the operation of the Na^+/H^+ transporter or the increased efficiency of intracellular buffering systems (see below). Cells with an increased ability to resist pH_i perturbations through more efficient organellar, metabolic, or physiochemical buffering would presumably be less reliant on acid extruding exchangers for immediate recovery from an induced acidification. This hypothesis is a possible explanation for the apparent inactivity of the Na^+ -independent $\text{HCO}_3^-/\text{Cl}^-$ exchanger at 37°C . Nevertheless, by imposing a large intracellular acid load, the probability of activating the otherwise dormant anion exchanger to aid in pH_i regulation appears to increase.

In an attempt to test whether the Na^+ -independent $\text{HCO}_3^-/\text{Cl}^-$ exchanger could be activated by lowering pH_i to extreme levels, imposed acidifications were employed at pH_o 6.8 instead of the normal 7.35. The lowering of pH_o indeed caused a reduction in the

minimum pH_i reached during the NH_4^+ -induced acid load. As a result, the rate of pH_i recovery increased, but the application of DIDS during this procedure had no appreciable effect. Though this suggests a possible connection between the rate of pH_i recovery and pH_o , the observed increase in the recovery rate could not be attributed to the activation of Na^+ -independent $\text{HCO}_3^-/\text{Cl}^-$ exchange.

In summary, the regulation of pH_i at 37°C (pH_o 7.3 - 7.4) in cultured hippocampal neurones is primarily governed by the activity of a Na^+ -dependent, HCO_3^- -independent acid extrusion mechanism. The most likely candidate for this mechanism is an amiloride-insensitive Na^+/H^+ exchanger, as suggested by Raley-Susman *et al* (1991) and Schwiening and Boron (1994).

Regulation of pH_i at room temperature:

At room temperature, and in neurones superfused with HCO_3^- -free HEPES-buffered medium (pH_o 7.32), steady-state pH_i was 6.85, which is considerably lower than the value of pH_i 7.23 observed at 37°C under similar buffering conditions. In the absence of HCO_3^- , the removal of $[\text{Na}^+]_o$ from the perfusate resulted in a fall in pH_i similar to that observed at 37°C (see Figure 17) suggesting that the Na^+ -dependent, HCO_3^- -independent acid extrusion mechanism described at 37°C continues to operate at room temperature. However, in contrast to observations at 37°C , the addition of HCO_3^- to the perfusion solution caused pH_i to rise to the substantially higher level of 7.15. Moreover, the net alkalinization caused by the transition from HCO_3^- -free to HCO_3^- -containing perfusion medium at constant pH_o was blocked by the application of the anion exchange inhibitor DIDS. Thus, when transferring into media buffered by $\text{HCO}_3^-/\text{CO}_2$ at room temperature, the likely cause of the alkalinizing tendency was the activation of $\text{HCO}_3^-/\text{Cl}^-$ exchange. In experiments carried out in the absence of $[\text{Na}^+]_o$, the transition into from HCO_3^- -free to HCO_3^- -containing medium similarly produced an increase in pH_i , which further

suggests that the activity of the $\text{HCO}_3^-/\text{Cl}^-$ exchanger at room temperature is Na^+ -independent.

Under steady-state conditions in the presence of HCO_3^- at room temperature, the application of 200 μM DIDS caused a reduction in pH_i of approximately 0.1 pH units. This acidification was likely a result of the inhibition of the Na^+ -independent $\text{HCO}_3^-/\text{Cl}^-$ exchange which therefore must participate in the regulation of pH_i at this temperature. Furthermore, the removal of $[\text{Cl}^-]_o$ caused an approximate 0.3 pH unit intracellular alkalinization, probably due to a 0 $[\text{Cl}^-]_o$ -induced enhancement of $\text{HCO}_3^-/\text{Cl}^-$ exchange as described previously by Gaillard and Dupont (1990). These results suggest that the maintenance of steady-state pH_i in the presence of HCO_3^- at room temperature is at least partially regulated by Na^+ -independent $\text{HCO}_3^-/\text{Cl}^-$ exchange. The activity of this anion counter-transporter, which exchanges intracellular Cl^- for extracellular HCO_3^- and thus acts as a cell alkalinizing mechanism, is presumably responsible for the higher resting pH_i observed in the presence as opposed to the absence of HCO_3^- .

Rates of pH_i recovery from an imposed acid load at room temperature were, in general, slower than those found at 37°C (see Figure 35). At this reduced temperature and in contrast to results obtained at 37°C , the rate of pH_i recovery from an induced acidification also appeared to depend on the presence of HCO_3^- . As seen in Figure 35, the addition of HCO_3^- to the perfusion medium at room temperature resulted in a substantial enhancement of the recovery rate, which possibly reflects the activation of Na^+ -independent $\text{HCO}_3^-/\text{Cl}^-$ exchange. The dependence of pH_i recovery on $\text{HCO}_3^-/\text{Cl}^-$ exchange (either Na^+ -dependent or Na^+ -independent) has also been demonstrated in lamprey reticulospinal neurones at room temperature (Chesler, 1986). The presence of $\text{HCO}_3^-/\text{CO}_2$ could also act to augment the apparent intracellular buffering power (see Roos and Boron, 1981), which would in turn contribute to reduce the magnitude and duration of imposed acid transients. Indeed, a comparison of the net decreases in pH_i caused by the NH_4^+ prepulse at room temperature (column 4, Table 6) indicates that a

greater acidification was obtained under HCO_3^- -free conditions than under conditions where HCO_3^- was present in the perfusate. However, the effects of buffering capacity on HCO_3^- -induced increases in pH_i recovery rates at room temperature were likely overshadowed by the contribution of anion exchange. In fact, several other observations indicate that the Na^+ -independent $\text{HCO}_3^-/\text{Cl}^-$ exchanger is actively involved in the recovery of pH_i from an imposed acid load at this temperature. In the presence of HCO_3^- , pH_i was restored to a higher resting level after the imposed acidification than that seen in the absence of HCO_3^- (see Figure 23). This result suggests that Na^+ -independent $\text{HCO}_3^-/\text{Cl}^-$ exchange, while participating in the restoration of pH_i following an induced acid load, continues to regulate pH_i to the higher resting level observed under HCO_3^- -containing steady-state perfusion at room temperature. Furthermore, in the presence of HCO_3^- at room temperature, the removal of $[\text{Cl}^-]_o$ enhanced the rate of pH_i recovery. As noted above, removal of external Cl^- likely increases the activity of $\text{HCO}_3^-/\text{Cl}^-$ exchange and thus the 0 $[\text{Cl}^-]_o$ -induced increase in the pH_i recovery rate may be due to an acceleration of the anion exchanger. This possibility is confirmed by the observed inhibitory influence of DIDS on the rate of pH_i recovery at room temperature during $\text{HCO}_3^-/\text{CO}_2$ perfusion in the presence or absence of $[\text{Cl}^-]_o$. However, the fact that DIDS did not completely block acid load recovery indicates that other regulators of pH_i , such as the Na^+ -dependent, HCO_3^- -independent acid extrusion mechanism, may also be operational at room temperature.

Overall, the results of this study suggest that, at room temperature, a combination of a Na^+ -dependent, HCO_3^- -independent acid extrusion mechanism and a Na^+ -independent $\text{HCO}_3^-/\text{Cl}^-$ exchanger contribute to the regulation of pH_i in hippocampal neurones at steady-state as well as during pH_i recovery from an induced intracellular acidification.

Comparison of pH_i regulation at 37°C and room temperature:

Based either on steady-state pH_i observations or on data from acid-load recoveries, the conclusions regarding pH_i regulation at 37°C or at room temperature were very similar. Both at 37°C and at room temperature, pH_i appears to be predominantly regulated by the activity of a Na^+ -dependent, HCO_3^- -independent acid extrusion mechanism, probably an amiloride-insensitive variant of the Na^+/H^+ exchanger. The dominance of Na^+/H^+ exchange over pH_i regulation has been demonstrated in a variety of vertebrate central neurones at 37°C (Nachshen and Drapeau, 1988; Raley-Susman *et al*, 1991; Ou-yang *et al*, 1993). However, Schwiening and Boron (1994) concluded that the primary acid extrusion mechanism in CA1 pyramidal neurones acutely dissociated from adult rat hippocampi at 37°C is a Na^+ -dependent $\text{HCO}_3^-/\text{Cl}^-$ exchanger. The findings of the present study, however, indicate that the $\text{HCO}_3^-/\text{Cl}^-$ exchanger present on cultured foetal hippocampal neurones is not dependent on $[\text{Na}^+]_o$, and furthermore, the activity of this anion exchanger appears to be minimal under steady-state conditions at 37°C. As the neurones employed in this study were cultured from hippocampi obtained from foetal rats, the difference between the present results and those reported by Schwiening and Boron (1994) may reflect developmental changes. In fact, Raley-Susman *et al* (1993) have reported that $\text{HCO}_3^-/\text{Cl}^-$ exchange, which could not be demonstrated in either acutely dissociated or cultured foetal rat hippocampal neurones at 37°C, actively regulates pH_i in acutely dissociated adult neurones. However, this observation may reflect the fact that $\text{HCO}_3^-/\text{Cl}^-$ exchange is simply not active in foetal neurones at 37°C, rather than being completely absent. Indeed, Raley-Susman *et al* (1993) reported that both adult and foetal neurones express mRNA for this anion exchanger.

The results of the present investigation suggest that, rather than being absent from cultured foetal rat hippocampal pyramidal neurones, the Na^+ -independent $\text{HCO}_3^-/\text{Cl}^-$ exchange actively regulates neuronal pH_i , but only at a reduced temperature. There were, in addition, other differences in steady-state pH_i caused by changing the temperature of

the perfusion medium from 37°C to room temperature. In the absence of HCO_3^- , pH_i rested approximately 0.4 pH units lower when experiments were performed at room temperature in comparison to 37°C. In addition, resting pH_i at 37°C was higher in the absence of HCO_3^- , whereas at room temperature pH_i was higher in the presence of HCO_3^- . pH_i recovery rates from induced acidifications were also substantially enhanced when the temperature of the perfusate was increased to 37°C. Temperature-induced changes in the regulators of pH_i may reflect differential activities of the acid extrusion mechanisms present, or perturbations in the intracellular buffering capacity.

Buffering capacity is the ability of cells to resist changes in pH_i imposed by the application of weak acids or bases. The total intracellular buffering power (β_T) is defined as the amount of acid or base required to change pH_i by one unit (Chesler, 1990). β_T is a combination of the intrinsic buffering capacity (β_i), and the buffering power caused specifically by the presence of $\text{HCO}_3^-/\text{CO}_2$ in a system (β_b). β_b , at constant CO_2 tensions, varies directly with the concentration of HCO_3^- , such that the contribution made by the presence of $\text{HCO}_3^-/\text{CO}_2$ to the buffering equation is $2.3 \times [\text{HCO}_3^-]$ (see Roos and Boron, 1981). β_i includes non-bicarbonate physiochemical buffering (e.g. sulphates, phosphates, and proteins), biochemical buffering, and organellar buffering (see Introduction). To calculate the total intracellular buffering power, a known concentration of weak acid or base is applied to the cells and, using the dissociation constant, the amount of base or acid entering the cell is calculated; the ensuing change in pH_i is then used to determine the buffering capacity. Experiments in which TMA or propionate were applied to the neurones employed in this study provided a potential means of calculating intracellular buffering power. In the presence of HCO_3^- at room temperature, 10 mM TMA induced an intracellular alkalinization, whereas 20 mM propionate induced an intracellular acidification. According to the above rationale, the imposed changes in pH_i should have provided sufficient information to calculate buffering power. However, errors are introduced into the computation of buffering values by the operation of pH_i

regulating mechanisms which are activated as soon as an intracellular acid or alkali load is imposed on the cells. This problem can only be alleviated by the application of pharmacological inhibitors which act to block these regulators (see Roos and Boron, 1981; Vaughan-Jones and Wu, 1990). Unfortunately, the pharmacological blockade of *all* acid extruding mechanisms was not possible in the present experiments due to the insensitivity of the neurones to inhibitors of cation exchange, which appears to be the dominant mechanism of pH_i regulation.

Despite these difficulties, an approximation of intracellular buffering capacity in these neurones was obtained by analyzing data resulting from the application of NH_4^+ . When exposed to extracellular NH_4Cl , pH_i increases due to the influx of NH_3 and its subsequent hydration to form NH_4^+ and OH^- . Knowing the concentration of the applied NH_4Cl , the magnitude of this induced alkalization could be used to estimate β_T . The limitation of this technique, in addition to the previously discussed inability to prevent errors introduced by the activation of pH_i regulating mechanisms, is that it does not account for the appearance of intracellular NH_4^+ from sources other than influxing NH_3 . During exposure to extracellular NH_4Cl , NH_4^+ will passively diffuse into the cell due to an electrochemical driving force. Moreover, there is evidence that a Na^+/K^+ pump, if present, can carry NH_4^+ into cells in place of K^+ (see Boron, 1989). Since the experiments performed could not exclude the effects of these phenomena, the results could not be used to formally determine buffering power. However, by measuring the alkaline changes in pH_i resulting from a 3 minute application of NH_4^+ under the various experimental conditions, an indication of the neuronal ability to buffer imposed pH_i shifts was obtained (see column 3, Table 6).

The magnitude of the pH_i increase resulting from a 3 minute exposure to NH_4^+ was greatest in neurones lacking HCO_3^- at room temperature. This increase was attenuated by the presence of HCO_3^- during the application of NH_4^+ . Therefore, at room temperature, these neurones are better able to resist pH_i changes when HCO_3^- and CO_2

are present in the extracellular medium. CO_2 -induced enhancement of internal buffering power has been demonstrated in a variety of neuronal preparations (e.g. Thomas, 1976b), and thus increased resistance to alkaline pH_i shifts probably reflects the contribution of $\text{HCO}_3^-/\text{CO}_2$ -dependent buffering processes (i.e. β_b). Increasing the temperature of the perfusion medium to 37°C also had a profound effect on the apparent buffering capacity. In the absence of HCO_3^- , a 3 minute application of NH_4^+ at 37°C produced a pH_i rise less than that observed at room temperature in the presence of HCO_3^- . With HCO_3^- present in the perfusion solution at 37°C , the pH_i rise was further reduced to approximately 0.1 of a pH unit. The internal buffering capacity at 37°C is therefore also enhanced by the presence of CO_2 and HCO_3^- . Furthermore, the results suggest that, whether in the presence or absence of HCO_3^- , the relative buffering power of these neurones is greatest at 37°C . Temperature considerations regarding intracellular buffering have not been well documented (see Roos and Boron, 1981). However, Burton (1978) indicates that the apparent dissociation constants of acid-base pairs which contribute to physiochemical buffering may be significantly altered by factors such as temperature. In addition to physiochemical buffering, there may also be an increase in biochemical and organellar buffering associated with an elevation in temperature. Accordingly, the effects of temperature on the regulation of pH_i may reflect, at least in part, the temperature dependence of intracellular buffering mechanisms, although other mechanisms are likely to participate in the observed temperature effects, including temperature-dependent changes in acid extrusion rates and passive fluxes of acid equivalents (see Roos and Boron, 1981).

In summary, at room temperature and at 37°C , the resulting steady-state pH_i during perfusion with $\text{HCO}_3^-/\text{CO}_2$ -buffered medium (pH_o 7.35) is approximately 7.15. This value may be the optimal level assumed by pH_i under conditions that allow for the expression of all pH_i regulating mechanisms. When HCO_3^- is removed at either temperature, pH_i deviates from this optimal value. At room temperature, pH_i falls

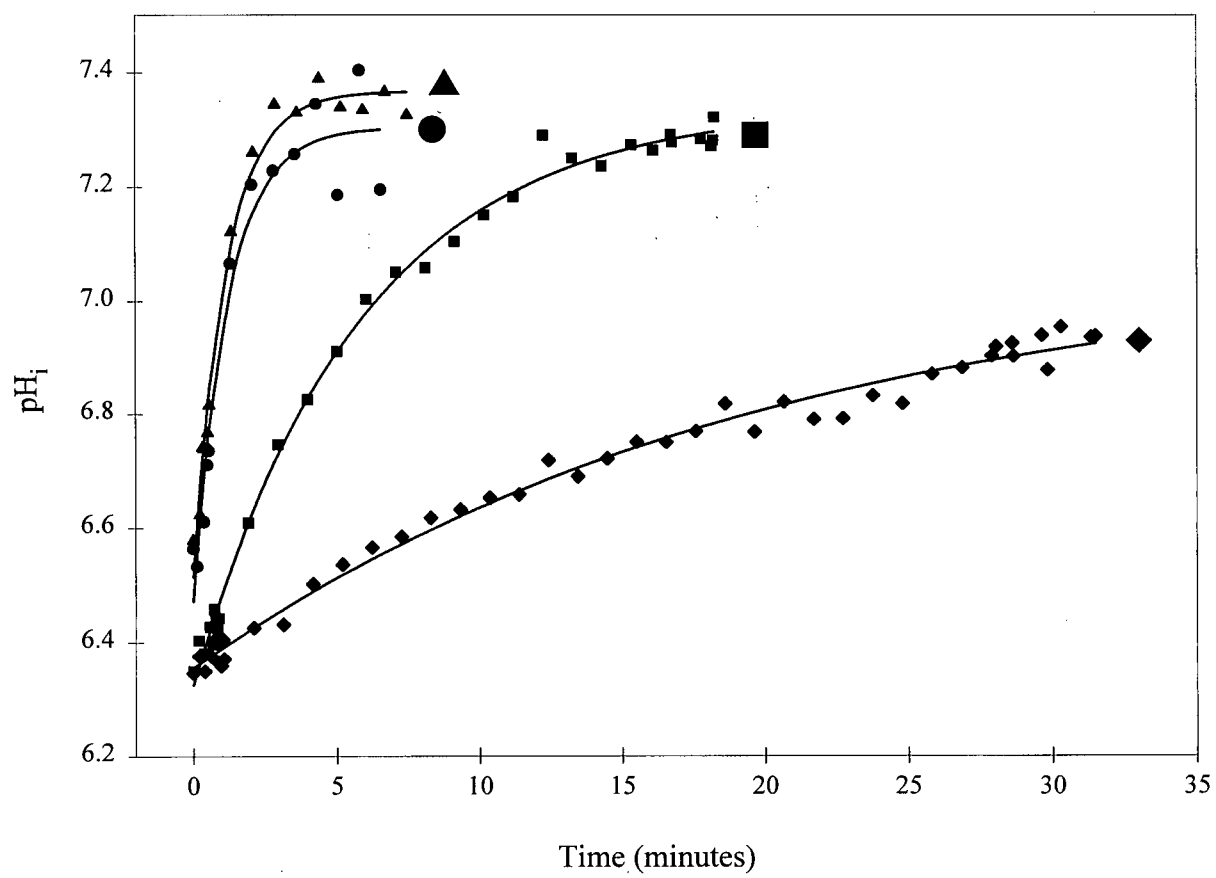
substantially when switched to HEPES-buffered perfusion solutions, whereas at 37°C, pH_i increases, albeit only slightly, when HCO_3^- is not present. The ability of the neurones employed in this study to maintain pH_i despite the absence of HCO_3^- at 37°C may reflect a temperature-dependent accentuation of the internal buffering power. At room temperature, this apparent buffering capacity is diminished, and thus the neurones may resort to other means, such as increased activity of Na^+ -independent $\text{HCO}_3^-/\text{Cl}^-$ exchange, to regulate steady-state pH_i to the optimal level. Intracellular buffering therefore contributes to the maintenance of resting pH_i in a manner that is dependent on the experimental temperature, and thus may explain the differences in pH_i regulation observed at room temperature and at 37°C.

Modulation of pH_i by pH_o :

In the presence of HCO_3^- , a shift in pH_o caused a qualitatively similar shift in pH_i , at both room temperature and at 37°C. This observation demonstrates the dependence of pH_i on pH_o , which has been documented in other vertebrate neurones (Tolkovsky and Richards, 1987; Nachshen and Drapeau, 1988; Ou-yang *et al*, 1993) and indicates that neuronal pH_i cannot be regulated back to normal levels until pH_o is normalized. In turn, this suggests the possibility that the mechanisms responsible for the maintenance of pH_i may be subject to modulation by the extracellular proton environment. Indeed, as discussed above, a decrease in pH_o causes an increase in the rate of recovery from an induced intracellular acidification. Moreover, the dependence of pH_i on pH_o suggests that changes in neuronal excitability which to date have been attributed to changes in pH_o (see Introduction) should be carefully analyzed since they may in fact reflect the accompanying alteration in pH_i , rather than just being due to changes in pH_o per se.

Figure 35. Diagrammatic representation of pH_i recovery from an acid load in the presence and absence of HCO_3^- , at room temperature and at 37°C .

The figure shows pH_i recovery from an NH_4^+ -induced acidification in the absence of HCO_3^- at room temperature (\blacklozenge), in the presence of HCO_3^- at room temperature (\blacksquare), in the presence of HCO_3^- at 37°C (\bullet), and in the absence of HCO_3^- at 37°C (\blacktriangle). pH_o ranged from 7.33 to 7.36 under the four conditions. The solid lines represent a least squares exponential best fit to data points indicated, which were obtained from four separate experiments under the conditions specified. Lines begin at the minimum pH_i reached during the acidification, and represent the trend found in all experiments conducted under similar conditions.



Conclusions:

The mechanisms operating to regulate pH_i were examined at steady-state or during recovery from an induced acidification in cultured foetal rat hippocampal pyramidal neurones. Temperature was found to exert a profound effect on the relative activities of these mechanisms (see Figure 36). At 37°C , the primary regulator of pH_i appears to be a Na^+ -dependent, HCO_3^- -independent acid extrusion mechanism (probably an amiloride insensitive variant of the Na^+/H^+ exchanger). At room temperature, the results of this study suggest that pH_i is regulated by a Na^+ -independent $\text{HCO}_3^-/\text{Cl}^-$ exchanger, which probably acts to supplement the activity of the same Na^+ -dependent acid extrusion mechanism observed at 37°C . The data do not support nor exclude the existence of a Na^+ -dependent $\text{HCO}_3^-/\text{Cl}^-$ exchanger on these neurones. However, if present, this Na^+ -dependent anion transporter would presumably play a minor role in the regulation of pH_i due to the demonstrated dominance of a HCO_3^- -independent acid extrusion mechanism governing pH_i , especially at 37°C .

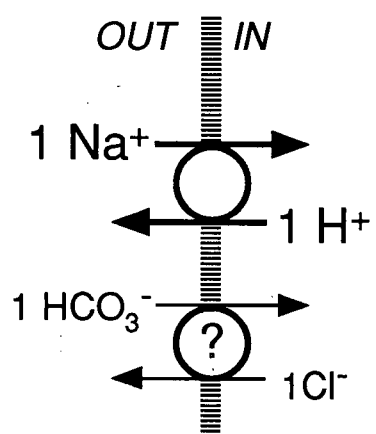
As noted in the Introduction, pH_i is an important modulator of many physiological and pathological events. The investigation of the mechanisms that are directly responsible for regulating pH_i may therefore help to provide information regarding the role of pH_i in such events. Future experimental directions include an investigation of the possible modulation of pH_i regulatory mechanisms by neurotransmitter candidates, and ways in which the effects of applied neuromodulators are in turn regulated by pH_i . Demonstrated on non-neuronal cell types, the activation of various cell surface receptors, including β -adrenergic, α_2 -adrenergic, somatostatin, D_2 -dopaminergic, and muscarinic cholinergic receptors, directly regulates the activity of Na^+/H^+ exchange (Isom *et al*, 1989; Barber *et al*, 1989; Ganz *et al*, 1990). Accordingly, it will be of interest to examine the effects of neurotransmitters, including norepinephrine, somatostatin, dopamine, and serotonin, on the pH_i regulating mechanisms present on hippocampal neurones. Such an investigation would include an examination of the

effects of intracellular second messengers on pH_i , since changes in cytoplasmic levels of cAMP, Ca^{2+} , and certain protein kinases have been shown to modulate pH_i in a variety of peripheral cell types (Grinstein and Rothstein, 1986). In a recent study of rat brain synaptosomes, Sánchez-Armass *et al* (1994) have indicated that Ca^{2+} , acting intracellularly, may play an important role in the modulation of Na^+/H^+ exchange. pH_i was not altered by enhancing the cytosolic levels of protein kinase C or kinase A (Sánchez-Armass *et al*, 1994). In addition, it is becoming increasingly apparent that a physiologically-relevant interdependence exists between pH_i and Ca^{2+} . For example, Dixon *et al* (1993) have demonstrated that high voltage activated Ca^{2+} currents in catfish horizontal cells are suppressed during glutamate application as a result of an associated increase in intracellular proton levels. Moreover, Irwin *et al* (1994) have suggested that an NMDA-induced intracellular acidosis observed in rat hippocampal neurones is dependent on Ca^{2+} influx resulting from the NMDA application. Therefore, further studies should include the investigation of pH_i in terms of its ability to modulate some of the intracellular processes which thus far have been attributed to changes in cytosolic Ca^{2+} and other intracellular second messengers.

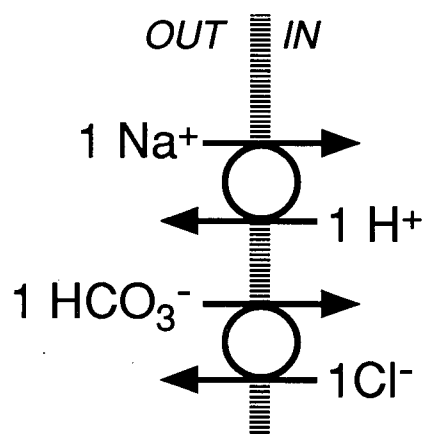
Figure 36. Schematic presentation of pH_i regulating mechanisms in cultured foetal hippocampal pyramidal neurones at 37°C and room temperature.

At 37°C, the dominant regulator in pH_i in these hippocampal neurones is a Na^+ -dependent, HCO_3^- -independent acid extrusion mechanism, which is probably a Na^+/H^+ exchanger. Though an anion exchanger was found to be present, its activity at 37°C appears to be minimal. At room temperature, pH_i is regulated by a Na^+ -independent $\text{HCO}_3^-/\text{Cl}^-$ exchanger acting to supplement the activity of the same Na^+ -dependent, HCO_3^- -independent acid extrusion mechanism observed at 37°C.

37°C



Room temperature



REFERENCES

- Ahmed, Z., and Connor, J. A. (1980). Intracellular pH changes induced by calcium influx during electrical activity in molluscan neurons. *Journal of General Physiology* **75**, 403-426.
- Aicken, C. C. (1984). Direct measurement of intracellular pH and buffering power in smooth muscle cells of guinea-pig vas deferens. *Journal of Physiology* **349**, 571-585.
- Aicken, C. C., and Thomas, R. C. (1977). An investigation of the ionic mechanism of intracellular pH regulation in mouse soleus muscle fibres. *Journal of Physiology* **273**, 295-316.
- Amoroso, S., Di Renzo, G., Tagliatela, M., Canzoniero, L. M. T., Cragoe, E. J., and Annunziato, L. (1991). Cytoplasmic alkalinization induced by insulin through an activation of $\text{Na}^+\text{-H}^+$ antiporter inhibits tyrosine hydroxylase activity in striatal synaptosomes. *Biochemical Pharmacology* **41**, 1279-1282.
- Amos, B. J., and Richards, C. D. (1994). Effect of glutamate on intracellular pH of rat neurones maintained in culture. *Journal of Physiology* **479**, 43P.
- Aram, J. A., and Lodge, D. (1987). Epileptiform activity induced by alkalosis in rat neocortical slices: block by antagonists of *N*-methyl-D-aspartate. *Neuroscience Letters* **83**, 345-350.
- Aronson, P. S. (1985). Kinetic properties of the plasma membrane $\text{Na}^+\text{-H}^+$ exchanger. *Annual Review of Physiology* **47**, 545-560.
- Aronson, P. S., and Bounds, S. E. (1980). Harmaline inhibition of Na-dependent transport in renal microvillus membrane vesicles. *American Journal of Physiology* **238**, F210-F217.
- Austin, C., and Wray, S. (1993). Extracellular pH signals affect vascular tone by rapid transduction into intracellular pH changes. *Journal of Physiology* **466**, 1-8.
- Baker, P. F., and Honerjäger, P. (1978). Influence of carbon dioxide on level of ionised calcium in squid axons. *Nature* **273**, 160-161.
- Balestrino, M., and Somjen, G. G. (1988). Concentration of carbon dioxide, interstitial pH and synaptic transmission in hippocampal formation of the rat. *Journal of Physiology* **396**, 247-266.
- Banker, G. A., and Cowan, W. M. (1977). Rat hippocampal neurons in dispersed cell culture. *Brain Research* **126**, 397-425.

- Barber, D. L., McGuire, M. E., and Ganz, M. B. (1989). β -adrenergic and somatostatin receptors regulate Na-H exchange independent of cAMP. *Journal of Biological Chemistry* **264**, 21038-21042.
- Barnes, S., and Bui, Q. (1991). Modulation of calcium-activated chloride current via pH-induced changes of calcium channel properties in cone photoreceptors. *Journal of Neuroscience* **11**, 4015-4023.
- Boron, W. F. (1989). Cellular buffering and intracellular pH. In: *The Regulation of Acid-Base Balance*, pp. 33-56. Eds. D. W. Seldin, and G. Giebisch. Raven Press.
- Boron, W. F., and Boulpaep, E. L. (1983). Intracellular pH regulation in the renal proximal tubule of the salamander. *Journal of General Physiology* **81**, 53-94.
- Boron, W. F., and De Weer, P. (1976). Intracellular pH transients in squid giant axons caused by CO₂, NH₃, and metabolic inhibitors. *Journal of General Physiology* **67**, 91-112.
- Bountra, C., Kaila, K., and Vaughan-Jones, R. D. (1988). Effect of repetitive activity upon intracellular pH, sodium and contraction in sheep cardiac Purkinje fibres. *Journal of Physiology* **398**, 341-360.
- Boyarski, G., Ganz, M. B., Sterzel, R. B., and Boron, W. F. (1988a). pH regulation in single glomerular mesangial cells. I. Acid extrusion in absence and presence of HCO₃⁻. *American Journal of Physiology* **255**, C844-C856.
- Boyarski, G., Ganz, M. B., Sterzel, R. B., and Boron, W. F. (1988b). pH regulation in single glomerular mesangial cells. II. Na⁺-dependent and -independent Cl⁻-HCO₃⁻ exchangers. *American Journal of Physiology* **255**, C857-C869.
- Brewer, G. J., and Cotman, C. W. (1989). Survival and growth of hippocampal neurons in defined medium at low density: advantages of a sandwich culture technique or low oxygen. *Brain Research* **494**, 65-74.
- Bright, G. R., Fisher, G. W., Rogowska, J., and Taylor, D. L. (1987). Fluorescence ratio imaging microscopy: temporal and spatial measurements of cytoplasmic pH. *Journal of Cell Biology* **104**, 1019-1033.
- Burton, R. F. (1978). Intracellular buffering. *Respiration Physiology* **33**, 51-58.
- Busa, W. B. (1986). Mechanisms and consequences of pH-mediated cell regulation. *Annual Review of Physiology* **48**, 389-402.
- Busa, W. B., and Nuccitelli, R. (1984). Metabolic regulation via intracellular pH. *American Journal of Physiology* **246**, R409-R438.

- Carbone, E., Testa, P. L., and Wanke, E. (1981). Intracellular pH and ionic channels in the *Loligo vulgaris* giant axon. *Biophysical Journal* **35**, 393-413.
- Chaillet, J. R., and Boron, W. F. (1985). Intracellular calibration of a pH-sensitive dye in isolated, perfused salamander proximal tubules. *Journal of General Physiology* **86**, 765-794.
- Chang, D., Kushman, N. L., and Dawson, D. C. (1991). Intracellular pH regulates basolateral K^+ and Cl^- conductances in colonic epithelial cells by modulating Ca^{2+} activation. *Journal of General Physiology* **98**, 183-196.
- Chesler, M. (1986). Regulation of intracellular pH in reticulospinal neurones of the lamprey, *Petromyzon marinus*. *Journal of Physiology* **381**, 241-261.
- Chesler, M. (1990). The regulation and modulation of pH in the nervous system. *Progress in Neurobiology* **34**, 401-427.
- Chesler, M., and Kaila, K. (1992). Modulation of pH by neuronal activity. *Trends in Neuroscience* **15**, 396-402.
- Chesler, M., and Kraig, R. P. (1987). Intracellular pH of astrocytes increases rapidly with cortical stimulation. *American Journal of Physiology* **22**, R666-R670.
- Church, J. (1992). A change from HCO_3^- - CO_2 - to HEPES-buffered medium modifies membrane properties of rat CA1 pyramidal neurones *in vitro*. *Journal of Physiology* **455**, 51-71.
- Church, J., and Baimbridge, K. G. (1991). Exposure to high-pH medium increases the incidence and extent of dye coupling between rat hippocampal CA1 pyramidal neurons *in vitro*. *Journal of Neuroscience* **11**, 3289-3295.
- Church, J., and McLennan, H. (1989). Electrophysiological properties of rat CA1 pyramidal neurones *in vitro* modified by changes in extracellular bicarbonate. *Journal of Physiology* **415**, 85-108.
- Clark, J. D., and Limbird, L. L. (1991). Na^+ - H^+ exchanger subtypes: a predictive review. *American Journal of Physiology* **261**, C945-C953.
- Conner, J. A., and Hockberger, P. P. (1984). Intracellular pH changes induced by injections of cyclic nucleotides into gastropod neurones. *Journal of Physiology* **354**, 163-172.
- Cook, D. L., Ikeuchi, M., and Fujimoto, W. Y. (1984). Lowering of pH_i inhibits Ca^{2+} -activated K^+ channels in pancreatic B-cells. *Nature* **311**, 269-271.
- Deutsch, C., and Lee, S. C. (1989). Modulation of K^+ currents in human lymphocytes by pH. *Journal of Physiology* **413**, 399-413.

- Dickens, C. J., Gillespie, J. I., and Greenwell, J. R. (1990). Measurement of intracellular calcium and pH in avian neuronal crest cells. *Journal of Physiology* **428**, 531-544.
- Dixon, D. B., Takahashi, K.-I., and Copenhagen, D. R. (1993). L-glutamate suppresses HVA calcium current in catfish horizontal cells by raising intracellular proton concentration. *Neuron* **11**, 267-277.
- Doering, A. E., and Lederer, W. J. (1993). The mechanism by which cytoplasmic protons inhibit the sodium-calcium exchanger in guinea-pig heart cells. *Journal of Physiology* **466**, 481-499.
- Ebine, Y., Fujiwara, N., and Shimoji, K. (1994). Mild acidosis inhibits the rise in intracellular Ca^{2+} concentration in response to oxygen-glucose deprivation in rat hippocampal slices. *Neuroscience Letters* **168**, 155-158.
- Endres, W., Ballanyi, K., Serve, G., and Grafe, P. (1986). Excitatory amino acids and intracellular pH in motoneurons of the isolated frog spinal cord. *Neuroscience Letters* **72**, 54-58.
- Fenn, W. O., and Cobb, D. M. (1934). The potassium equilibrium in muscle. *Journal of General Physiology* **17**, 629-656.
- Fenn, W. O., and Maurer, F. W. (1935). The pH of muscle. *Protoplasma* **28**, 337-345.
- Fitz, J. G., Lidofsky, S. D., Xie, M.-H., and Scharschmidt, B. F. (1992). Transmembrane electrical potential difference regulates $\text{Na}^+/\text{HCO}_3^-$ cotransport and intracellular pH in hepatocytes. *Proceedings of the National Academy of Science, U.S.A.* **89**, 4197-4201.
- Fornai, F., Dybdal, D. J., Proctor, M. R., and Gale, K. (1994). Focal intracerebral elevation of L-lactate is anticonvulsant. *European Journal of Pharmacology* **254**, R1-R2.
- Freudenrich, C. C., Murphy, E., Levy, L. A., London, R. E., and Lieberman, M. (1992). Intracellular pH modulates cytosolic free magnesium in cultured chicken heart cells. *American Journal of Physiology* **262**, C1024-C1030.
- Gaillard, S., and DuPont, J.-L. (1990). Ionic control of intracellular pH in rat cerebellar Purkinje cells maintained in culture. *Journal of Physiology* **425**, 71-83.
- Ganz, M. B., and Boron, W. F. (1994). Long-term effects of growth factors on pH and acid-base transport in rat glomerular mesangial cells. *American Journal of Physiology* **266**, F576-F585.
- Ganz, M. B., Pachter, J. A., and Barber, D. L. (1990). Multiple receptors coupled to adenylate cyclase regulate Na-H- exchange independent of cAMP. *Journal of Biological Chemistry* **265**, 8989-8992.

- Ganz, M. B., Rasmussen, J., Bollag, W. B., and Rasmussen, H. (1990). Effect of buffer systems and pH_i on the measurement of $[\text{Ca}^{2+}]_i$ with fura-2. *FASEB Journal* **4**, 1638-1644.
- Giffard, R. G., Monyer, H., Christine, C. W., and Choi, D. W. (1990). Acidosis reduces NMDA receptor activation, glutamate neurotoxicity, and oxygen-glucose deprivation neuronal injury in cortical cultures. *Brain Research* **506**, 339-342.
- Gottfried, J. A., and Chesler, M. (1994). Endogenous H^+ modulation of NMDA receptor-mediated EPSCs revealed by carbonic anhydrase inhibition in rat hippocampus. *Journal of Physiology* **478.3**, 373-378.
- Harris, R. J., Richards, P. G., Symon, L., Habib, A.-H. A., and Rosenstein, J. (1987). pH , K^+ , and PO_2 of the extracellular space during ischaemia of primate cerebral cortex. *Journal of Cerebral Blood Flow and Metabolism* **7**, 599-604.
- Hartley, Z., and Dubinsky, J. M. (1993). Changes in intracellular pH associated with glutamate excitotoxicity. *Journal of Neuroscience* **13**, 4690-4699.
- Hesketh, T. R., Moore, J. P., Morris, J. D. H., Taylor, M. V., Rogers, J., Smith, G. A., and Metcalfe, J. C. (1985). A common sequence of calcium and pH signals in the mitogenic stimulation of eukaryotic cells. *Nature* **313**, 481-484.
- Hill, A. V. (1955). The influence of the external medium on the internal pH of muscle. *Proceedings of the Royal Society London B Series* **144**, 1-22.
- Irwin, R. P., Lin, S.-Z., Long, R. T., and Paul, S. M. (1994). *N*-methyl-D-aspartate induces a rapid, reversible, and calcium-dependent intracellular acidosis in cultured fetal rat hippocampal neurons. *Journal of Neuroscience* **14**, 1352-1357.
- Isom, L. L., Cragoe, E. J., and Limbird, L. E. (1987). Multiple receptors linked to inhibition of adenylate cyclase accelerate Na^+/H^+ exchange in neuroblastoma \times glioma cells via a mechanism other than decreased cAMP accumulation. *Journal of Biological Chemistry* **262**, 17504-17509.
- Jarolimek, W., Misgeld, U., and Lux, H. D. (1989). Activity dependent alkaline and acid transients in guinea pig hippocampal slices. *Brain Research* **505**, 225-232.
- Johnson, J. D., Epel, D., and Paul, M. (1976). Intracellular pH and activation of sea urchin eggs after fertilization. *Nature* **262**, 661-664.
- Kaibara, M., and Kameyama, M. (1988). Inhibition of the calcium channel by intracellular protons in single ventricular myocytes of the guinea-pig. *Journal of Physiology* **403**, 621-640.

- Kaila, K., Saarikoski, J., and Voipio, J. (1990). Mechanism of action of GABA on intracellular pH and on surface pH in crayfish muscle fibres. *Journal of Physiology* **427**, 241-260.
- Kaila, K., and Voipio, J. (1987). Postsynaptic fall in intracellular pH induced by GABA-activated bicarbonate conductances. *Nature* **330**, 163-165.
- Kaila, K., and Voipio, J. (1990). Dependence of intracellular free calcium and tension on membrane potential and intracellular pH in single crayfish muscle fibres. *Pflügers Archiv* **416**, 501-511.
- Kaku, D. A., Giffard, R. G., and Choi, D. W. (1993). Neuroprotective effects of glutamate antagonists and extracellular acidity. *Science* **260**, 1516-1518.
- Katsura, K., Kristián, T., Nair, R., and Siesjö, B. K. (1994). Regulation of intra- and extracellular pH in the rat brain in acute hypercapnia: a re-appraisal. *Brain Research* **651**, 47-56.
- Koch, R. A., and Barish, M. E. (1994). Perturbation of intracellular calcium and hydrogen ion regulation in cultured mouse hippocampal neurons by reduction of the sodium ion concentration gradient. *Journal of Neuroscience* **14**, 2585-2593.
- Kraig, R. P., Petito, C. K., Plum, F., and Pulsinelli, W. A. (1987). Hydrogen ions kill brain at concentrations reached in ischemia. *Journal of Cerebral Blood Flow and Metabolism* **7**, 379-386.
- Krishtal, O. A., Osipchuk, Y. V., Shelest, T. N., and Smirnov, S. V. (1987). Rapid extracellular pH transients related to synaptic transmission in rat hippocampal slices. *Brain Research* **436**, 352-356.
- Kristián, T., Katsura, K., Gidö, G., Siesjö, B. K. (1994). The influence of pH on cellular calcium influx during ischemia. *Brain Research* **641**, 295-302.
- Kume, H., Takagi, K., Satake, T., Tokuno, H., and Tomita, T. (1990). Effects of intracellular pH on calcium-activated potassium channels in rabbit tracheal smooth muscle. *Journal of Physiology* **424**, 445-457.
- Kurachi, Y. (1982). The effects of intracellular protons on the electrical activity of single ventricular cells. *Pflügers Archiv* **394**, 264-270.
- Laurido, C., Candia, S., Wolff, D., and Latorre, R. (1991). Proton modulation of a Ca^{2+} -activated K^{+} channel from rat skeletal muscle incorporated into planar bilayers. *Journal of General Physiology* **98**, 1025-1043.
- Lea, T. J., and Ashley, C. C. (1978). Increase in free Ca^{2+} in muscle after exposure to CO_2 . *Nature* **275**, 236-238.

- Lennox, W. G., Gibbs, F. A., and Gibbs, E. L. (1936). Effect on the electroencephalogram of drugs and conditions which influence seizures. *Archives of Neurology and Psychiatry* **36**, 1236-1250.
- Ludt, J., Tønnessen, T. I., Sandvig, K., Olsnes, S. (1991). Evidence for involvement of protein kinase C in regulation of intracellular pH by $\text{Cl}^-/\text{HCO}_3^-$ antiport. *Journal of Membrane Biology* **119**, 179-186.
- Mabe, H., Blomqvist, P., and Siesjö, B. K. (1983). Intracellular pH in the brain following transient ischemia. *Journal of Cerebral Blood Flow and Metabolism* **3**, 109-114.
- MacVicar, B. A., and Jahnsen, H. (1985). Uncoupling of CA3 pyramidal neurons by propionate. *Brain Research* **330**, 141-145.
- Martínez-Zaguilán, R., Gillies, R. J., and Sánchez-Armass, S. (1994). Regulation of pH in rat brain synaptosomes. II. Role of Cl^- . *Journal of Neurophysiology* **71**, 2249-2257.
- Martínez-Zaguilán, R., Martínez, G. M., Lattanzio, F., and Gillies, R. J. (1991). Simultaneous measurement of intracellular pH and Ca^{2+} using the fluorescence of SNARF-1 and fura-2. *American Journal of Physiology* **260**, C297-C307.
- Meech, R. W., and Thomas, R. C. (1977). The effect of calcium injection on the intracellular sodium and pH of snail neurones. *Journal of Physiology* **265**, 867-879.
- Meech, R. W., and Thomas, R. C. (1987). Voltage-dependent intracellular pH in *Helix aspersa* neurones. *Journal of Physiology* **390**, 433-452.
- Messeter, K., and Siesjö, B. K. (1971). The intracellular pH in the brain in acute and sustained hypercapnia. *Acta Physiologica Scandinavica* **83**, 210-219.
- Moody, W. (1980). Appearance of calcium action potentials in crayfish slow muscle fibres under conditions of low intracellular pH. *Journal of Physiology* **302**, 335-346.
- Moody, W. (1984). Effects of intracellular H^+ on the electrical properties of excitable cells. *Annual Review of Neuroscience* **7**, 257-278.
- Moody, W. J., and Hagiwara, S. (1982). Block of inward rectification by intracellular H^+ in immature oocytes of the starfish *Mediaster aequalis*. *Journal of General Physiology* **79**, 115-130.
- Moolenaar, W. H., de Laat, S. W., Mummery, C. L., and van der Saag, P. T. (1982). Na^+/H^+ exchange in the action of growth factors. In: *Ions, Cell Proliferation, and Cancer*, pp. 151-162. Eds. A. L. Boyton, W. L. McKeehan, and J. F. Whitfield. Academic Press.

- Mrkic, B., Tse, C.-M., Forgo, J., Helmle-Kolb, C., Donowitz, M., and Murer, H. (1993). Identification of PTH-responsive Na/H-exchanger isoforms in a rabbit proximal tubule cell line (RKPC-2). *Pflügers Archiv* **424**, 377-384.
- Murer, H., Hopfer, U., and Kinne, R. (1976). Sodium/proton antiport in brush-border-membrane vesicles isolated from rat small intestine and kidney. *Biochemical Journal* **154**, 597-604.
- Mutch, W. A. C., and Hansen, A. J. (1984). Extracellular pH changes during spreading depression and cerebral ischemia: mechanisms of brain pH regulation. *Journal of Cerebral Blood Flow and Metabolism* **4**, 17-27.
- Nachshen, D. A., and Drapeau, P. (1988). The regulation of cytosolic pH in isolated presynaptic nerve terminals from rat brain. *Journal of General Physiology* **91**, 289-303.
- Nedergaard, M., Goldman, S. A., Desai, S., and Pulsinelli, W. A. (1991). Acid-induced death in neurons and glia. *Journal of Neuroscience* **11**, 2489-2497.
- Nonner, W., Spalding, B. C., and Hille, B. (1980). Low intracellular pH and chemical agents slow inactivation gating in sodium channels of muscle. *Nature* **284**, 360-363.
- Orlowski, J., Kandasamy, R. A., and Shull, G. E. (1992). Molecular cloning of putative members of the Na/H exchanger gene family. *Journal of Biological Chemistry* **267**, 9331-9339.
- Ou-yang, Y., Kristián, T., Møllergård, P., and Siesjö, B. K. (1994). The influence of pH on glutamate- and depolarization-induced increases of intracellular calcium concentration in cortical neurons in primary culture. *Brain Research* **646**, 65-72.
- Ou-yang, Y., Møllergård, P., and Siesjö, B. K. (1993). Regulation of intracellular pH in single rat cortical neurons in vitro: a microspectrofluorometric study. *Journal of Cerebral Blood Flow and Metabolism* **13**, 827-840.
- Peers, C., and Green, F. K. (1991). Inhibition of Ca^{2+} -activated K^{+} currents by intracellular acidosis in isolated type I cells of the neonatal rat carotid body. *Journal of Physiology* **437**, 589-602.
- Pocock, G., and Richards, C. D. (1989). Hydrogen ion regulation in rat cerebellar granule cells maintained in tissue culture. *Journal of Physiology* **412**, 68P.
- Preissler, M., and Williams, J. A. (1981). Pancreatic acinar cell function: measurement of intracellular ions and pH and their relation to secretion. *Journal of Physiology* **321**, 437-448.

- Prod'hom, B., Pietrobon, D., and Hess, P. (1987). Direct measurement of proton transfer rates to a group controlling the dihydropyridine-sensitive Ca^{2+} channel. *Nature* **329**, 243-246.
- Raley-Susman, K. M., Cragoe, E. J., Sapolsky, R. M., and Kopito, R. R. (1991). Regulation of intracellular pH in cultured hippocampal neurones by an amiloride-insensitive Na^+/H^+ exchanger. *Journal of Biological Chemistry* **266**, 2739-2745.
- Raley-Susman, K. M., Sapolsky, R. M., and Kopito, R. B. (1993). $\text{Cl}^-/\text{HCO}_3^-$ exchange function differs in adult and fetal rat hippocampal neurons. *Brain Research* **614**, 308-314.
- Richards, C. D., and Pocock, G. (1989). Hydrogen ion regulation in cultured mammalian CNS neurones. *Acta Physiologica Scandinavica Supplementum* **136**, 36.
- Rink, T. J., Tsien, R. Y., and Pozzan, T. (1982). Cytoplasmic pH and free Mg^{2+} in lymphocytes. *Journal of Cell Biology* **95**, 189-196.
- Roos, A. (1975). Intracellular pH and distribution of weak acids across cell membranes. A study of D- and L-lactate and of DMO in rat diaphragm. *Journal of Physiology* **249**, 1-25.
- Roos, A., and Boron, W. F. (1981). Intracellular pH. *Physiological Reviews* **61**, 296-434.
- Rosario, L. M., Stutzin, A., Cragoe, E. J., and Pollard, H. B. (1991). Modulation of intracellular pH by secretagogues and the Na^+/H^+ antiporter in cultured bovine chromaffin cells. *Neuroscience* **41**, 269-276.
- Rowe, W. A., Lesho, M. J., and Montrose, M. H. (1994). Polarized Na^+/H^+ exchange function is pliable in response to transepithelial gradients of propionate. *Proceedings of the National Academy of Science, U.S.A.* **91**, 6166-6170.
- Russell, J. M., and Boron, W. F. (1976). Role of chloride transport in regulation of intracellular pH. *Nature* **264**, 73-74.
- Sachs, G. (1987). The gastric proton pump: the H^+ , K^+ , ATPase. In: *Physiology of the Gastrointestinal Tract, Second Edition*, pp. 865-881. Ed. L. R. Johnson. Raven Press.
- Sachs, G., Chang, H. H., Rabon, E., Schackman, R., Lewin, M., and Saccomani, G. (1976). A nonelectrogenic H^+ pump in plasma membranes of hog stomach. *Journal of Biological Chemistry* **251**, 7690-7698.
- Sánchez-Armass, S., Martínez-Zaguilán, R., and Martínez, G. M. (1994). Regulation of pH in rat brain synaptosomes. I. Role of sodium, bicarbonate, and potassium. *Journal of Neurophysiology* **71**, 2236-2248.

- Sardet, C., Fafournoux, P., and Pouyssegur, J. (1991). α -thrombin, epidermal growth factor, and okadaic acid activate the Na^+/H^+ exchanger, NHE-1, by phosphorylating a set of common sites. *Journal of Biological Chemistry* **266**, 19166-19171.
- Sardet, C., Franchi, A., and Pouyssegur, J. (1989). Molecular cloning, primary structure, and expression of the human growth factor-activatable Na^+/H^+ antiporter. *Cell* **56**, 271-280.
- Schmid, A., Scholz, W., Lang, H.-J., and Popp, R. (1992). Na^+/H^+ exchange in porcine cerebral capillary endothelial cells is inhibited by a benzoylguanidine derivative. *Biochemical and Biophysical Research Communications* **184**, 112-117.
- Schuldiner, S., and Rozengurt, E. (1982). Na^+/H^+ antiport in swiss 3T3 cells: mitogenic stimulation leads to cytoplasmic alkalinization. *Proceedings of the National Academy of Science, U.S.A.* **79**, 7778-7782.
- Schwiening, C. J., and Boron, W. F. (1992). Fractional rate of dye signal decrease as an aid in assessing membrane permeability. *Journal of Physiology* **452**, 187P.
- Schwiening, C. J., and Boron, W. F. (1994). Regulation of intracellular pH in pyramidal neurones from the rat hippocampus by Na^+ -dependent $\text{Cl}^-/\text{HCO}_3^-$ exchange. *Journal of Physiology* **475.1**, 59-67.
- Sharp, A. P., and Thomas, R. C. (1981). The effects of chloride substitution on intracellular pH in crab muscle. *Journal of Physiology* **312**, 71-80.
- Siesjö, B. K. (1985). Acid-base homeostasis in the brain: physiology, chemistry, and neurochemical pathology. In: *Progress in Brain Research*, Vol. 63, pp. 121-154. Eds. K. Kogure, K.-A. Hossmann, B. K. Siesjö, and F. A. Welsh. Elsevier.
- Siesjö, B. K., Ekholm, A., Katsura, K., and Theander, S. (1990). Acid-base changes during complete brain ischemia. *Stroke* **21** (Suppl III), 194-199.
- Siesjö, B. K., and Messeter, K. (1971). Factors determining intracellular pH. In: *Ion Homeostasis of the brain. Alfred Benzon Symposium III*, pp. 244-269. Eds. B. K. Siesjö, and S. C. Sorensen. Munksgaard, Copenhagen.
- Siesjö, B. K., von Hanwehr, R., Nergelius, G., Nevander, G., and Ingvar, M. (1985). Extra- and Intracellular pH in the brain during seizures and in the recovery period following the arrest of seizure activity. *Journal of Cerebral Blood Flow and Metabolism* **5**, 47-57.
- Silver, R. A., Whitaker, M., and Bolsover, S. R. (1992). Intracellular ion imaging using fluorescent dyes: artefacts and limits to resolution. *Pflügers Archiv* **420**, 595-602.

- Simon, R. P., Niiro, M., and Gwinn, R. (1993). Brain acidosis induced by hypercarbic ventilation attenuates focal ischemic injury. *Journal of Pharmacology and Experimental Therapeutics* **267**, 1428-1431.
- Siskind, M. S., McCoy, C. E., Chobanian, A., and Schwartz, J. H. (1989). Regulation of intracellular calcium by cell pH in vascular smooth muscle cells. *American Journal of Physiology* **256**, C234-C240.
- Somjen, G. G. (1984). Acidification of interstitial fluid in hippocampal formation caused by seizures and by spreading depression. *Brain Research* **311**, 186-188.
- Somjen, G. G., Allen, B. W., Balestrino, M., and Aitken, P. G. (1987). Pathophysiology of pH and Ca^{2+} in bloodstream and brain. *Canadian Journal of Physiology* **65**, 1078-1085.
- Spray, D. C., and Bennett, M. V. L. (1985). Physiology and pharmacology of gap junctions. *Annual Review of Physiology* **47**, 281-303.
- Spray, D. C., Stern, J. H., Harris, A. L., and Bennett, M. V. L. (1982). Gap junctional conductances: comparison of sensitivities to H and Ca ions. *Proceedings of the National Academy of Science, U.S.A.* **79**, 441-445.
- Sun, B., and Vaughan-Jones, R. D. (1994). Effect of extracellular pH on intracellular pH in isolated guinea-pig ventricular myocytes. *Journal of Physiology* **475.P**, 83P.
- Taggart, M., Austin, C., and Wray, S. (1994). A comparison of the effects of intracellular and extracellular pH on contraction in isolated rat portal vein. *Journal of Physiology* **475**, 285-292.
- Taira, T., Smirnov, S., Voipio, J., and Kaila, K. (1993). Intrinsic proton modulation of excitatory transmission in rat hippocampal slices. *NeuroReport* **4**, 93-96.
- Takahashi, K.-I., Dixon, D. B., and Copenhagen, D. R. (1993). Modulation of a sustained calcium current by intracellular pH in horizontal cells of fish retina. *Journal of General Physiology* **101**, 695-714.
- Tang, C.-M., Dichter, M., and Morad, M. (1990). Modulation of *N*-methyl-D-aspartate channel by extracellular H^+ . *Proceedings of the National Academy of Science, U.S.A.* **87**, 6445-6449.
- Thomas, R. C. (1976a). Ionic mechanisms of the H^+ pump in snail neurone. *Nature* **262**, 54-55.
- Thomas, R. C. (1976b). The effect of CO_2 on the intracellular pH and buffering power of snail neurones. *Journal of Physiology* **255**, 715-735.

- Thomas, R. C. (1977). The role of bicarbonate, chloride and sodium ions in the regulation of intracellular pH in snail neurones. *Journal of Physiology* **273**, 317-338.
- Thomas, R. C. (1984). Experimental displacement of intracellular pH and the mechanism of its subsequent recovery. *Journal of Physiology* **354**, 3P-22P.
- Tolkovsky, A. M., and Richards, C. D. (1987). Na^+/H^+ exchange is the major mechanism of pH regulation in cultured sympathetic neurons: measurements in single cell bodies and neurites using a fluorescent pH indicator. *Neuroscience* **22**, 1093-1102.
- Tombaugh, G. C. (1994). Mild acidosis delays hypoxic spreading depression and improves neuronal recovery in hippocampal slices. *Journal of Neuroscience* **14**(9), 5635-5643.
- Tombaugh, G. C., and Sapolsky, R. M. (1993). Evolving concepts about the role of acidosis in ischemic neuropathology. *Journal of Neurochemistry* **61**, 793-803.
- Traynelis, S. F., and Cull-Candy, S. G. (1991). Pharmacological properties and H^+ sensitivity of excitatory amino acid receptor channels in rat cerebellar granule neurones. *Journal of Physiology* **433**, 727-763.
- Tse, C.-M., Levine, S. A., Yun, C. H. C., Brant, S. R., Pouyssegur, J., Montrose, M. H., and Donowitz, M. (1993). Functional characteristics of a cloned epithelial Na^+/H^+ exchanger (NHE3): resistance to amiloride and inhibition by protein kinase C. *Proceedings of the National Academy of Science, U.S.A.* **90**, 9110-9114.
- Tse, C. M., Watson, A. J. M., Ma, A. I., Pouyssegur, J., and Donowitz, M. (1991). Cloning and functional expression of a second novel rabbit ileal villus epithelial cell Na^+/H^+ exchanger (NHE-2). *Gastroenterology* **100**, A258.
- Tsien, R. Y. (1989). Fluorescent indicators of ion concentration. In: *Methods in Cell Biology, Volume 30*, pp. 127-156. Eds. Y. Wang, and D. L. Taylor. Academic Press.
- Umbach, J. A. (1982). Changes in intracellular pH affect calcium currents in *Paramecium caudatum*. *Proceedings of the Royal Society of London B* **216**, 209-224.
- Vaughan-Jones, R. D., Eisner, D. A., and Lederer, W. J. (1987). Effects of changes of intracellular pH on contraction in sheep cardiac Purkinje fibers. *Journal of General Physiology* **89**, 1015-1032.
- Vaughan-Jones, R. D., and Wu, M.-L. (1990). pH dependence of intrinsic H^+ buffering power in the sheep cardiac Purkinje fibre. *Journal of Physiology* **425**, 429-448.
- Velíšek, L., Dreier, J. P., Stanton, P. K., Heinemann, U., and Moshé, S. L. (1994). Lowering of extracellular pH suppresses low- Mg^{2+} -induces seizures in combined entorhinal cortex-hippocampal slices. *Experimental Brain Research* **101**, 44-52.

- Voipio, J., and Kaila, K. (1993). Intestinal PCO_2 and pH in rat hippocampal slices measured by means of a novel fast CO_2/H^+ -sensitive microelectrode based on a PVC-gelled membrane. *Pflügers Archiv* **423**, 193-201.
- Voipio, K., Pasternack, M., Rydqvist, B., and Kaila, K. (1991). Effect of γ -aminobutyric acid on intracellular pH in the crayfish stretch-receptor neurone. *Journal of Experimental Biology* **156**, 349-361.
- Vyklický, L., Vlachová, V., and Krušek, J. (1990). The effect of external pH changes on responses to excitatory amino acids in mouse hippocampal neurones. *Journal of Physiology* **430**, 497-517.
- Wanke, E., Carbone, E., and Testa, P. L. (1979). K^+ conductance modified by a titratable group accessible to protons from the intracellular side of the squid axon membrane. *Biophysical Journal* **26**, 319-324.
- Wanke, E., Carbone, E., and Testa, P. L. (1980). The sodium channel and intracellular H^+ blockage in squid axons. *Nature* **287**, 62-63.
- Wilkie, D. R. (1979). Generation of protons by metabolic processes other than glycolysis in muscle cells: a critical view. *Journal of Molecular and Cellular Cardiology* **11**, 325-330.
- Wöll, E., Ritter, M., Offner, F., Lang, H.-J., Schölkens, B., Häussinger, D., and Lang, F. (1993). Effects of HOE 694 - a novel inhibitor of Na^+/H^+ exchange - on NIH 3T3 fibroblasts expressing the *RAS* oncogene. *European Journal of Pharmacology - Molecular Pharmacology Section* **246**, 269-273.
- Zeilhofer, H. U., Müller, T. H., and Swandulla, D. (1993). Inhibition of high voltage-activated calcium currents by L-glutamate receptor-mediated calcium influx. *Neuron* **10**, 879-887.